IDENTIFICATION AND CHARACTERIZATION OF EPITOPES ON THE MEROZOITE SURFACE PROTEIN-1_{42} (MSP-1_{42}) OF *PLASMODIUM KNOWLESI*

CHEONG FEI WEN

THESIS SUBMITTED IN FULFILMENT OF THE REQUIREMENTS FOR THE DEGREE OF DOCTOR OF PHILOSOPHY

DEPARTMENT OF PARASITOLOGY
FACULTY OF MEDICINE
UNIVERSITY OF MALAYA
KUALA LUMPUR

2014

UNIVERSITI MALAYA

ORIGINAL LITERARY WORK DECLARATION

Name of Candidate: Cheong Fei Wen

Registration/Matric No: MHA100032

Name of Degree: Doctor of Philosophy

Title of Project Paper/Research Report/Dissertation/Thesis ("this Work"):

Identification and characterization of epitopes on the merozoite surface protein-1_{42} (MSP-1_{42}) of *Plasmodium knowlesi*

Field of Study: Parasitology

I do solemnly and sincerely declare that:

(1) I am the sole author/writer of this Work;
(2) This Work is original;
(3) Any use of any work in which copyright exists was done by way of fair dealing and for permitted purposes and any excerpt or extract from, or reference to or reproduction of any copyright work has been disclosed expressly and sufficiently and the title of the Work and its authorship have been acknowledged in this Work;
(4) I do not have any actual knowledge nor do I ought reasonably to know that the making of this work constitutes an infringement of any copyright work;
(5) I hereby assign all and every rights in the copyright to this Work to the University of Malaya ("UM"), who henceforth shall be owner of the copyright in this Work and that any reproduction or use in any form or by any means whatsoever is prohibited without the written consent of UM having been first had and obtained;
(6) I am fully aware that if in the course of making this Work I have infringed any copyright whether intentionally or otherwise, I may be subject to legal action or any other action as may be determined by UM.

Candidate's Signature Date

Subscribed and solemnly declared before,

Witness's Signature Date

Name:

Designation:

ABSTRACT

Malaria is one of the infections that causes high global mortality and morbidity annually. *Plasmodium knowlesi* has been recognised as the fifth human *Plasmodium* species that can cause human malaria and it can be potentially life threatening.

The merozoite surface protein 1 (MSP-1) undergoes two proteolytic steps during maturation of merozoites and invasion of merozoites into erythrocytes. During the first process, the MSP-1 precursor polypeptide is cleaved into four major fragments including MSP-1_{42}. The secondary process further cleaves the MSP-1_{42} into two fragments, MSP-1_{33} and MSP-1_{19}.

In the present study, the ~28 kDa recombinant protein MSP-1_{33} and ~42 kDa recombinant protein MSP-1_{42} of *P. knowlesi* (pkMSP-1_{33} and pkMSP-1_{42} respectively) were expressed using *Escherichia coli* system. The purified proteins were evaluated with malaria and non-malaria human patient sera using Western Blot and ELISA assays. In the Western Blot assays, pkMSP-1_{33} showed sensitivity of 98.3% and specificity of 97.4% in detecting malaria antibodies. In ELISA, the sensitivity for pkMSP-1_{33} was 76.3%, with the specificity 94.9%. The pkMSP-1_{42} had a sensitivity of 91.0% for detection of human malaria in both assays. Specificity of pkMSP-1_{42} was 97.5% and 92.6% in Western blots and ELISA, respectively. High sensitivity and specificity of pkMSP-1_{33} and pkMSP-1_{42} in immunoassays reveals that these two recombinant proteins could be useful in general sero-epidemiological screening.

Sensitivity and specificity obtained for pkMSP-1_{42} in Western Blot and ELISA assays were consistently higher (>90%) as compared to pkMSP-1_{33} which had lower sensitivity in ELISA (<80%). Besides, the MSP-1_{42}, which is made up of the MSP-1_{33} and MSP-1_{19} regions, has immunodominant T cell and B cell epitopes. Hence, this study aimed to evaluate the immunogenicity of pkMSP-1_{42} using mouse model and to identify

the potential epitopes. Mice immunized with pkMSP-1_{42} had increased levels of cytokine interferon-gamma, interleukin-2, interleukin-4, and interleukin-10 significantly as compared to the levels in negative control mice. Furthermore, the endpoint titres of pkMSP-1_{42}-raised antibody were high, with the following IgG isotype distribution: IgG1 > IgG2b > IgG3 > IgG2a.

Potential epitopes on *P. knowlesi* MSP-1_{42} were identified using synthetic peptide library and phage display library approaches. In these approaches, pkMSP-1_{42}-immunized mice sera were used for screening of the potential epitopes. Nine potential epitopes were identified using synthetic peptide library, and 14 using the phage display library. Two regions (residues 37-95 and residues 240-289) were identified to be the potential dominant epitope regions. Two peptides from the peptide library, P10 (TAKDGMEYYNKMGELYKQ) and P31 (RCLLGFKEVGGKCVPASI), were selected and evaluated using mouse model. P10 and P31-immunized mice sera reacted with recombinant *P. knowlesi* MSP-1_{42}, and the IgG isotype distribution was IgG2b > IgG1 > IgG2a > IgG3. Antibodies raised against P10 and P31 recognised *P. knowlesi* blood stage parasites, indicating that both peptides were immunogenic and might correspond to the epitopes that serve as the binding sites for antibodies on the parasites. Furthermore, interferon-gamma and interleukin-2 levels were significantly higher in P31-immunized mice. With further evaluations, P10 and P31 can potentially be used in the development of malaria vaccine and therapeutic agents.

Abstrak

Malaria merupakan salah satu jangkitan yang menyebabkan mortaliti dan morbiditi yang tinggi di dunia setiap tahun. *Plasmodium knowlesi* telah diiktiraf sebagai spesies *Plasmodium* yang kelima yang boleh menyebabkan malaria pada manusia dan ia berkemungkinan mengancam nyawa.

Protein permukaan merozoit-1 (merozoite surface protein-1, MSP-1) menjalani dua langkah proteolisis iaitu semasa kematangan merozoit dan semasa serangan merozoit ke atas eritrosit. Semasa proses pertama, MSP-1 polipeptida prekursor dibahagi kepada empat fragmen major termasuk MSP-1_{42}. Proses sekunder seterusnya membahagi MSP-1_{42} kepada dua fragmen MSP-1_{33} dan MSP-1_{19}.

Dalam kajian ini, ~28 kDa protein rekombinan MSP-1_{33} dan ~42 kDa protein rekombinan MSP-1_{42} *P. knowlesi* masing-masing (pkMSP-1_{33} dan pkMSP-1_{42}) telah diekspresikan dengan menggunakan sistem *Escherichia coli*. Protein yang ditulenkan telah diuji dengan serum pesakit malaria dan bukan pesakit malaria menggunakan asai Western Blot dan ELISA. Dalam asai Western Blot, pkMSP-1_{33} menunjukkan sensitiviti 98.3% dan spesifisiti 97.4% bagi mengesan antibodi malaria. Bagi ELISA, sensitiviti untuk pkMSP-1_{33} ialah 76.3% dan spesifisiti ialah 94.9%. pkMSP-1_{42} mempunyai sensitiviti 91.0% bagi mengesan malaria manusia dalam kedua-dua asai. Spesifisiti bagi pkMSP-1_{42} ialah 97.5% and 92.6% masing-masing bagi Western Blot dan ELISA. Sensitiviti dan spesifisiti yang tinggi bagi pkMSP-1_{33} dan pkMSP-1_{42} dalam imunoasai menunjukkan bahawa kedua-dua protein rekombinan ini berkemungkinan berguna dalam penyaringan sero-epidemiologi secara am.

Sensitiviti dan spesifisiti yang diperolehi untuk pkMSP-1_{42} dalam asai Western Blot dan ELISA adalah secara konsisten lebih tinggi (>90%) berbanding dengan pkMSP-1_{33} yang mempunyai sensitiviti yang lebih rendah bagi ELISA (<80%). Selain itu, MSP-1_{42} yang terdiri dari kawasan MSP-1_{33} dan MSP-1_{19} mempunyai sel T dan sel

B imunodominan epitop. Oleh itu, kajian ini bertujuan untuk menilai imunogenisiti pkMSP-1_{42} dengan menggunakan model tikus dan untuk mengenalpasti epitop berpotensi. Tikus yang diimunisasikan dengan pkMSP-1_{42} mempunyai tahap kenaikan sitokin interferon-gamma, interleukin-2, interleukin-4, dan interleukin-10 yang signifikan berbanding dengan tahap dalam tikus kawalan negatif. Lagipun titik akhir titer bagi kenaikan pkMSP-1_{42} antibodi adalah tinggi dengan taburan isotip IgG seperti berikut: IgG1 > IgG2b > IgG3 > IgG2a.

Epitop berpotensi bagi *P. knowlesi* pkMSP-1_{42} telah dikenalpasti menggunakan 'library' peptida sintetik dan pendekatan 'library' pameran faj. Dalam pendekatan ini pkMSP-1_{42} serum tikus yang telah diimunisasi digunakan untuk saringan bagi epitop berpotensi. Sembilan epitop berpotensi telah dikenalpasti menggunakan 'library' peptida sintetik dan 14 menggunakan 'library' pameran faj. Dua kawasan (residue 37-95 dan residue 240-289) telah dikenalpasti sebagai kawasan berpotensi epitop dominan. Dua peptida dari 'library' peptida, P10 (TAKDGMEYYNKMGELYKQ) dan P31 (RCLLGFKEVGGKCVPASI), telah dipilih dan dinilai menggunakan model tikus. P10 dan P31-serum tikus yang telah diimunisasikan bertindak balas dengan rekombinan *P. knowlesi* MSP-1_{42} dan taburan isotip IgG adalah IgG2b > IgG1 > IgG2a > IgG3. Antibodi yang meningkat naik terhadap P10 dan P31 dapat mengecam parasit peringkat darah *P. knowlesi*, menunjukkan bahawa kedua-dua peptida ini adalah imunogenik dan berkemungkinan ada persamaan terhadap epitop yang bertindak sebagai tapak pengikat bagi antibodi ke atas parasit. Lagipun, tahap interferon-gamma dan interleukin-2 adalah tinggi secara signifikan dalam tikus P31- yang telah diimunisasikan. Dengan penilaian seterusnya, P10 dan P31 berpotensi digunakan dalam pembangunan vaksin malaria dan agen terapeutik.

ACKNOWLEDGMENTS

After three years of learning, struggling and troubleshooting, finally this study is approaching the end of the journey. I would like to take this opportunity to express my sincere gratitude and appreciation to various people for their help and guidance throughout the study.

First of all, I would like to thank my supervisors, Prof. Dr. Fong Mun Yik and Assoc. Prof. Dr. Lau Yee Ling. Thank you for offering me this project and giving me so much of trust on my ability, with that, I built up confidence to work independently and gained valuable experience to troubleshoot the obstacles throughout the study. This study would not be successfully accomplished without their excellent supervision, guidance, inspirations, continuous support and advice.

Besides, I would also like to thank all the lecturers and staffs in Department of Parasitology, Faculty of Medicine, University of Malaya, for their assistance rendered to me during the study. Special thanks to Head of Department, Prof. Dr. Rohela Mahmud for her precious advice and support during my dilemma in the journey of study. And not forgetting to thank the staffs in PARASEAD for teaching me some techniques.

A special word of thanks goes to all of my labmates Meng Yee, Jeremy, Behram, Yit Han, Jonathan, Amirah, Jia Siang, Leong, Mira, Idzzan, Marzira, Pn. Ruhani and Dr. Atique. Thank you for always giving me a hand whenever I need help. Special thanks to Xiao Teng and Wenn Chyau for spending time to listen and discuss with me, and providing idea on solving obstacles and difficulties throughout the study.

Furthermore, I wish to dedicate this study to my beloved parents, family members and friends for their constant encouragement and support. Without you all, I wouldn't have gained enough strength and courage to overcome the depressions and frustrations and keep fighting till the end of the study.

Last but not least, I would like to convey my thanks to whoever participated in various ways to help me in accomplishing this mission.

The path for pursuing PhD. Degree is full of challenges. I cherish the laughter of success in experiments and tears of depression and failure throughout the journey, as these would all be valuable experiences and enlightenments for my directions in future. Thoughts to be shared with whomever that reads this thesis: Be patient, sometimes you have to go through the worst in order to get the best. Just embrace failure as part of success and get going. If you never try, you'll never know. Cheers.

TABLE OF CONTENTS

LIST OF FIGURES

LIST OF TABLES

LIST OF ABBREVIATIONS

%	Percent
℃	Degree Celcius
et al.	et alia (and others)
× g	Gravitational field (centrifuging)
pg	Picogramme
µg	Microgramme
mg	Miligramme
g	Gramme
µl	Microlitre
ml	Mililitre
µm	Micrometre
nm	Nanometre
µM	Micromolar
mM	Milimolar
M	Molar
N	Normality
min	Minute
mm^3	Cubic mililitre
rpm	Revolutions per minute
sp.	Species
v/v	Volume per volume
w/v	Weight per volume
V	Volt

LIST OF APPENDICES

LIST OF PUBLICATIONS

Cheong, F. W., Fong, M. Y., Lau, Y. L., & Mahmud, R. (2013a). Immunogenicity of bacterial-expressed recombinant *Plasmodium knowlesi* merozoite surface protein-142 (MSP-142). *Malaria Journal, 12*(1), 454.

Cheong, F. W., Lau, Y. L., Fong, M. Y., & Mahmud, R. (2013b). Evaluation of recombinant *Plasmodium knowlesi* Merozoite Surface Protein-133 for detection of human malaria. *The American Journal of Tropical Medicine and Hygiene, 88*(5), 835-840.

Publications which are not included in the thesis:

Fong, M. Y., Noordin, R., Lau, Y. L., Cheong, F. W., Yunus, M. H., & Idris, Z. M. (2013). Comparative analysis of ITS1 nucleotide sequence reveals distinct genetic difference between *Brugia malayi* from Northeast Borneo and Thailand. *Parasitology, 140*(1), 39-45.

Lau, Y. L., Fong, M. Y., Mahmud, R., Chang, P. Y., Palaeya, V., Cheong, F. W., Chin, L. C., Anthony, C. N., Al-Mekhlafi, A. M., & Chen, Y. (2011). Specific, sensitive and rapid detection of human *Plasmodium knowlesi* infection by loop-mediated isothermal amplification (LAMP) in blood samples. *Malaria Journal, 10*, 197.

Lau, Y. L., Lee, W. C., Tan, L. H., Kamarulzaman, A., Syed Omar, S. F., Fong, M. Y., Cheong, F. W., & Mahmud, R. (2013). Acute respiratory distress syndrome and acute renal failure from *Plasmodium ovale* infection with fatal outcome. *Malaria Journal, 12*, 389.

CHAPTER 1: INTRODUCTION

Malaria is one of the important infectious diseases which causes high global mortality and morbidity. *Plasmodium knowlesi* has recently been recognised as the fifth *Plasmodium* species that can cause malaria in humans (Singh *et al.*, 2004; Bronner *et al.*, 2009). *Plasmodium knowlesi* replicates every 24 hours, which is one of the most rapid replication rates among *Plasmodium* species. Hence, quoditian fever, hyperparasitaemia, life-threatening complications and death may occur if the patient remains untreated (Daneshvar *et al.*, 2009).

Merozoite surface protein 1 (MSP-1) is a high molecular mass glycoprotein expressed on the surface of *Plasmodium* merozoites. MSP-1 undergoes two proteolytic steps to produce several fragments. During the first processing, the MSP-1 precursor polypeptide is cleaved into four major fragments of ~83 ($MSP\text{-}1_{83}$), 30 ($MSP\text{-}1_{30}$), 38 ($MSP\text{-}1_{38}$), and 42 kDa ($MSP\text{-}1_{42}$) (Holder *et al.*, 1987). The secondary processing further cleaves the C-terminal $MSP\text{-}1_{42}$ into fragments $MSP\text{-}1_{33}$ and $MSP\text{-}1_{19}$. The soluble $MSP\text{-}1_{33}$ is shed from merozoite surface whereas the membrane-bound $MSP\text{-}1_{19}$ remains on the merozoite surface and is carried into the new erythrocyte (Blackman *et al.*, 1996).

$MSP\text{-}1_{42}$ is one of the leading candidates for blood-stage malaria vaccines as it is able to induce protective immune responses (Good, 2001; Quin & Langhorne, 2001; Richards & Beeson, 2009), and antibodies directed against $MSP\text{-}1_{42}$ and $MSP\text{-}1_{19}$ can interrupt merozoite invasion *in vitro* (Blackman *et al.*, 1990; Egan *et al.*, 1999) and delay the intracellular parasite development (Moss *et al.*, 2012). Protective immune response is found to be elicited against challenge of *Plasmodium* parasites in $MSP\text{-}1_{42}$ and $MSP\text{-}1_{19}$ immunization studies using animal models such as rodents, mice and primates (Chang *et al.*, 1996; Darko *et al.*, 2005; Dutta *et al.*, 2005; Singh *et al.*, 2006).

MSP-1_{19}-mediated protective responses are mainly antibody-dependent humoral immunity, while protective T cell responses are induced by epitopes on MSP-1_{33} instead of MSP-1_{19} (Udhayakumar *et al.*, 1995; Egan *et al.*, 1997; Stowers *et al.*, 2001). MSP-1_{33} regulates cell mediated responses, inducing effector T cells which in turn help in protective B cells response, cytokines production and antiparasitic activity regulation against *Plasmodium* in an antibody-independent manner (Wipasa *et al.*, 2002; Draper *et al.*, 2009). Hence, MSP-1_{42} which elicits both cell-mediated and humoral immune responses, is considered as a suitable candidate for malaria vaccine (Dutta *et al.*, 2001; Epp *et al.*, 2003).

B cell epitope is the region of an antigen which is recognised by B cells and antibodies. These epitopes could be further divided into two categories, linear and conformational epitopes, based on their structure and interaction with the antibody (Huang & Honda, 2006). Linear epitope consists of a continuous segment of amino acids along the polypeptide and interacts with the antibody based on its primary structure, while conformational epitope consists of discontinuous sections of amino acids and interacts with the antibody based on the tertiary structure of the antigen (Barlow *et al.*, 1986).

Epitope mapping is the process for epitope identification of T cell receptors or antibodies on their target antigens. Identification and characterization of these epitopes are useful in vaccine designs and development of immunodiagnostic assays (Gershoni *et al.*, 2007). One of the approaches for the identification of B cell epitopes is the use of overlapping synthetic peptide library scanning, in which the peptides in the library represent the entire sequence of the antigen. Potential B cell epitopes on an antigen can be recognised by characterizing the reactivity of antigen-raised antibodies to each of the peptide in the library. This method has been used by Villard *et al.* (2007) to identify the malaria vaccine candidates, by synthesising the synthetic peptides that represent the α-

helical coiled coil domains on erythrocytic stage parasites of *P. falciparum*. Other previous studies of epitope mapping on *Plasmodium* sp. antigen by using synthetic peptide libraries include epitope mapping of *P. falciparum* MSP-1_{42} (Udhayakumar *et al.*, 1995; Cowan *et al.*, 2011), *P. falciparum* MSP-1_{33} (Malhotra *et al.*, 2008), *P. vivax* Duffy binding protein (DBP) (Chootong *et al.*, 2010), *P. berghei* ookinete surface antigen (Spano *et al.*, 1996) and *P. chabaudi* MSP-1 (McKean *et al.*, 1993). However, for the synthetic peptides that are considerably short in length (lesser than 15 amino acid residues), the secondary structure formation is unlikely to occur, thus preclude the possibility of those peptides to identify conformational epitopes.

Phage display is another approach for epitope mapping. Each recombinant phage expresses and displays a unique peptide or protein on the surface of phage virion with the genetic information that encodes them resides on the inside (Smith, 1985). The phage which displays the targeted peptides or epitopes can be accessed through immunological methods such as immunoprecipitation by antigen-antibody binding, and can be concentrated by panning process (Parmley & Smith, 1988). Epitope mapping of *Plasmodium* sp. antigens by using pre-made random phage libraries or customised phage libraries has been conducted on *P. falciparum* apical membrane antigen-1 (AMA-1) (Coley *et al.*, 2001; Casey *et al.*, 2004; Harris *et al.*, 2005), erythrocyte binding antigen (EBA-175) (Ambroggio *et al.*, 2013), ring-infected erythrocyte surface antigen (RESA) (Adda *et al.*, 1999) and macrophage migration inhibitory factor (MIF) (Wang *et al.*, 2009).

Considerable amount of studies on MSP-1_{42} have been carried out on several *Plasmodium* sp. but not much is known about *P. knowlesi* MSP-1_{42}. Hence, this study aimed to evaluate the immunogenicity of *P. knowlesi* MSP-1_{42} and identify the potential B cell epitopes (including the *P. knowlesi* MSP-1_{33} region). The recombinant MSP-1_{33} and MSP-1_{42} of *P. knowlesi* (pkMSP-1_{33} and pkMSP-1_{42} respectively) were produced

and evaluated using ELISA and Western blot assays. Immunogenicity test of pkMSP-1_{42} was carried out using the mouse model. Cytokine levels in the pkMSP-1_{42}-immunized mice were determined and antibody responses to pkMSP-1_{42} were characterized. Identification of epitopes with pkMSP-1_{42}-immunized mice sera was done by using synthetic peptide library and pre-made random phage display library, and the potential epitopes were evaluated and characterized by using animal models.

OBJECTIVES

a) To clone, express and purify pkMSP-1_{33} and pkMSP-1_{42} using *Escherichia coli* bacterial expression system.
b) To evaluate the purified pkMSP-1_{33} and pkMSP-1_{42} with Western blot assays and ELISA using patient sera.
c) To evaluate the immunogenicity of recombinant pkMSP-1_{42} using mouse models.
d) To identify and characterize the potential epitopes on the MSP-1_{42} of *P. knowlesi* by using pkMSP-1_{42}-immunized mice sera with synthetic peptide library and phage display library.
e) To evaluate the identified potential epitopes using ELISA, immunoblots and animal models.

CHAPTER 2: LITERATURE REVIEW

2.1 General history of *Plasmodium* sp.

Plasmodium sp. is a sporozoan obligate intracellular parasite which lives in hepatocytes or erythrocytes. The number of species in the *Plasmodium* genus is large, which currently exceeds 250. Generally, the *Plasmodium* sp. undergoes sexual and asexual stage in its life cycle which requires both vertebrate and invertebrate hosts. Mosquito is the invertebrate host, while the vertebrate host consists of reptiles, birds and mammals. Therefore, *Plasmodium* sp. is able to be transmitted by mosquito biting to a large range of animals and human. *Plasmodium* sp. is placed in the Kingdom Chromalveolata, Superphylum Alveolata, Phylum Apicomplexa, Class Aconoidasida, Order Haemosporida, Family Plasmodiidae and Genus *Plasmodium* (Levine, 1988). More than 90 species of *Plasmodium* such as *P. weyoni*, *P. agamae* and *P. minasense* infect reptilian hosts, which include 3200 species of lizards and 29 species of snakes. These species belong to the subgenera Asiamoeba, Carinamoeba, Fallisia, Garnia, Lacertamoeba, Ophidiella, Paraplasmodium and Sauramoeba (Schall, 2000). Species of *Plasmodium* that infect birds such as *P. relictum, P. elongatum, P. juxtanucleare* have been classified into five subgenera i.e., Bennettinia, Giovannolaia, Haemamoeba, Huffia and Novyella (Wiersch *et al.*, 2005). Species which infect mammals other than primates are divided into the subgenus Vinckeia. *Plasmodium aegyptensis, P. bergei, P. chabaudi,* and *P. yoelli* are examples of *Plasmodium* that infect rodents (Abd-el-Aziz *et al.*, 1975). *Plasmodium* sp. that infect primates and human include *P. falciparum, P. vivax, P. ovale, P. malariae, P. knowlesi, P. brasilianum, P. cynomolgi, P. inui, P. rhodiani, P. schwetz, P. simiovale* and *P. simium* (Coatney *et al.*, 1966; Contacos *et al.*, 1970).

2.2 Malaria

The disease which is caused by *Plasmodium* is called malaria. Mortality and morbidity rate caused by malaria globally is very high. According to World Malaria Report (2013), a total of 103 countries or areas still suffer from malarial infection and approximately 207 million clinical cases resulted in 627000 deaths. About 2.5 billion people, approximately 40% of the world's populations, are at risk. Among malarial-infected people, about 90% of them live in sub-Saharan Africa, and more than 90% of the mortality cases occur in sub-Saharan Africa as well. Most of the deaths are in children under five years age. This makes malaria responsible for almost 50% of deaths of children under five years old in Africa. According to the Global Malaria Action Plan, funding for research, treatment and control of malaria has increased significantly over years and reached approximately US $1.97 billion in year 2013. The four *Plasmodium* sp. which cause malarial infections in human are *P. falciparum, P. vivax, P. malariae* and *P. ovale*. *Plasmodium falciparum* contributes the most to the mortality and morbidity due to its high rate of complications and malignancies (Perlmann & Troye-Blomberg, 2000). Recently, *P. knowlesi* has been recognised as the fifth species of *Plasmodium* that can infect human populations (Cox-Singh & Singh, 2008; White, 2008; Bronner *et al.*, 2009).

2.3 *Plasmodium knowlesi*

2.3.1 General history

Plasmodium knowlesi is a malaria parasite which is naturally found in long-tailed (*Macaca fascicularis*) and pig-tailed (*M. nemestrina*) macaques. However, it can be transmitted to human from macaques through vector mosquito by zoonotic transmission. *Plasmodium knowlesi* was first observed by

Franchiti in 1927. He noticed differences between *P. knowlesi* to *P. inui* and *P. cynomolgi* during blood examination of *Silenus cynomolgus* (*M. fascicularis)*. In year 1931, Campbell and Napier investigated the tendency of *P. knowlesi* to produce haemoglobinuria in *M. fascicularis* and rhesus macaque *M. mulatta*. They found that *P. knowlesi* could lead to serious lethal infection in *M. mulatta*, which is an accidental host. In 1932, Knowles and Das Gupta described blood forms of *P. knowlesi* for the first time and demonstrated that it could be transmitted to human. Sinton and Mulligan (1933) confirmed that the parasite which Knowles and Das Gupta described as a new species. They named the parasite as *P. knowlesi* in honor of Knowles. In the early 1930s, *P. knowlesi* was used in treating patients with neurosyphillis (van Rooyen & Pile, 1935). In 1957, *P. knowlesi* was suggested to be the fifth species of *Plasmodium* which could lead to endemic human malaria (Garnham *et al.*, 1957).

2.3.2 Life cycle

The life cycle of *P. knowlesi* involves two hosts. Sporozoites are inoculated by a malaria-infected female *Anopheles* mosquito (invertebrate host) into the vertebrate human host during blood meal. Sporozoites are transported by the circulatory system to the liver and then infect the hepatocytes. This exo-erythrocytic cycle (Figure 2.1a) requires approximately five days to reach maturity. The mature schizonts rupture and release active merozoites. Among the human malaria parasites, *P. vivax* and *P. ovale* can exist in human host as a dormant stage called hypnozoite. These hypnozoites can persist in the liver and cause relapse by invading the peripheral blood stream after a dormant period of several weeks, or even up to years. Until now, hypnozoites of *P. knowlesi* in the

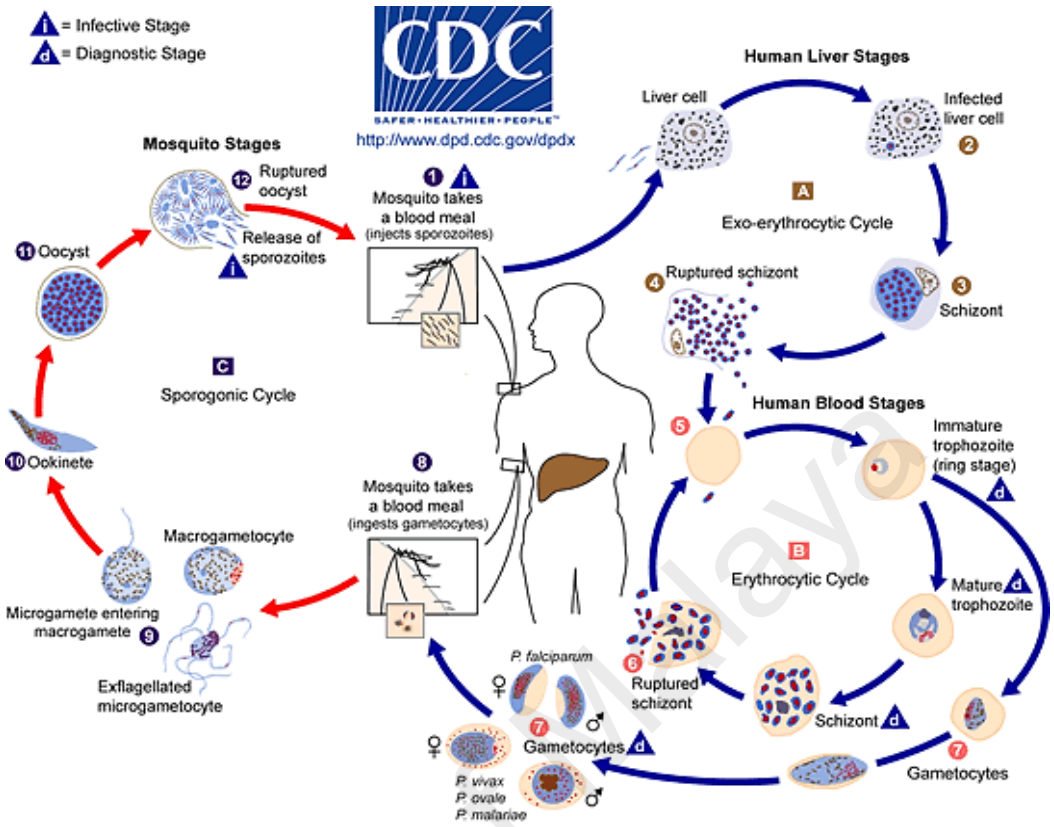

Figure 2.1. Sexual and axesual life cycle of *Plasmodium knowlesi* (adapted from Centre for Disease Control and Prevention, 2010). Life cycle of *P. knowlesi* consists of (a) exo-erythrocytic cycle, (b) erythrocytic cycle and (c) sporogonic cycle. (a) The sporozoites infect the hepatocytes of host and mature into schizonts. Mature schizonts rupture and release active merozoites which invade into blood stream. (b) The merozoites released from schizonts infect the erythrocytes, and develop into trophozoites, then into schizonts which consist of merozoites. Rupture of schizonts release merozoites and these merozoites infect new erythrocytes. (c) The microgametes and macrogametes form fertilised zygotes in the midgut of the mosquito. The zygotes mature into ookinetes and then develop into oocysts which contain sporozoites. The sporozoites invade the salivary gland of mosquito and the mosquito infects a new human host with inoculation of sporozoites.

liver has not yet been found. After the exo-erythrocytic cycle in liver, the parasites invade into blood stream after the hepatocytes rupture and undergo asexual multiplication. During this erythrocytic cycle (Figure 2.1b), the merozoites released from schizonts infect the erythrocytes. The ring stages of parasite then develop into trophozoites, and the mature trophozoites turn into schizonts which contain merozoites. Mature schizonts rupture and then release the invasive merozoites. These merozoites again infect new erythrocytes and the multiplication of blood stage parasites repeat every 24 hours, which is the shortest asexual life cycle among the known human and non-human primate malaria parasites (Chin *et al.*, 1968; Cox-Singh *et al.*, 2008). As an alternative to the asexual multiplication, some of the parasites differentiate into gametocytes. These sexual forms take longer time, which is approximately 48 hours to complete their development. The male (mircogametocytes) and female (macrogametocytes) gametocytes remain in the blood stream and ingested by female *Anopheles* mosquitoes during blood meal. These gametocytes then undergo sporogonic cycle (Figure 2.1c) in the mosquito. In the stomach of mosquito, an increase of carbon dioxide concentration and mosquito metabolites induce the maturation of microgametocytes and macrogametocytes into microgametes and macrogametes respectively. The flagellated microgametes penetrate the macrogametes and form fertilised zygotes. The zygotes mature into ookinetes which are motile and elongated. Ookinetes then invade into the midgut wall of the mosquito and develop into oocysts which contain sporozoites. Rupture of the mature oocysts release sporozoites and these sporozoites migrate to and invade the salivary gland of the mosquito. The mosquito then infects a new human host with inoculation of sporozoites during blood meal. This cycle repeats and perpetuates the malaria life cycle.

2.3.3 Epidemiology and prevalence

The natural hosts for *P. knowlesi* are the macaque species *M. fascicularis* and *M. nemestrina*. However, *P. knowlesi* is transmissible from macaques to humans through mosquito bites. In the early days, macaques which live in jungle did not have close association with humans. However, due to development and deforestation in South East Asian developing countries, the macaques which lost their habitats are forced to come close to human habitations in suburban and semi-urban areas. Furthermore, workers for deforestation, populations who live near to the forest fringe, and active participants of jungle activities have a higher risk to acquire knowlesi infection (Vythilingam *et al.*, 2008). The geographical distribution of knowlesi malarial infection is in South East Asian countries, which includes Borneo (Singh *et al.*, 2004), Myanmar (Jiang *et al.*, 2010), Thailand (Jongwutiwes *et al.*, 2004), the Philippines (Luchavez *et al.*, 2008), Singapore (Ng *et al.*, 2008), Vietnam (Cox-Singh, 2009; Van den Eede *et al.*, 2009) (Figure 2.2). It also occurs in malaria-free areas which are not subjected to control activities. Imported knowlesi malaria cases have been reported in Japan (Tanizaki *et al.*, 2013), Finland (Kantele *et al.*, 2008), Sweden (Bronner *et al.*, 2009), Germany (Orth *et al.*, 2013), and Spain (Ta *et al.*, 2010). All the patients in the imported case reports had previously travelled to forested areas of South East Asia countries, indicating that the knowlesi infections can be acquired from knowlesi malaria endemic areas. However, *P. knowlesi* is absent in Africa. The reason could be due to the absence of reservoir macaque of *P. knowlesi* in Africa. Besides, large populations of the West Africans lack of Duffy antigen, which serves as a binding target for *P. knowlesi* Duffy binding proteins during merozoites invasion into erythrocytes (Singh *et al.*, 2005). This thus inhibits the

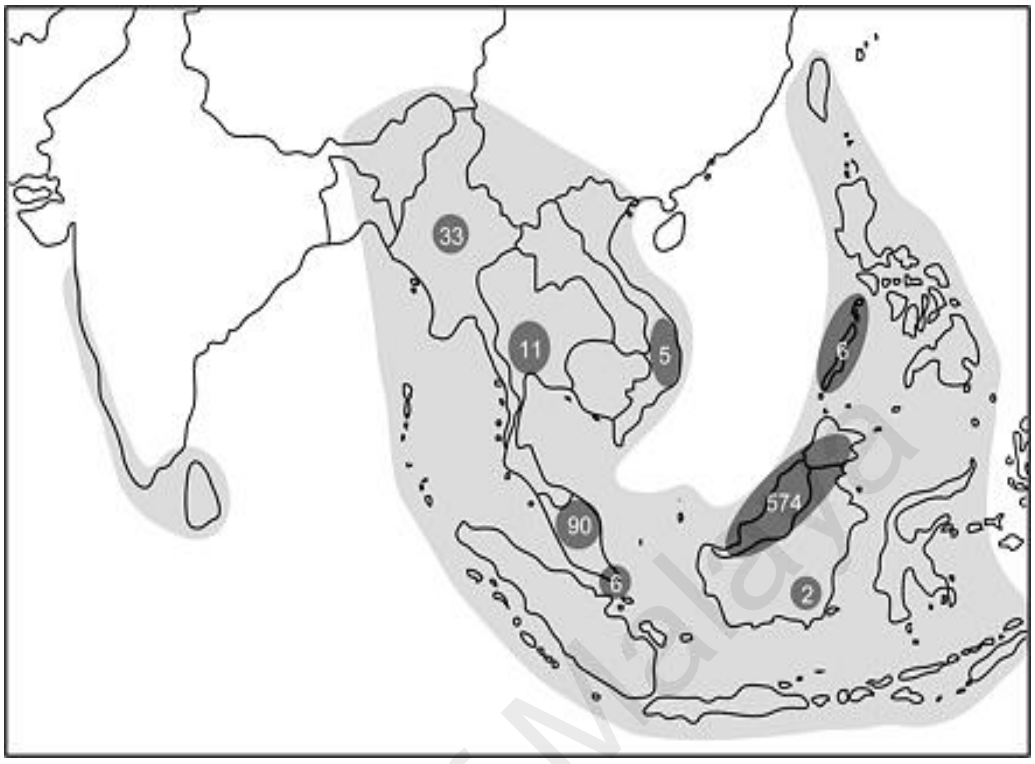

Figure 2.2. Geographical area of *Plasmodium knowlesi* infections reported in humans in South East Asia (adapted from Cox-Singh & Singh, 2008). The grey area indicates the geographical distribution of main vectors of *P. knowlesi*, *Anopheles leucosphyrus* group mosquitoes. The figures in dark grey areas indicate the reported number of knowlesi-infected patients, including both local citizens and travellers returning from that area.

invasion of parasites into the erythrocytes and interrupts the transmission of infection.

The first case of naturally acquired infection of *P. knowlesi* in humans was reported in 1965, in which an American man was infected by knowlesi malaria after working in the jungle in Pahang, Peninsular Malaysia (Chin *et al.*, 1965). According to the Ministry of Health Malaysia Annual Report, malaria cases in Malaysia have gradually decreased from 12,705 cases in year 2000 to 5,297 cases in year 2006 due to effective control activities. There were only 852 cases in Peninsular Malaysia in 2006 compared to 3918 cases in 2000. However, malaria cases have increased from 5456 cases in 2007 to 6650 cases in 2010. *Plasmodium knowlesi* contributes to the high percentage of the malaria incidences in Malaysia. For example, it contributed to one fifth of the malaria cases diagnosed in Kapit Division of Sarawak, Malaysian Borneo (Singh *et al.*, 2004). Besides, *P. knowlesi* is responsible as the most common cause of malaria in children age 15 years old and below in Kudat District of Sabah (Barber *et al.*, 2011). Recently, the infection has extended to most states of Peninsular Malaysia (Cox-Singh *et al.*, 2008; Yusof *et al.*, 2014).

2.3.4 Vectors and mode of transmissions

Four modes of transmission for *P. knowlesi* infection have been proposed, which include macaques to macaques, macaques to humans, human to human, and human back to macaques (Vythilingam *et al.*, 2008). The known mosquito vectors belong to the genus *Anopheles*, subgenus Cellia, series *Neomyzomyia* and group *Leucosphyrus* (Wharton *et al.*, 1962; Singh *et al.*, 2004). This group of mosquito is typically found in rainforest areas or forest fringes in South East Asia. After the discovery of *P. cynomolgi* as being able to be transmitted to

human via mosquito bites (Eyles *et al.*, 1960), numerous studies have been carried out in peninsular Malaysia in order to determine the species of malaria parasites in macaques, the vectors of monkey malaria, and the possibility of monkey malaria to be transmitted to human (Wharton & Eyles, 1961; Wharton *et al.*, 1962; Eyles *et al.*, 1963). A study that was conducted in the coastal area of Selangor proposed *Anopheles hackeri* (*An. hackeri*) as a natural vector of monkey malaria in peninsular Malaysia (Wharton & Eyles, 1961). However, although *An. hackeri* is capable of transmitting malaria to humans, it is not normally attracted to humans. Hence, *An. hackeri* is believed to be a vector of *P. knowlesi* in monkey populations, but unlikely to be a vector for transmission of *P. knowlesi* to humans (Reid & Weitz, 1961). On the other hand, *An. latens* which is attracted to both macaques and humans with the biting ratio of monkey to human 1:1.3 (Vythilingam *et al.*, 1995) has been incriminated as the main vector of *P. knowlesi* among humans and macaques in Sarawak, Malaysian Borneo (Vythilingam *et al.*, 2006; Tan *et al.*, 2008). Vythilingam *et al.* (2008) reported that *An. cracens* was the predominant species in areas where only *P. knowlesi* infections were reported. However, *An. cracens* has a biting ratio of monkey to human 1:5.6, showing that this species prefers to bite humans compared to monkeys. Hence the possibility for transmission of parasites from monkeys to humans is lower and this could be the reason for fewer *P. knowlesi* infection cases in Peninsular Malaysia compared to Sabah and Sarawak, Malaysian Borneo. Besides, a single bite from a *P. knowlesi*-infected mosquito is sufficient to inoculate the parasites to humans (Vythilingam *et al.*, 2008).

2.3.5 Pathogenesis

Symptoms of *P. knowlesi* infection in humans include headache, fever, chills, rigor, cough, vomiting, nausea, diarrhea and cold sweats (Singh *et al.*, 2004; Bronner *et al.*, 2009). Symptoms typically begin approximately 11 days after bitten by infected mosquitoes, and the parasites can be detected in blood stream approximately 10-12 days after infection (Bronner *et al.*, 2009). *Plasmodium knowlesi* causes non-relapsing malaria, as no hypnozoites could be detected in the exo-erythrocytic cycle (Krotoski & Collins, 1982). *Plasmodium knowlesi* completes its erythrocytic cycle every 24 hours and can lead to quotidian fever with fever spikes every day (Chin *et al.*, 1965). Patients of older age, female gender and pregnant women are more susceptible to severe knowlesi malaria infection (Daneshvar *et al.*, 2009). Comparison between severe knowlesi malaria and uncomplicated knowlesi malaria showed haemoglobin concentrations, platelet counts, sodium and albumin concentrations were significantly lower in the former. Leukocyte counts, prothrombin time, partial thromboplastin time, creatinine, potassium, lactate dehyrdogenase, total bilirubin level and amino transferase values were increased in severe malaria patients compared with uncomplicated malaria patients (William *et al.*, 2011). Other complications and manifestations seen in severe knowlesi malaria include acute renal failure, anemia, jaundice, shock and hyperbilirubinemia (Daneshvar *et al.*, 2009; Lee *et al.*, 2013). Thrombocytopenia is a consistent feature in *P. knowlesi* infection (Jongwutiwes *et al.*, 2004; Cox-Singh *et al.*, 2008; Bronner *et al.*, 2009; Cox-Singh *et al.*, 2010; Rajahram *et al.*, 2012; Lee *et al.*, 2013). Therefore, malaria tests should be carried out on patients who were thrombocytopenic. Besides, severe malaria patients may also suffer chest infiltrates and acute respiratory distress syndrome (ARDS) with hypoxemia. Ibiwoye *et al.* (1993)

demonstrated cerebral malaria in rhesus monkey *M. mulatta* by intravenous inoculation of a virulent strain of *P. knowlesi*. The macaques developed acute malaria and died after varying periods of illness. Cerebral vascular congestion was noted and parasite-packed microvessels were found in many areas. In fatal human knowlesi malaria, widespread microvascular parasite accumulation was found within the brain. Multiple petechial haemorrhages in the brain and endocardium are also found (William *et al.*, 2011). Life-threatening hyperparasitaemia and fatal complications such as multi-organ failure may occur (one in 10 patients) due to the rapid asexual replication cycle of *P. knowlesi* and delay in accurate diagnosis and treatment (Bronner *et al.*, 2009; Cox-Singh *et al.*, 2010; Rajahram *et al.*, 2012). Hence, rapid diagnosis and immediate effective treatment are crucial.

2.3.6 Morphology

Morphology of *P. knowlesi* blood stage parasites can be observed using microscopy examination of Giemsa- of Field-stained thick and thin blood films. The films have to be made before anti-malarial treatment in order to preserve the native morphologies of the parasites. All the *P. knowlesi* blood stage parasites which include early and late trophozoites, mature schizonts, free merozoites and gametocytes can be observed in the peripheral blood film. Detailed morphological features of *P. knowlesi* parasites are described by Lee *et al.* (2009b). *Plasmodium knowlesi* infections are not highly synchronous and few forms of blood stage parasites can be detected in a single peripheral blood film. Early trophozoites are characterized by a round dot of nuclear chromatin surrounded by a fine ring-like cytoplasm enclosing a vacuole. These ring form trophozoites are approximately one third to half (2.5-4 μm) the diameter of the

infected erythrocytes. Although single nuclear chromatin dot is the prominent ring form trophozoite, double chromatin dots and "headset" ring form can also be observed. Other rare forms of *P. knowlesi* early trophozoites include trophozoites with triple chromatin dots or appliqué form. Multiple infections especially double infections in a single erythrocyte occur frequently (Figure 2.3a). Late trophozoites have denser and thicker cytoplasm, with slightly amoeboid and irregular in shape. The size of the trophozoites is slightly increased to 3-5 µm. In some cases, the cytoplasm is stretched across the erythrocyte forming the 'band' form of trophozoite. Mature trophozoites are slightly larger (5-6 µm), have more solid cytoplasm and malarial pigments can be observed in the form of scattered fine dark brown grains or clumps of dense golden brown granules (Figure 2.3b). Stippling which resembled Schüffner's dots is not found in the erythrocytes. Only faint stippling that appears as light, irregular and sparse dots, referred to as "Sinton and Mullingan's stippling", has been observed in some of the infected erythrocytes with mature trophozoite and schizont stages (Fong *et al.*, 1971; Jongwutiwes *et al.*, 2004). Young schizonts consist of two to five divided nuclear chromatin masses and approximately two thirds of the infected erythrocytes, while mature schizonts consist of a maximum number of 16 merozoites and occupy nearly the whole infected erythrocytes. The merozoites are irregularly scattered or clustered in a grape-like form and fine stippling is found in most of the erythrocytes containing schizonts (Figure 2.3c). Young gametocytes are difficult to be distinguished from mature trophozoites. The macrogametocytes have bluish cytoplasm and pinkish chromatin distributed at the periphery of the parasites (Figure 2.3d), while the microgametocytes have pinkish-purple cytoplasm and darker large chromatin

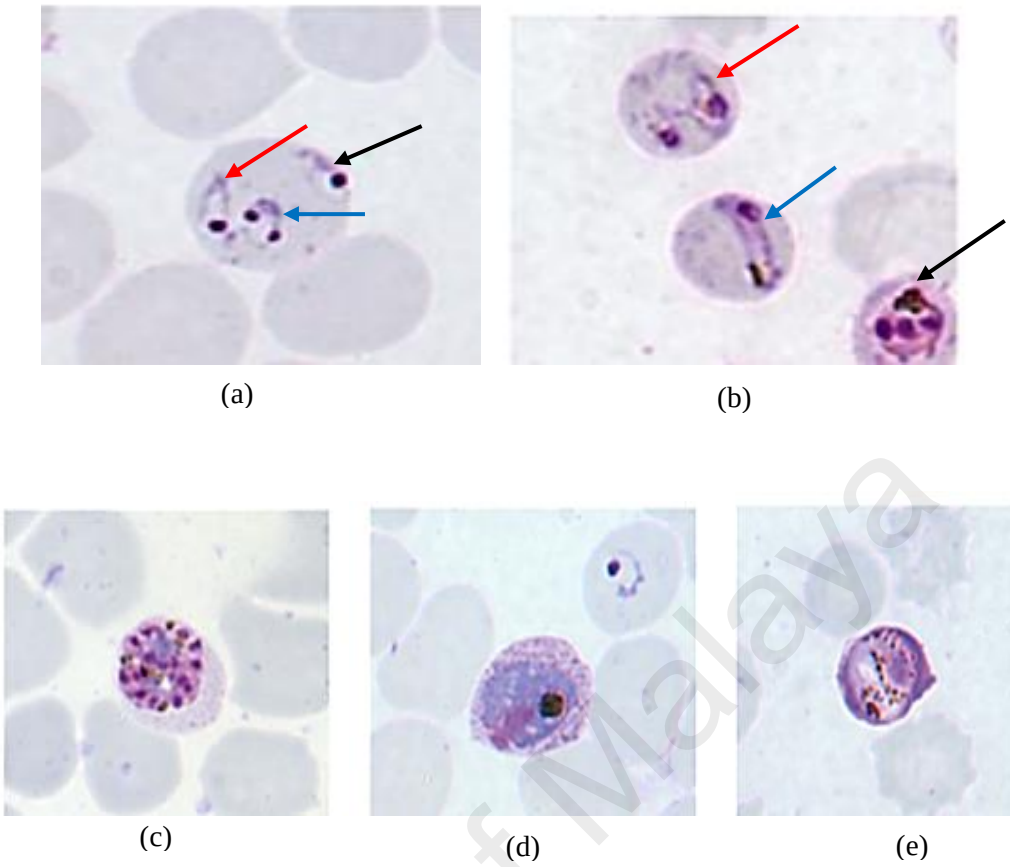

Figure 2.3. *Plasmodium knowlesi* blood stage parasites in human infection (modified from Lee *et al*, 2009b). (a) Early trophozoites with single chromatin dot (red arrow), double chromatin dots and fine ring-like cytoplasm (blue arrow), and appliqué form at the peripheral site of infected erythrocyte (black arrow). (b) Mature trophozoites with thicker and amoeboid-like cytoplasm (red arrow), 'band' form (blue arrow), and clumps of dense golden brown granules malaria pigments (black arrow). (c) Mature schizont with irregularly scattered merozoites. (d) Macrogametocyte with bluish cytoplasm and pinkish chromatin. (e) Microgametocyte with pinkish cytoplasm and darker chromatin mass.

mass which situated variably (Figure 2.3e). Unevenly distributed pigment grains are observed in both micro and macrogametocytes. Infected erythrocytes containing *P. knowlesi* blood stage parasites are generally not enlarged compared to uninfected erythrocytes.

2.3.7 Diagnosis

Malaria diagnosis relies on microscopy examination of Giemsa- of Field-stained thick and thin blood films. Microscopic examination of blood films is the gold standard diagnosis method for the four common human malaria parasites. Detection and identification of *Plasmodium* sp., determination of parasitaemia level, rational decisions and considerations for patient treatment and management can be done by examining the morphological characteristics of the parasites under microscope. However, *P. knowlesi* is easily misdiagnosed as *P. malariae* or *P. falciparum* infections under microscopy due to their morphology similarities. Early trophozoites of *P. knowlesi* appear as ring forms with occasional double chromatin dots, multiple infected erythrocytes and appliqué form in the infected erythrocyte, which morphologically resemble the early trophozoites of *P. falciparum* (Lee *et al.*, 2009b). Hence, if blood smear for human knowlesi infection is prepared when the infecting parasites are predominantly at the developmental ring form stage, it could be misdiagnosed as falciparum malaria. On the other hand, the late and mature trophozoites, schizonts and gametocytes of human knowlesi infections are generally indistinguishable from those of *P. malariae*. Elongated trophozoite stretching across the erythrocyte, called 'band' form trophozoite, is previously characterized as the unique morphology feature for *P. malariae* (Coatney *et al*., 1971). However, these 'band' form trophozoites are observed in knowlesi

infection (Figtree *et al.*, 2010; Lee *et al.*, 2013; Tanizaki *et al.*, 2013) and may lead to misdiagnosis as malariae infection. For instance, Singh *et al.* (2004) and Lee *et al.* (2009a) demonstrated that most of the microscopic-identified *P. malariae* infections in Sarawak, Malaysia, were actually *P. knowlesi* infections. There are some morphological differences between blood stage parasites of *P. knowlesi* and *P. malariae*. For example, a maximum of 16 merozoites can be detected in mature *P. knowlesi* schizonts, while only 12 in mature *P. malariae* schizonts. Besides, merozoites in mature *P. malariae* schizonts are typically arranged in a rosette pattern, which the merozoites are arranged in a symmetrical form surrounding clumps of malaria pigments in the centre, while this rosette form is not detected in *P. knowlesi*. However, the morphological differences in knowlesi infection and malariae infection are difficult to be detected and require experienced and well-trained personnel. Therefore, laboratory misdiagnosis of *P. knowlesi* as *P. malariae* by microscopy is highly unavoidable (Lee *et al.*, 2009b). Misdiagnosis of *P. knowlesi* malaria as *P. malariae* infection may lead to underestimation of the severity of infection. Delayed treatment and management may cause vital-organ dysfunction and other fatal complications. Another limitation of microscopic examination is difficulty in detecting the parasite in blood film when the parasitaemia level is low. False negative results may be reported. Rapid diagnostic tests (RDTs) such as BinaxNOW Malaria, OptiMAL Rapid Malaria, Animalaria^{TM} and Entebe Malaria Cassette are unable to detect *P. knowlesi* infection, or unable to distinguish *P. knowlesi* infection from other malarial infections due to cross-reactivity (McCutchan *et al.*, 2008; Kawai *et al.*, 2009; van Hellemond *et al.*, 2009). Both OptiMAL test and Entebe Malaria Cassette test are designed to detect a *Plasmodium* intracellular metabolic enzyme, *Plasmodium* lactate dehydrogenase (pLDH). Interestingly, when

knowlesi-infected blood samples are examined with these RDTs, OptiMAL test results have been interpreted as falciparum malaria-positive, while Entebe Malaria Cassette test results have been interpreted as vivax malaria-positive. Moreover, the sensitivity of both tests in detecting *P. knowlesi* parasite is similar to those for *P. falciparum* and higher than *P. vivax*. Thus, commercial RDTs based on detection of pLDH should be used with great caution, especially in diagnosis of suspected cases of knowlesi malaria. On the other hand, BinaxNOW malaria which is designed based on detection of *P. falciparum* histidine-rich protein 2 and pan-malarial aldolase, detect *P. knowlesi* as non-*P. falciparum* malaria (Lee *et al.*, 2013); whilst Tanizaki *et al.* (2013) indicated that BinaxNOW was unable to detect *P. knowlesi* and demonstrated malaria-negative result. Other methods for detection of knowlesi infections include PCR, loop-mediated isothermal amplification (LAMP) and real-time PCR assays. PCR diagnostic method is time-consuming, complicated, and requires the use of a high-precision thermal cycler which is too expensive for most endemic countries to be used for routine diagnosis (Singh *et al.*, 2004). Moreover, cross-reactivity has been observed between *P. vivax* and *P. knowlesi* in nested PCR for malaria targeting the *small subunit ribosomal RNA* (*SSU rRNA*) gene due to high sequence homology of this gene (Imwong *et al.*, 2009). Hence, development and improvement in malarial diagnostic methods is crucial in order to detect knowlesi infections accurately and efficiently.

2.3.8 Treatments

Early treatment for knowlesi infection is important as it can prevent complications and fatal outcomes. Majority of Malaysian patients who were naturally infected with *P. knowlesi* were primarily treated with chloroquine and

primaquine (Singh *et al.*, 2004; Daneshvar *et al.*, 2009; Daneshvar *et al.*, 2010). High efficiency has been observed and no recrudescences or re-infections have been detected after the patients were given oral chloroquine for three days, and oral primaquine (as gametocidal agent) for two consecutive days at 24 hours. Unlike falciparum malaria which is highly resistant to chloroquine, evidence of drug resistance has not been detected in knowlesi malaria. The chloroquine plus primaquine combination is inexpensive and highly effective for uncomplicated knowlesi malaria infections (Daneshvar *et al.*, 2009; Daneshvar *et al.*, 2010). Besides, artemether-lumefantrine, mefloquine, combination of atovaquone and proguanil have also been found to be effective for uncomplicated knowlesi malaria (Kantele & Jokiranta, 2011; William *et al.*, 2011). In cases of high parasitaemia and severely ill patients, intravenous quinine is given (Singh *et al.*, 2004; Cox-Singh *et al.*, 2008; Daneshvar *et al.*, 2009). However, quinine may lead to many adverse effects. In its therapeutic dose, quinine can cause cinchonism (quinism) or even death by pulmonary edema, and it is extremely toxic if overdose. Artesunate has been found to be well tolerated, no serious drug-related adverse effects and has lower mortality rate compared to quinine (Dondorp *et al.*, 2005; Dondorp *et al.*, 2010). Lee *et al.* (2013) reported that intravenous artesunate and oral doxycycline worked efficiently in a hyperparasitaemic knowlesi-infected patient by killing most of the parasites within one day after the course of treatment. Therefore, artesunate has been suggested as an alternative treatment for knowlesi malaria, especially for patients who cannot use quinine and primaquine due to glucose-6-phosphate dehydrogenase (G6PD) deficiency.

2.3.9 Control and prevention

Control and prevention of malaria involve three living beings: human (host), *Anopheles* mosquito (vector) and *Plasmodium* sp. (parasite) (Figure 2.4). People who live in malaria endemic areas should be educated to use protective measures against mosquito bites. Closure of doors and windows in the evening can prevent entry of nocturnal *Anopheles* mosquito into human dwellings. Avoiding contact with mosquito during dust-to-dawn hours is an important malaria control measure. Insecticide-impregnated materials (permethrin-containing products) such as bed nets and curtains have been used. Insecticide-treated bed nets could effectively reduce malaria morbidity and morbidity rate up to 60%. Health authorities in malaria endemic countries organise campaigns for distribution of free insecticide-treated bed nets to their citizens (Thwing *et al.*, 2008; Hightower *et al.*, 2010). However, due to the low awareness and compliance of the net owners, this strategy faces difficulties in implementation (Atieli *et al.*, 2011). For travelers and workers in jungle, clothes which cover most parts of body are worn and effective repellents cream, lotion, mats and coils are used. Chemoprophylaxis for prevention of malaria is taken one to two weeks before travel to jungle and malaria endemic areas. A wide range of medication is used for chemoprophylaxis under consultancy of medical doctors. These medications include atovaquone/proguanil (Malarone), chloroquine (Aralen) and hydroxychloroquine (Plaquenil), doxycycline, mefloquine, primaquine, and sulfadoxine-pyrimethamine (Fernando *et al.*, 2011). On the other hand, few strategies could be applied in mosquito vector control. Larvae of mosquitoes are controlled by using larvicide or biological control. Control of adult mosquitoes is done by killing them with effective insecticides especially in

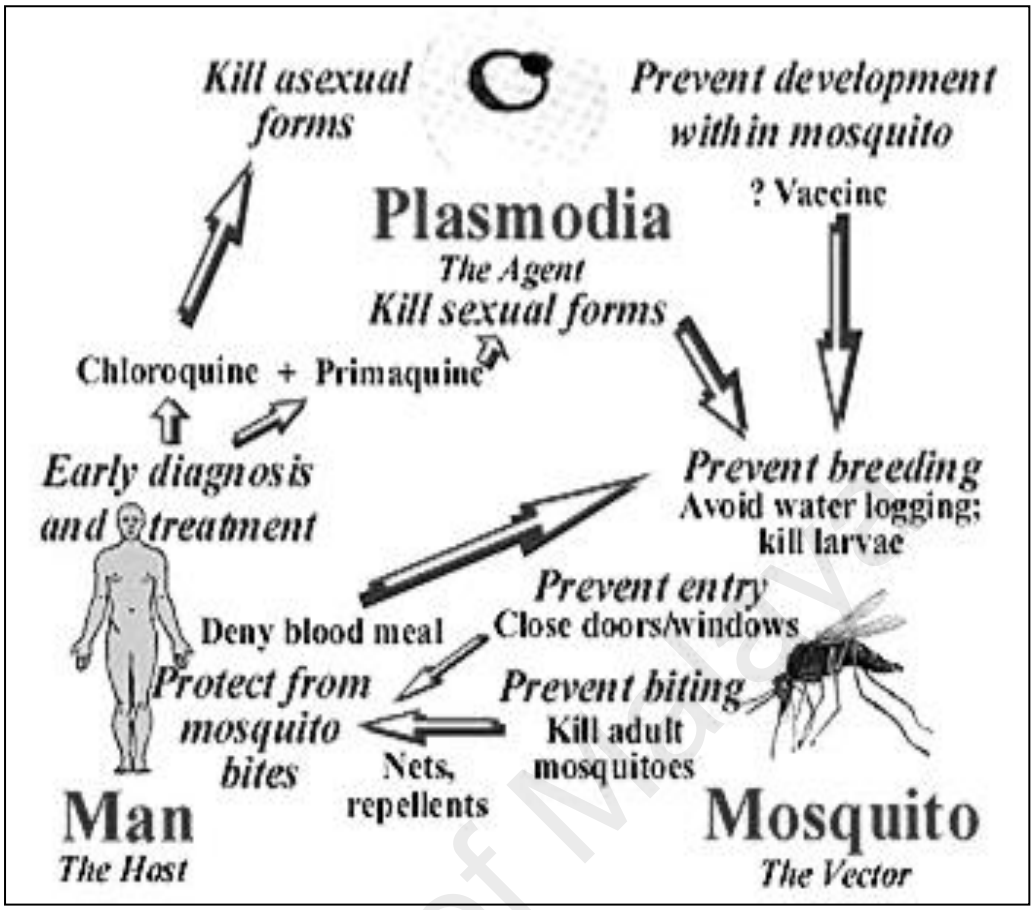

Figure 2.4. Chain map of control and prevention of malaria, which involves three parties: human, mosquito and *Plasmodium* sp. (adapted from Malaria Site, 2009). Summary of the control and prevention chain: use of personal protective measures and chemoprophylaxis, control of adult and larvae of mosquito by insecticides and larvicides, early diagnosis and effective treatments on infections, and vaccine developments and genetic modifications of vector mosquito.

indoor spraying. Besides, accurate diagnosis and effective treatment are also crucial steps for control of malaria. Compliance of treatment is important to achieve complete clearance of parasitaemia and to prevent further spreading of infection to other humans. Other efforts on elimination and eradication of malaria include development of vaccines, and also genetic modifications of mosquito vectors to prevent transmission of parasites from mosquitoes to humans.

2.4 Merozoite surface protein 1 (MSP-1) of *Plasmodium* sp.

The merozoite surface protein 1 (MSP-1) is a high molecular mass (~185 to 225kDa) glycoprotein which is fixed to the merozoite surface membrane via a glycosylphosphatidylinositol (GPI) anchor. This protein is found in all *Plasmodium* species (Holder & Freeman, 1982; McBride & Heidrich, 1987). It is divided into highly polymorphic (repetitive N-terminal block 2 region) and conserved regions (MSP-1_{19}) (Polley *et al.*, 2003). MSP-1 is essential for initial attachment of merozoites to the erythrocyte surface by forming a complex of co-ligands with MSP-9 (Goel *et al.*, 2003; Li *et al.*, 2004), maturation of merozoites, and invasion of merozoites into erythrocytes (Good, 2001). In order for the merozoites to enter into an erythrocyte, the MSP-1 undergoes two proteolytic processing by proteases. Proteolytic processing has been most extensively studied in *P. falciparum* MSP-1. The primary processing occurs during schizonts rupture, where merozoites are released from an infected erythrocyte. The *P. falciparum* MSP-1 precursor polypeptide is cleaved into four major fragments of ~83 (MSP-1_{83}), 30 (MSP-1_{30}), 38 (MSP-1_{38}), and 42 kDa (MSP-1_{42}). These fragments are held together by non-covalent contacts and form a multi-component protein complex. This protein complex is membrane-bound to

the merozoite surface via the C-terminal MSP-1_{42} fragment and remains on the merozoite surface (Holder & Freeman, 1982; Holder *et al.*, 1987; McBride & Heidrich, 1987). During invasion of merozoites into erythrocytes, the secondary processing, which is catalysed by a Ca^{2+}-activated serine protease, further cleaves *P. falciparum* MSP-1_{42} into two fragments with molecular masses of 33 (MSP-1_{33}) and 19 kDa (MSP-1_{19}) (Blackman & Holder, 1992). The MSP-1_{33}, corresponding to the N-terminal region of MSP-1_{42}, is shed from the merozoite surface with the rest of the complex, including the MSP-1_{38}, MSP-1_{30} and MSP-1_{83} in a fully soluble form (Blackman *et al.*, 1991b). The membrane-bound MSP-1_{19} remains anchored to the merozoite surface membrane by the GPI tail attached to the C-terminal residue and is carried into new erythrocyte (Blackman *et al.*, 1990; Blackman *et al.*, 1991a). Shedding of MSP-1_{33} is unlikely to occur prior to attachment of merozoites to the target erythrocytes. Hence, complete shedding of MSP-1_{33} from the merozoite surface serves as an indicator for successful invasion of merozoites into erythrocytes (Blackman *et al.*, 1991b; Blackman *et al.*, 1993). *Plasmodium knowlesi* MSP-1 undergoes proteolytic processing in a similar manner to *P. falciparum* MSP-1 (Blackman *et al.*, 1996) (Figure 2.5).

2.4.1 MSP-1_{42} and MSP-1_{19} of *Plasmodium* sp.

MSP-1 is one of the leading candidates for blood stage malaria vaccines. Among the MSP-1 proteolytic fragments, the MSP-1_{42} fragment is of particular interest due to certain reasons. Studies have shown that antibodies directed against MSP-1_{42} and MSP-1_{19} can interrupt merozoite invasion *in vitro* (Blackman *et al.*, 1990; Egan *et al.*, 1999; O'Donnell *et al.*, 2001). Furthermore, these antibodies could also inhibit the secondary proteolytic processing of

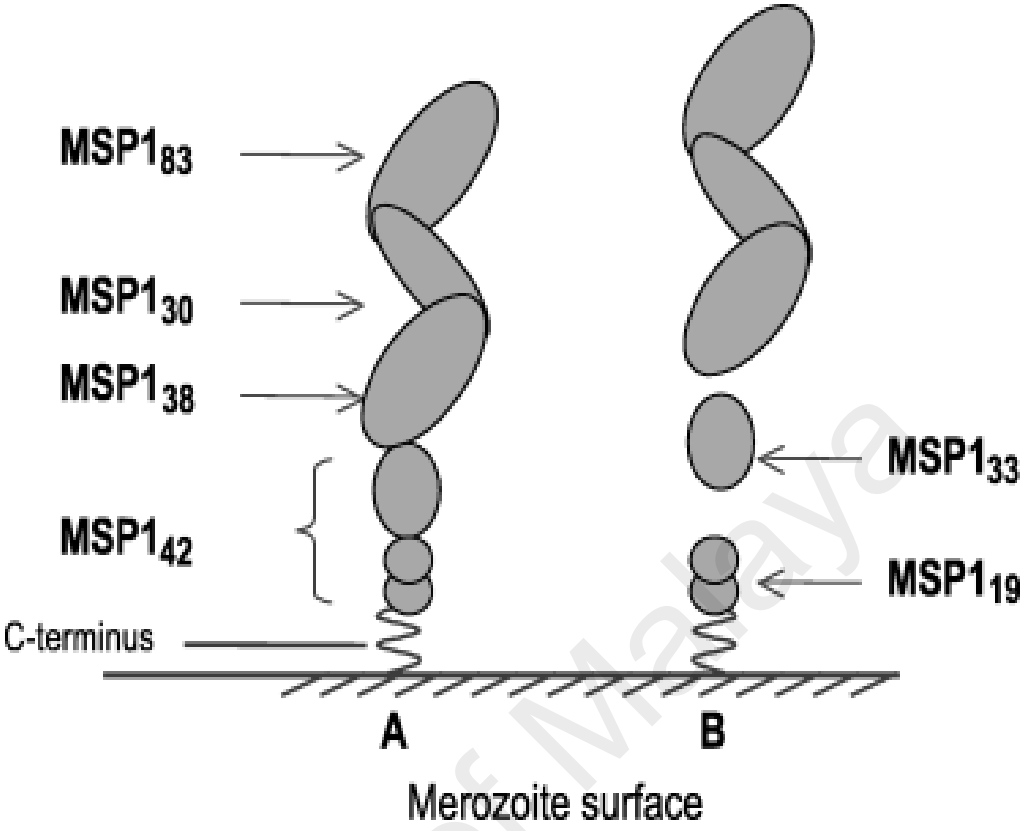

Figure 2.5. Primary and secondary processing of *Plasmodium knowlesi* MSP-1 on merozoite surface (adapted from Blackman *et al.*, 1996). (A) shows primary processing which MSP-1 precursor polypeptide is cleaved into four fragments MSP-1_{83}, MSP-1_{30}, MSP-1_{38}, and MSP-1_{42}. These fragments are held together and remain on the merozoite surface via C-terminal MSP-1_{42}. (B) shows secondary processing which MSP-1_{42} is further cleaved into MSP-1_{33} and MSP-1_{19}. Soluble MSP-1_{33} sheds from the merozoite surface whereas membrane-bound MSP-1_{19} remains on merozoite and is carried into new erythrocyte.

MSP-1 (Blackman *et al.*, 1994) and delay the intracellular parasite development (Moss *et al.*, 2012). Besides, anti-MSP-1_{19} antibodies have been shown to play an important role in protection from symptomatic disease. Children with naturally acquired immune response to *P. falciparum* developed antibodies to MSP-1_{19} are significantly associated with resistance towards malarial infection and clinical manifestations such as fever associated with high parasitaemia (Riley *et al.*, 1992), while pregnant women with anti-MSP-1_{19} antibodies are protected against placental infection and infection in infants (Branch *et al.*, 1998). Immunization using MSP-1_{42} and MSP-1_{19} in animal models such as rodents, mice and primates provided protective immune response against live *Plasmodium* parasites (Daly & Long, 1993; Ling *et al.*, 1994; Chang *et al.*, 1996; Renia *et al.*, 1997; Angov *et al.*, 2003; Darko *et al.*, 2005; Dutta *et al.*, 2005; Singh *et al.*, 2006; Kaushal *et al.*, 2007).

2.4.2 MSP-1_{33} of *Plasmodium* sp.

MSP-1_{19}-mediated protective responses are mainly responsible for humoral immunity. MSP-1_{19}-vaccinated mice have been shown to have high protection level with high titer of anti-MSP-1_{19} antibodies, predominantly IgG1 and IgG2b. However, the effector $CD4^+$ T cells induced by MSP-1_{19} failed to induce any level of protection or resistant to infection. These T cell epitopes might provide help to B cells for antibody response, but may not function as effector T cells for reducing parasitaemia level (Hirunpetcharat *et al.*, 1997; Tian *et al.*, 1998). Besides, low level of T cell responses to MSP-1_{19} is observed due to limited T cell epitopes on this fragment. Protective T cell responses, on the other hand, are induced by epitopes within the dimorphic regions of MSP-1_{33} instead of MSP-1_{42} (Udhayakumar *et al.*, 1995; Egan *et al.*, 1997; Stowers *et al.*,

2001). It has been shown that T cell epitopes on MSP-1_{33} could mediate cellular immune response and protection against the malarial parasites by inducing effector T cells which are capable of producing protective cytokines and controlling parasite growth in an antibody-independent manner (Wipasa *et al.*, 2002). Draper *et al.* (2009) observed that vaccine-induced $CD4^+$ T cells against MSP-1_{33} could assist in priming MSP-1_{19}-specific B cells in protective B cells responses, while $CD8^+$ T cells against MSP-1_{33} could mediate significant antiparasitic activity against *Plasmodium*. Sun *et al.* (2012) showed that inadequate T cell responses, particularly the memory T cell response, may lead to persistent blood stage malaria parasite infection. It is thus logical to include both MSP-1_{19} and MSP-1_{33} fragments in malaria vaccine design in order to elicit both humoral and cell mediated responses. Therefore, MSP-1_{42} which has both immunodominant B and T cell epitopes, is considered as a potential vaccine candidate (Dutta *et al.*, 2001; Epp *et al.*, 2003).

2.5 *Escherichia coli* as cloning and expression host

Escherichia coli has been widely used in the biotechnology industry and still the common choice of host for most gene cloning experiments. The advantage of bacterial host includes its genetic simplicity, with relatively small genome size compared to eukaryotes. *Escherichia coli* can easily undergo transduction and can be readily transformed with plasmids or other vectors with a very high successful rate. Besides, the preparation of competent cells of *E. coli* is easy and convenient. *Escherichia coli* expression system is probably the most popular expression system among all the present expression system due to its safety, simplicity, known genetic properties, established working protocol and rapid growth rate. The growth rate of *E. coli* is approximately one generation per

twenty minutes under typical growth conditions, which is few fold higher compared to mammalian cells, therefore enabling efficient yields in a short time. Large amount of proteins can be produced in an inexpensive way compared to other expression systems which use virus, yeast or mammalian cells as the growth medium for *E. coli* is cheap and easily prepared (Pan *et al.*, 1999; Epp *et al.*, 2003). Moreover, *E. coli* expression system can overcome unwanted and aberrant secondary structures in the expressed recombinant protein. The expressed protein does not undergo post-translational modifications such as glycosylation, methylation and multi-subunit formation (Terpe, 2006). This expression system has been extensively used in numerous studies for expression of *Plasmodium* proteins, which include *P. falciparum* MSP-1_{42} (Epp *et al.*, 2003; Singh *et al.*, 2003; Sachdeva *et al.*, 2006), *P. falciparum* pLDH (Bzik *et al.*, 1993), *P. falciparum* AMA-1 (Casey *et al.*, 2004), *P. vivax* MSP-1_{42} (Dutta *et al.*, 2001; Sachdeva *et al.*, 2004), *P. vivax* MSP-3α (Lima-Junior *et al.*, 2011), *P. vivax* thrombospondin related adhesive protein (Ogunbanwo *et al.*, 2006), *P. cynomolgi* MSP-1_{42} (Kaushal *et al.*, 2007), and *P. knowlesi* surface protein containing an altered thrombospondin repeat domain (Palaeya *et al.*, 2013).

2.6 Antigenic epitopes

Antigen is a substance that when introduced into the body, stimulates the production of antibody by the immune system. Antigenic epitope, which is also known as antigenic determinant, is the region of an antigen which is recognised and bound by antigen-specific membrane receptors on B cells, T cells or to secreted antibodies (Goldsby *et al.*, 2002). A paratope is a part of an antibody that recognises the epitope, which serves as antigen-binding site on the antibody. Large antigens can possess many different epitopes on the same molecule and

therefore stimulate the production of different antibodies with different paratopes. Epitopes are involved in specific interaction with the paratopes or T cell receptors. T cell epitopes, which are recognised by T cell receptors, are usually linear peptide. B cell epitopes, which are recognised by B cells and antibodies, can be in a range of small chemical compounds or large marcomolecules components such as lipids, glycans and proteins. Epitopes from marcomolecules, such as proteins, can be further divided into two categories: linear and discontinuous/conformational epitopes, based on their structure and interaction with paratopes (Huang & Honda, 2006) (Figure 2.6). Linear epitope is a segment composed of a continuous sequence of amino acids along the polymer chain and it interacts with the paratope based on its primary structure; whereas conformational epitope is constituted by discontinuous sections of the antigen's amino acid sequence and these amino acids are brought together by folding of the antigen into its native structure. Conformational epitope interacts with the paratope based on the three dimensional surface features and shape or tertiary structure of the antigen (Barlow *et al.*, 1986).

2.7 Epitope mapping

Epitope mapping is the process of identifying the binding sites (or epitopes) of T cell receptors or antibodies on their target antigens. Identification and characterization of these binding sites are useful in the development of new vaccines and diagnostic assays (Gershoni *et al.*, 2007). Several approaches have been used for epitope mapping. The gold standard approach for epitope mapping is X-ray co-crystallography. Interaction between antigen and antibody can be

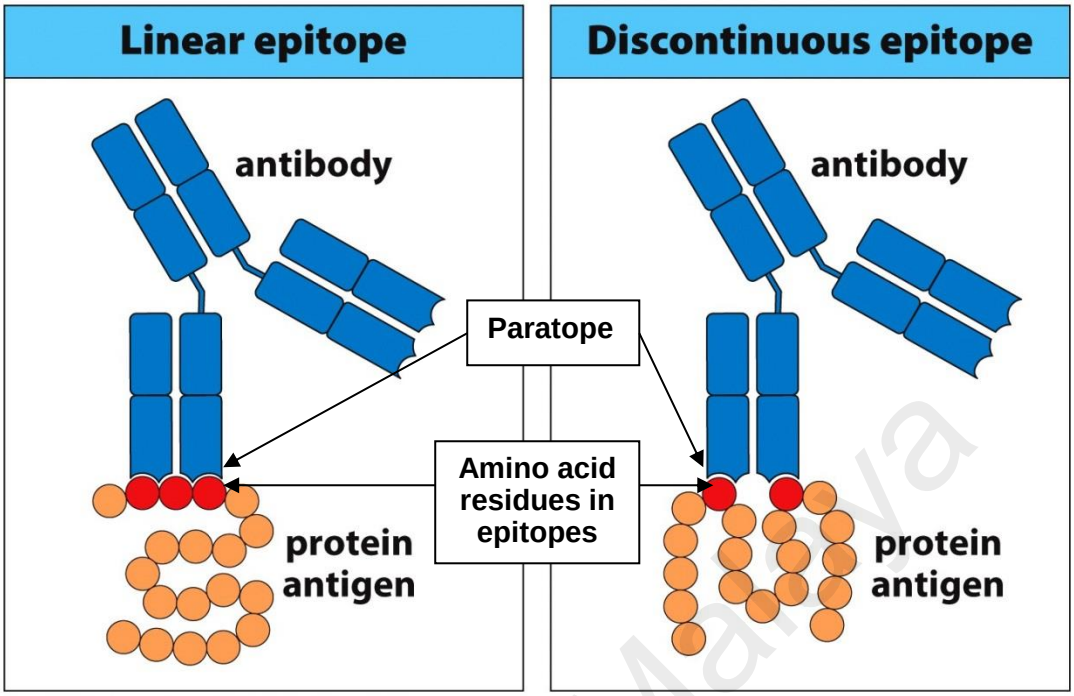

Figure 2.6. Linear and discontinuous/conformational epitopes (modified from Parham, 2009). Amino acid residues in linear epitope are adjacent in the polypeptide chain, while discontinuous/conformational epitope is created from amino acid residues located in different parts of the polypeptide chain and these amino acids are brought together by antigen folding.

directly visualised by analysing the crystals of antigen-antibody complexes, and the atomic resolution of the epitope could be provided. Guthridge *et al.* (2001) successfully identified a highly inhibitory monoclonal antibody that directly recognises the complement receptor type 2 (CR2)-B lymphocyte cell membrane C3d interface by using the X-ray crystallographic structure of CR2/CD21. This finding provides useful information for further study of *in vivo* roles of CR2 and allows the therapeutic targeting of this receptor. However, this method is not readily applicable to many antigens and antibodies as it requires large amount of purified proteins, time consuming, expensive, technically challenging and high degree of expertise is needed. Another approach used is site-directed mutagenesis. Systematic point mutations of amino acids are introduced into a protein sequence by substitution of a particular amino acid residue with another. Then, the effect of the amino acid change is assessed by measuring the binding strength of antibody to the sequence. Loss of binding strength due to point modification of an amino acid residue is considered as an indication of an epitope component. With this, amino acids that comprise an epitope can be identified. For instance, Kam-Morgan *et al.* (1993) functionally mapped a portion of monoclonal antibody HyHEL-10 epitope on hen egg white lysozyme (HEL) by introducing 20 single amino acid substitutions on four positions of HEL. Epitope prediction software by using protein sequence as input have been developed such as ADEPT (Maksyutov & Zagrebelnaya, 1993) and BEPITOPE (Odorico & Pellequer, 2003). These software are generally for prediction of hydrophilicity, surface accessibility, flexibility and propensity of the amino acids and are more suitable for prediction of linear epitopes (Hopp & Woods, 1981; Hopp, 1985). Several novel computational algorithms and software have been developed based on amino acid statistics, spatial information and X-ray

crystallography determined-surface accessibility such as DiscoTope (Haste Andersen *et al.*, 2006) and Mapitope (Bublil *et al.*, 2007). These novel algorithms are used to predict the residues in discontinuous B cell epitopes by using the protein 3D structures. Results have shown that the novel structure-based method can perform better for predicting residues of discontinuous epitopes than methods based solely on sequence information, and these algorithms are useful in guiding experimental epitope mapping especially in vaccine design and diagnostic assay development.

2.7.1 Epitope mapping using array-based synthetic peptide scanning

Array-based oligo-peptide scanning, also known as overlapping peptide scanning or pepscan analysis, is another approach in epitope mapping. A library of synthetic peptides (overlapping or non-overlapping segments) of a target protein is obtained and the ability of each peptide to bind to the antibody is evaluated in immunoassays (Figure 2.7). This method is rapid, simple and inexpensive. Discontinuous epitopes can also be mapped with high reliability and prevision by using synthetic peptide scanning (Cragg, 2011). Non-adjacent peptide sequences from the different parts of the target protein are combined and conformational rigidity is enforced onto this combined peptide. Gaseitsiwe *et al.* (2010) constructed a 15-mer peptide microarray derived from *Mycobacterium tuberculosis* proteins and the immunogenic *M. tuberculosis* epitopes that bind to major histocompatibility complex (MHC) class I or class II molecules were successfully identified. The immunogenic potential of these epitopes can be further characterized from least to most immunogenic based on their binding strength. Several studies on epitope mapping of *Plasmodium* antigens have

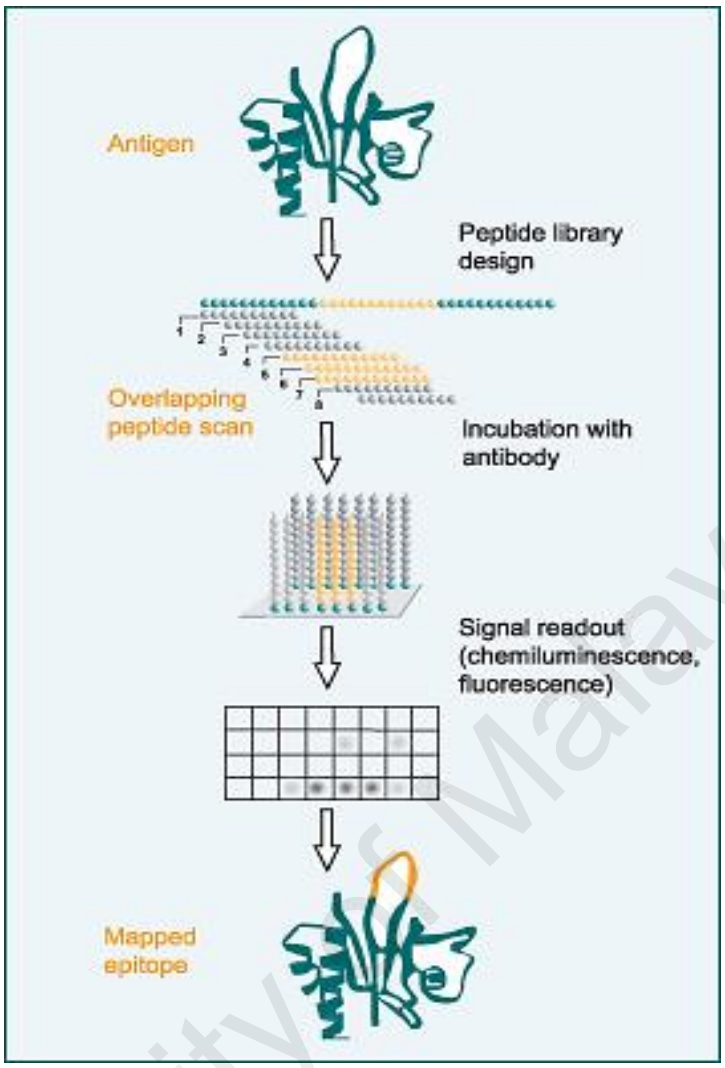

Figure 2.7. Overview of epitope mapping using peptide library (adapted from Creative Diagnostics, 2014). A library of overlapping peptides of a target antigen was synthesised. The ability of each peptide to bind to the antibody was evaluated in immunoassays such as ELISA by incubating the peptides with the antibody. The binding strength of the peptides with antibody was determined by signal readout including absorbance reading at particular wavelengths, chemiluminescence or fluorescence.

been carried out by using synthetic peptide libraries such as *P. chabaudi* MSP-1 (McKean *et al.*, 1993), *P. falciparum* MSP-1 (Herrera *et al.*, 1993), *P. falciparum* MSP-1_{42} (Udhayakumar *et al.*, 1995; Cowan *et al.*, 2011), *P. falciparum* MSP-1_{33} (Malhotra *et al.*, 2008), *P. falciparum* circumsporozoite protein (CSP) (Calvo-Calle *et al.*, 2006), *P. vivax* DBP (Xainli *et al.*, 2003; Chootong *et al.*, 2010) and *P. berghei* ookinete surface antigen (Spano *et al.*, 1996). These studies provide fundamental information for malaria vaccine designs and can be useful in studies of immune responses to *Plasmodium.*

2.7.2 Epitope mapping using phage display library

Phage display library is a collection of millions of recombinant phage, each expressing and displaying a different antigen-binding domain, peptide or protein variants on the surface of a phage virion, while the genetic material encoding each variant resides inside the phage. Phage display was developed by George P. Smith in 1985. He demonstrated that foreign DNA fragments can be inserted into filamentous phage genome to create a fusion protein that is incorporated into the virion. The peptide of interest was fused on to gene III of the filamentous phage and the peptide of interest was displayed on virion surface. The displayed foreign amino acids or peptide could be accessed through immunological methods such as antigen-antibody binding and immunoprecipitation. The phage can be pooled and concentrated up to 1000 fold over the ordinary unfused phage by affinity of the antibodies directed against the foreign peptide (Smith, 1985). The physical linkage which connects the variant protein sequence and the DNA encoding it enables large libraries of proteins to be screened, selected, amplified and purified through *in vitro* selection. Rapid partitioning based on binding affinity of some tagged molecules (such as

antibodies and enzymes) towards the target molecule or peptide (such as antigens) on the phage can be done by a process called panning (Parmley & Smith, 1988). The identity of the displayed peptide responsible for binding to the tagged molecules can be confirmed by direct sequencing analysis of the encoding insert in the genome of the recombinant phage (Wang & Yu, 2009) (Figure 2.8). Hence, phage display can be used for study of protein-protein, protein-peptide and protein-DNA interactions. This panning strategy can further allow the identification and characterization of the peptide of interest and protein-protein interaction by screening the fused phage against affinity baits (Hertveldt *et al.*, 2009). The phage display system can also be modified and designed into promising alternative expression vector compared to conventional expression systems due to the advantages of selection and affinity enrichment (Parmley & Smith, 1988). The most common and prominent surface display technology is M13-based bacteriophage surface display. Besides M13, other bacteriophages such as T4, T7 and λ phage have also been used (Castagnoli *et al.*, 2001). These alternative phage display systems can enable the display of the expression products on the viral coat which are unable to be displayed by M13 bacteriophage (Konthur & Crameri, 2003). Phage display technology can be used for epitope mapping (Coley *et al.*, 2001; Spillner *et al.*, 2003; Casey *et al.*, 2004), characterization of small molecule binders (Harris *et al.*, 2005), and identification of novel enzyme substrate (Sugimura *et al.*, 2006). For instance, construction and biopanning of *P. falciparum* phage display expression libraries against human purified erythrocyte binding proteins demonstrated a new approach to map unidentified interactions between the parasite and the human erythrocyte membrane (Lauterbach *et al.*, 2003). By screening a phage display peptide library on the surface of *P. falciparum*-infected red blood cells (iRBCs),

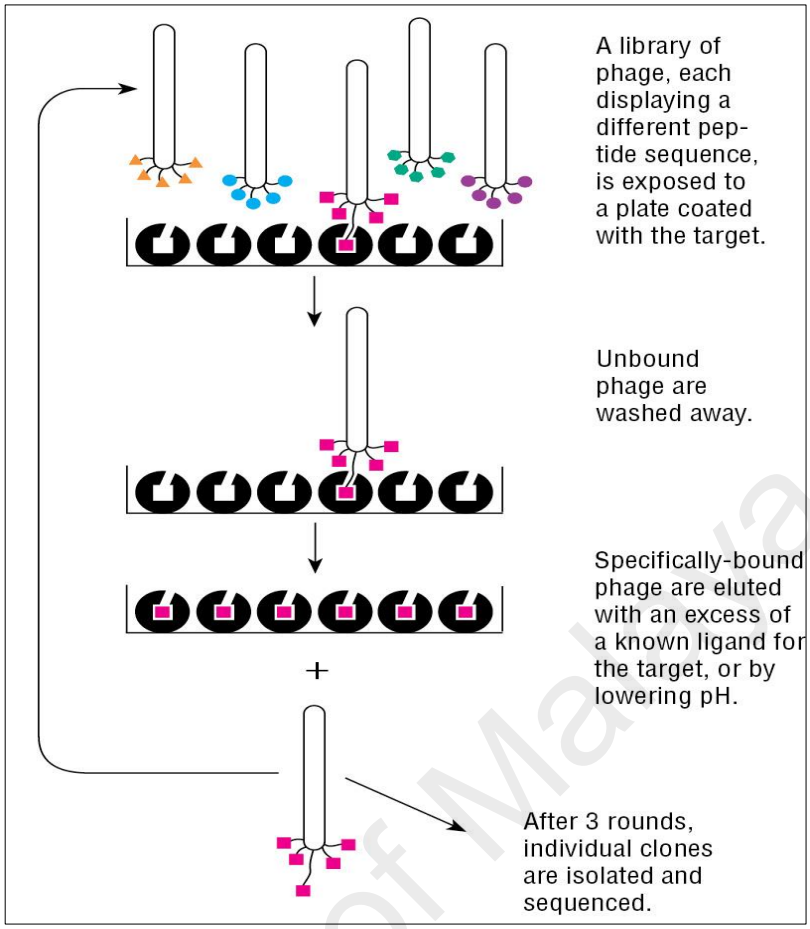

Figure 2.8. Overview of biopanning of phage display library (adapted from New England Biolabs, 2014). Phage display library, which each phage displaying a different peptide sequence, was incubated with the target. The unbound phage were washed away and the specifically-bound phage were eluted. After the final round of panning, individual clones of phage were isolated and sequenced.

Eda *et al.* (2004) successfully identified a small peptide that specifically recognised the altered surface of iRBCs. This peptide is a potential candidate for the development of anti-malarial agents that targets the surface of iRBCs. Phage display libraries have been used for epitope mapping of several *Plasmodium* proteins. By using pre-made random phage libraries or customised phage libraries, epitope map of *P. falciparum* AMA-1 (Coley *et al.*, 2001; Casey *et al.*, 2004; Harris *et al.*, 2005), EBA-175 (Ambroggio *et al.*, 2013), RESA (Adda *et al.*, 1999) and MIF (Wang *et al.*, 2009) was obtained. The identified epitopes can be further characterized for development of malaria vaccine and diagnostic assays.

CHAPTER 3: METHODOLOGY

3.1 Overview

Knowlesi malaria blood samples were collected from patients admitted to University Malaya Medical Centre (UMMC). *Plasmodium knowlesi* genomic DNA was extracted from blood sample using DNeasy® blood & tissue extraction kit (Qiagen, Hilden, Germany). Polymerase chain reaction (PCR) of the *P. knowlesi MSP-1$_{33}$* (*pkMSP-1$_{33}$*) and *MSP-1$_{42}$* (*pkMSP-1$_{42}$*) gene were performed by specific primers. The PCR products were purified with QIAquick® Gel Extraction Kit (Qiagen, Hilden, Germany) and cloned into pCR® 2.1-TOPO® vector using TOPO® TA cloning® kit (Invitrogen Corp., U.S.A.). Restriction enzymes *Sac*I (New England Biolabs, U.S.A.) and *Bam*HI (New England Biolabs, U.S.A.) were used to digest TOPO-*pkMSP-1$_{33}$* and TOPO-*pkMSP-1$_{42}$* plasmids respectively at 37℃ for 3 hours, and the digested target fragments were ligated with expression vector pRSET A (Invitrogen Corp., U.S.A.) at 4℃ overnight. Transformation into *E. coli* maintenance host TOP10F' strain was done with the resulting ligation mixtures for propagation and maintenance of the plasmids. Before expressions, the plasmids were transformed into *E. coli* expression host BL21 (DE3)pLysS strain. Suitable clones were selected from Luria-Bertani (LB) plates with antibiotics.

Expression of recombinant pkMSP-1$_{33}$ and pkMSP-1$_{42}$ was induced by isopropyl β-D-1-thiogalactopyranoside (IPTG) (Invitrogen Corp., U.S.A.). Expressed pkMSP-1$_{33}$ and pkMSP-1$_{42}$ were purified with ProBond™ purification system (Invitrogen Corp., U.S.A.). The purified pkMSP-1$_{33}$ and pkMSP-1$_{42}$ were dialysed, analysed and evaluated using sodium dodecylsulfate-polyacrylamide gel electrophoresis (SDS-PAGE), Western Blot assay and enzyme-linked immunosorbent assay (ELISA). The sensitivity and specificity of

purified pkMSP-1_{33} and pkMSP-1_{42} for detection of malarial infection in Western Blot assay and ELISA was evaluated by using human patient sera.

The immunogenicity of purified pkMSP-1_{42} was assessed using mouse model. Levels of cytokine interleukin-2 (IL-2), interleukin-4 (IL-4), interleukin-10 (IL-10) and interferon gamma (IFN-γ) in pkMSP-1_{42}-immunized mice were determined by using mouse cytokine ELISA kits (Thermo Scientific, U.S.A.). IgM/IgG level, IgG isotype distribution and end point titre of raised anti-pkMSP-1_{42} antibodies was determined. Anti-pkMSP-1_{42} antibodies were further confirmed by immunofluorescence assay (IFA) of thin blood smear from *P. knowlesi*-infected patient.

Epitope mapping of antibody responses to *P. knowlesi* MSP-1_{42} in pkMSP-1_{42}-immunized mice was done using synthetic peptide library. A peptide library with 18-mer peptides covered the entire *P. knowlesi* MSP-1_{42} protein sequence was synthesised by GenScript Inc., U.S.A. The peptide library which consists of 36 peptides was used to fine-scale map the antibody responses of pkMSP-1_{42}-immunized mice sera. Reactivity strength of pkMSP-1_{42}-immunized mice sera towards each peptide was evaluated and potential epitopes were identified. On the other hand, pkMSP-1_{42}-immunized sera were affinity-purified by using pkMSP-1_{42} as coating antigen in ELISA. Panning of phage towards the affinity-purified anti-pkMSP-1_{42} antibodies was carried out using Ph.D.™ dodecapeptide (Ph.D.-12) premade random phage display library (New England Biolabs, U.S.A.). Three rounds of panning were carried out. After final round of panning, ELISA was performed to screen several hundred individual phage clones for binding to anti-pkMSP-1_{42} antibodies. Phage clones with high binding affinity were chosen and the DNA of selected phage clones was extracted. The nucleotide sequences of each clone were confirmed by sequence analysis. The

DNA sequences in the region encoding the random dodecapeptide were assessed for homology to the primary sequence of *P. knowlesi* MSP-1_{42}. Epitopes identified using synthetic peptide library and phage display library were compared. These potential epitopes were characterized and evaluated in mouse model. Cytokine levels IL-2, IL-4, IL-10 and IFN-γ in peptide-immunized mice were determined (Thermo Scientific, U.S.A.) and the antibody responses were characterized.

3.2 Oligonucleotide primers

Oligonucleotide primers used in this study were synthesised by NHK Bioscience Sdn. Bhd., Malaysia. The stock concentration of all primers used in this project was 100 μM. The details for each primer were presented in Table 3.1.

3.3 Reagents and chemicals

All commonly used chemicals were of Analar grade or of the highest grade available from Amresco Inc., U.S.A.; Amersham Pharmacia Biotech Inc., Sweden; Difco, U.S.A.; Conda Pronadisa, Spain; Gibco BRL, Life Technologies Inc., U.S.A.; Invitrogen Corp., U.S.A; MBI Fermentas, U.S.A.; Promega Corp, U.S.A. and Sigma Chemical Co., U.S.A. These commonly used chemicals include methanol, acetic acid glacial, absolute ethanol, glycerol, glycine, tris, magnesium chloride, calcium chloride, hydrochloric acid, sulphuric acid, sodium hydroxide, sodium chloride, bacto agar powder, sodium bicarbonate, tryptone, yeast extract, acetone, sodium iodide, sodium phosphate dibasic, ammonium persulfate, SDS, tris-hydrochloride, urea, imidazole, sodium phosphate monobasic, dimethyl formamide, Tween-20, urea and guanidinine hydrochloride.

Table 3.1. List of oligonucleotide primers used

Purpose	Primer	Sequence (5' to 3')
PCR of *pkMSP-1*$_{33}$ gene	pkMSP-1$_{33}$_F	GAGCTCGAGAATCACGTGGCTGCATTCA
	pkMSP-1$_{33}$_R	GAGCTCCTACATCTGAGTTTGTACATTTAAC
PCR of *pkMSP-1*$_{42}$ gene	pkMSP-1$_{42}$_F	CGCGGATCCGAGAATCACGTGGCTGCATTCA
	pkMSP-1$_{42}$_R	CGCGGATCCCTAGCTGGAGGAGCTACAGAA
Selection of positive recombinant TOPO-*pkMSP-1*$_{33}$ and TOPO-*pkMSP-1*$_{42}$ clones	M13F	GTAAAACGACGGCCAG
	M13R	CAGGAAACAGCTATGAC
Selection of positive recombinant pRSET A-*pkMSP-1*$_{33}$ and pRSET A-*pkMSP-1*$_{42}$ clones	T7 terminator	CTAGTTATTGCTCAGCGGTGG

F, forward primer; R, reverse primer.

For *P. knowlesi* DNA extraction, DNeasy® blood & tissue kit was purchased from Qiagen, Hilden, Germany. For PCR, *i-Taq*™ DNA polymerase, 10X PCR buffer (with 20 mM $MgCl_2$) and deoxyribonucleotide triphosphates (dNTPs) were from iNtRON Biotechnology, Inc., Korea. For PCR product purification, QIAquick® gel extraction kit was purchased from Qiagen, Hilden, Germany. For agarose gel electrophoresis, Ethylenediaminetetraacetic acid (EDTA) was obtained from Sigma Chemical Co., U.S.A.; GeneRuler™ 100 bp ladder and 1 kb DNA ladder were from Thermo Scientific, U.S.A.; SYBR® safe DNA gel stain was from Invitrogen Corp., U.S.A.; Agarose powder was obtained from Promega Corp., U.S.A.; 6X DNA loading dye was provided together with the DNA ladder.

For cloning of PCR product, TOPO® TA cloning® kit was purchased from Invitrogen Corp., U.S.A. One Shot® Chemically Competent *E. coli* TOP10F' strain was provided together with the TOPO® TA cloning® kit. For growth and propagation of *E. coli* strains, LB broth and agar which are the growth media, were prepared by tryptone and yeast extract obtained from Conda Pronadisa, Spain; Antibiotics ampicillin and chloramphenicol were obtained from Bio Basic Inc., Canada. For digestion and ligation of targeted fragment into expression vector, T4 DNA ligase, restriction enzymes (RE) *Sac*I and *Bam*HI, and calf intestine alkaline phosphatase (CIAP) were obtained from New England Biolabs, U.S.A. For plasmid extraction, QIAprep® spin Miniprep kit was purchased from Qiagen, Hilden, Germany.

For protein expression, IPTG was purchased from Invitrogen Corp., U.S.A. For SDS-PAGE, acrylamide-bisacrylamide (30%) pre-mix solution, N, N, N', N'-tetramethylethylenediamine (TEMED), Coomassie Brilliant Blue powder were obtained from Bio-Rad Laboratories, U.S.A.; ammonium persulfate from

Amresco Inc., U.S.A.; PageRuler™ prestained protein ladder from Thermo Scientific, U.S.A.

For ELISA, bovine serum albumin (BSA) powder and phosphate-buffered-saline (PBS) tablets were purchased from Sigma Chemical Co., U.S.A.; Horseradish peroxidase (HRP)-labelled goat anti-human antibodies and HRP-labelled goat anti-mouse antibodies were purchased from Kirkegaard & Perry Laboratories, Inc. (KPL Inc.), U.S.A.; 3, 3', 5, 5'-tetramethylbenzidine (TMB) was purchased from Amresco Inc., U.S.A.

For Western Blot assay, polyvinylidene difluoride (PVDF) membrane was purchased from Bio-Rad Laboratories, U.S.A.; Biotin-labelled goat anti-human antibodies, biotin-labelled goat anti-mouse antibodies and streptavidin-alkaline phosphatase were purchased from KPL Inc., U.S.A.; Anti-Xpress™ antibody was from Invitrogen Corp., U.S.A.; 5-bromo-4-chloro-3-indolyl phosphate/nitro blue tetrazolium (BCIP/NBT) tablets were from Sigma Chemical Co., U.S.A.

For protein purification, ProBond™ purification kit was purchased from Invitrogen Corp., U.S.A.; Polypropylene column and nickel-NTA agarose resin were purchased from Qiagen, Hilden, Germany; Guanidinine hydrochloride was obtained from Sigma Chemical Co., U.S.A.; Urea was from Bio Basic Inc., Canada. For protein dialysis, SnakeSkin dialysis tubing, 10K MWCO, was purchased from Thermo Scientific, U.S.A. For protein quantification, Quick Start™ Bradford protein assay was purchased from Bio-Rad Laboratories, U.S.A.

For immunogenicity tests using mouse model, Complete Freund's Adjuvant (CFA), Incomplete Freund's Adjucant (IFA), Fluka® Trypan blue solution, fetal bovine serum (FBS) and Penicillin-Streptomycin were purchased

from Sigma Chemical Co., U.S.A.; Cell strainer with 70 µm nylon mesh was obtained from BD (Becton, Dickinson and Co., U.S.A.); Incomplete Gibco® Roswell Park Memorial Institute (RPMI) 1640 medium was purchased from Invitrogen Corp., U.S.A.; Mouse cytokine assays included mouse IL-2, IL-4, IL-10 and IFN-γ ELISA kit were purchased from Thermo Scientific, U.S.A.; Concanavalin A (ConA) was obtained from Merck KGaA, Germany. For IFA, fluorescein isothiocyanate (FITC)-labelled anti-mouse antibodies were purchased from Kirkegaard & Perry Laboratories, Inc., U.S.A.; 4', 6-diamidino-2-phenylindole (DAPI)/Antifade solution and Calbiochem® FluorSave™ reagent were obtained from Merck Millipore Corp., U.S.A.

For identification of potential epitopes by using pkMSP-1_{42}-immunized mice sera and synthetic peptide library, total of 36 peptides (18-mer each) were purchased from GenScript Inc., U.S.A.; Nunc MaxiSorp® flat-bottom 96 well plates were obtained from Thermo Scientific, U.S.A.

For panning of purified anti-MSP-1_{42} antibodies using phage display library, Ph.D.-12 premade random phage display library kit and HRP-labelled anti-M13 pIII monoclonal antibody were purchased from New England Biolabs, U.S.A.; 5-bromo-4-chloro-3-indolyl-β-D-galactopyranoside (X-gal) was purchased from Molekula Ltd., U.K.; Polyethylene glycol-8000 (PEG-8000) was purchased from Promega Corp., U.S.A.; -96 gIII sequencing primer and *E. coli* ER2738 host strain were provided in the phage library kit.

3.4 Stock solutions and buffers

3.4.1 Materials for agarose gel electrophoresis

50X Tris-Acetate-EDTA (TAE) electrophoresis buffer

Tris base		242	g
Acetic acid		57.1	ml
0.5 M EDTA		100	ml
ddH_2O	to	1000	ml

The solution was mixed well and stored at room temperature. The solution was diluted 50X with ddH_2O before used.

3.4.2 Materials for cloning of PCR product and recombinant protein expression

LB broth

Tryptone		10.0	g
Yeast extract		5.0	g
NaCl (ANALAR grade)		5.0	g
ddH_2O	to	1000	ml

The medium was sterilized by autoclaving at 121 ℃ for 15 min and stored at 4 ℃.

Ampicillin (100 mg/ml)

Ampicillin sodium powder, 1.0 g, was dissolved in 10 ml of ddH_2O. The solution was filter-sterilized using 0.22 μm filter, aliquoted and stored at -20°C.

Chloramphenicol (34 mg/ml)

Chloramphenicol, 0.34 g, was dissolved in 10 ml of absolute ethanol. The solution was filter-sterilized using 0.22 μm filter, aliquoted and stored at -20 ℃.

LB agar plates containing ampicillin (100 µg/ml)

Tryptone		10.0	g
Yeast extract		5.0	g
NaCl (analar grade)		5.0	g
Bacto-Agar		15.0	g
ddH_2O	to	1000	ml

The mixture was sterilized by autoclaving at 121 ℃ for 15 min. When the mixture was cooled to about 55^{o}C, ampicillin stock (100 mg/ml) was added to a final concentration of 100 µg/ml and approximately 20 ml of mixture was poured into each petri dish. Plates were stored at 4°C.

LB agar plates containing ampicillin (100 µg/ml) and chloramphenicol (34 µg/ml)

LB agar was prepared as mentioned above. The mixture was sterilized by autoclaving at 121 ℃ for 15 min. When the mixture was cooled to about 55^{o}C, ampicillin stock (100 mg/ml) and chloramphenicol stock (34 mg/ml) was added to a final concentration of 100 µg/ml and 34 µg/ml respectively. Approximately 20 ml of mixture was poured into each petri dish. Plates were stored at 4°C.

Isopropyl β-D-1-thiogalactopyranoside (IPTG) solution (100 mM)

IPTG, 0.238 g was dissolved in 10 ml of ddH_2O. The solution was filter-sterilized using 0.22 µm filter and stored at -20°C.

50% glycerol

Absolute glycerol, 25 ml was added to 25 ml of ddH_2O. The solution was filter-sterilized using 0.45 µm filter and stored at 4°C.

3.4.3 Solutions for Tris-Glycine SDS-PAGE

12% resolving gel solution

ddH_2O	1.6	ml
Acrylamide-bisacrylamide (30%)	2.0	ml
1.5 M Tris-HCl, pH 8.8	1.3	ml
10% SDS	50.0	µl
10% ammonium persulfate (APS)	50.0	µl
TEMED	2.0	µl

All the components were mixed thoroughly and poured immediately after the addition of TEMED.

5% stacking gel solution

ddH_2O	1.1	ml
Acrylamide-bisacrylamide (30%)	0.33	ml
0.5 M Tris-HCl, pH 6.8	0.5	ml
10% SDS	20.0	µl
10% APS	20.0	µl
TEMED	2.0	µl

All the components were mixed thoroughly and poured immediately after the addition of TEMED.

10X Tris-Glycine electrophoresis buffer (running buffer)

Tris base		30.3	g
Glycine		144.0	g
SDS		10.0	g
ddH_2O	to	1000	ml

The buffer was diluted 10X with ddH_2O before used.

2X sample buffer (SDS reducing buffer)

0.5M Tris-HCl, pH 6.8	4.0	ml
10% SDS	8.0	ml
Bromophenol blue	0.04	g
Glycerol	4.0	ml
β-mercaptoethanol	0.5	ml

β-mercaptoethanol was added to reduce disulfide bonds in protein samples. The solution was stored at 4 ℃.

Coomassie Brilliant Blue staining solution

Coomassie Brilliant Blue	1.25	g
Methanol	250	ml
Acetic acid	50	ml
ddH_2O to	500	ml

The solution was filtered with filter paper and stored at room temperature.

Destaining solution

Acetic acid	70	ml
Methanol	50	ml
ddH_2O to	1000	ml

3.4.4 Solutions for Western Blot assay

Blotting buffer (transfer buffer), pH 8.3

Tris base		3.03	g
Glycine		14.4	g
Methanol		200	ml
ddH_2O	to	1000	ml

5X Tris-borate-saline (TBS), pH 7.5

Trizma base		12.11	g
NaCl		48.85	g
ddH_2O	to	1000	ml

The buffer was diluted 5X with ddH_2O before used.

0.2% (v/v) TBS-Tween-20 (TBS-T) (washing buffer)

1X TBS		1000	ml
Tween-20		2	ml

5% (w/v) blocking buffer

Skimmed milk powder		0.5	g
1X TBS	to	10	ml

3.4.5 Solutions for ELISA

0.05 M sodium bicarbonate buffer (coating buffer), pH 9.6

Sodium bicarbonate, 0.21 g was dissolved in 50 ml of ddH_2O. The pH of the solution was adjusted to pH 9.6. The solution was stored at room temperature.

1% (w/v) BSA/PBS (blocking buffer)

BSA, 1 g was dissolved in 100 ml of 1X PBS. The solution was stored at 4°C.

0.1% (v/v) PBS-Tween-20 (PBS-T) (washing buffer)

1X PBS		1000	ml
Tween-20		1	ml

2 N sulphuric acid (stop solution)

Absolute sulphuric acid		49.04	ml
ddH_2O	to	500	ml

3.4.6 Buffers for recombinant protein purification and dialysis

10X stock solution A

Sodium phosphate, monobasic (NaH_2PO_4)		2.76	g
NaCl		29.29	g
ddH_2O	to	100	ml

The solution was mixed well and stored at room temperature.

10X stock solution B

Sodium phosphate, dibasic (Na_2HPO_4)		2.84	g
NaCl		29.29	g
ddH_2O	to	100	ml

The solution was mixed well and stored at room temperature.

5X native purification buffer

Sodium phosphate, monobasic (NaH_2PO_4)		7.0	g
NaCl		29.2	g
ddH_2O	to	200	ml

The buffer was mixed well and pH was adjusted to pH 8.0. Buffer was stored at room temperature and diluted 5X with ddH_2O before used.

1X native purification buffer, pH 8.0

5X native purification buffer, 20 ml was diluted with 80 ml of ddH_2O and pH was adjusted to pH 8.0.

3 M imidazole, pH 6.0

Imidazole		20.6	g
10X stock solution A		8.77	ml
10X stock solution B		1.23	ml
ddH_2O	to	100	ml

The solution was mixed well and pH was adjusted to pH 6.0. Buffer was stored at room temperature.

Guanidinium lysis buffer, pH 7.8

10X stock solution A		0.58	ml
10X stock solution B		9.42	ml
Guanidine hydrochloride		57.3	g
ddH_2O	to	100	ml

The pH of solution was adjusted to pH 7.8. The solution was filter-sterilized using 0.45 μm filter and stored at room temperature.

Denaturing binding buffer, pH 7.8

10X stock solution A		0.58	ml
10X stock solution B		9.42	ml
Urea		48.1	g
ddH_2O	to	100	ml

The solution was gently heated to 50-60 ℃ and stirred until completely dissolved. The pH was adjusted to pH 7.8. The solution was filter-sterilized using 0.45 µm filter and stored at room temperature.

Denaturing wash buffer, pH 6.0

10X stock solution A		7.38	ml
10X stock solution B		2.62	ml
Urea		48.1	g
ddH_2O	to	100	ml

The solution was gently heated to 50-60 ℃ and stirred until completely dissolved. The pH was adjusted to pH 6.0. The solution was filter-sterilized using 0.45 µm filter and stored at room temperature.

Native wash buffer, pH 8.0

1X native purification buffer	50	ml
3 M imidazole, pH 6.0	335	µl

The pH of solution was adjusted to pH 8.0 and stored at room temperature.

Native elution buffer, pH 8.0

1X native purification buffer	13.75	ml
3 M imidazole, pH 6.0	1.25	ml

The solution was mixed and pH was adjusted to pH 8.0 and stored at room temperature.

Dialysis buffer

1.0 M Tris-HCl, pH 8.0		10	ml
0.5 M EDTA		2	ml
ddH_2O	to	1000	ml

3.4.7 Materials for mice immunization

Complete RPMI 1640 medium

Penicillin-Streptomycin		10	ml
FBS		100	ml
Incomplete RPMI 1640 medium	to	1000	ml

FBS was heat-inactivated at 56 ℃ for 1 hour before used.

Ammonium-chloride-potassium (ACK) lysis buffer, pH 7.4

Ammonium chloride		4.14	g
Potassium bicarbonate		0.5	g
EDTA		0.037	g
ddH_2O	to	500	ml

The pH of the buffer was adjusted to pH 7.4 and filter-sterilized using 0.22 μm filter.

ConA (1 mg/ml)

ConA, 0.1 g was dissolved in 100 ml of complete RPMI 1640 medium. The solution was stored at -20 ℃.

3.4.8 Solutions for IFA

Acetone-methanol mixture (9:1, v/v) (fixative)

Methanol, 10 ml was added to 90 ml of acetone. The solution was stored at -20 ℃.

3% (w/v) BSA/PBS (blocking buffer)

BSA, 3 g was dissolved in 100 ml of 1X PBS. The solution was stored at 4°C.

3.4.9 Solutions for ELISA and panning using phage display library

Tetracycline (20 mg/ml)

Tetracycline, 0.2 g was dissolved in 5 ml of ddH_2O and 5 ml of absolute ethanol. The solution was filter-sterilized using 0.22 µm filter, aliquoted and stored at -20°C.

IPTG/ X-gal stock

IPTG, 1.25 g and X-gal, 1.0 g was dissolved in 25 ml dimethyl formamide. The solution was filter-sterilized using 0.22 µm filter, aliquoted and stored at -20°C.

LB agar plates containing tetracycline (20 µg/ml)

LB agar was prepared as mentioned above. The mixture was sterilized by autoclaving at 121 ℃ for 15 min. When the mixture was cooled to about 55^{o}C, tetracycline stock (20 mg/ml) and was added to a final concentration of 20 µg/ml. Approximately 20 ml of mixture was poured into each petri dish. Plates were stored at 4°C in the dark.

LB agar plates containing IPTG/X-gal

LB agar, 1000 ml was prepared as mentioned above. The mixture was sterilized by autoclaving at 121 ℃ for 15 min. When the mixture was cooled to about 55^{o}C, IPTG/X-gal stock, 1 ml was added. Approximately 10 ml of mixture was poured into each petri dish. Plates were stored at 4°C in the dark.

TOP Agar

Tryptone		10.0	g
Yeast extract		5.0	g
NaCl		5.0	g
Bacto-Agar		7.0	g
ddH_2O	to	1000	ml

The mixture was sterilized by autoclaving at 121 ℃ for 15 min. The mixture was dispensed into 25 ml aliquots, stored solid at room temperature. The agar was melted in microwave as needed.

1% (w/v) BSA/TBS (blocking buffer)

BSA, 1 g was dissolved in 100 ml of 1X TBS. The solution was stored at 4°C.

0.1% (v/v) TBS-T (washing buffer)

1X TBS	1000	ml
Tween-20	1	ml

0.5% (v/v) TBS-T (washing buffer)

1X TBS	1000	ml
Tween-20	5	ml

20% (w/v) PEG/ 2.5 M NaCl

PEG-8000		40	g
NaCl		29.2	g
ddH_2O	to	200	ml

The solution was sterilized by autoclaving at 121 ℃ for 15 min. The solution was mixed well to combine separated layers while still warm and stored at room temperature.

Iodide buffer

Sodium iodide		59.96	g
1.0 M Tris-HCl, pH 8.0		1.0	ml
0.1 M EDTA		1.0	ml
ddH_2O	to	100	ml

The solution was stored at room temperature in the dark.

0.2 M Glycine-HCl in 1 mg/ml BSA (elution buffer), pH 2.2

Glycine		0.75	g
BSA		0.05	g
1X TBS	to	50	ml

The pH of the solution was adjusted to pH 2.2 using 1 M HCl. The solution was filter-sterilized using 0.22 μm filter and stored at 4°C.

1 M Tris-HCl (neutralising buffer), pH 9.1

Tris, 6.06 g was dissolved in 50 ml ddH_2O. The pH of the solution was adjusted to pH 9.1 using HCl or NaOH. The solution was filter-sterilized using 0.22 μm filter and stored at 4°C.

0.1 M sodium bicarbonate buffer (coating buffer), pH 8.6

Sodium bicarbonate, 0.42 g was dissolved in 50 ml of ddH_2O. The pH of the solution was adjusted to pH 8.6. The solution was stored at room temperature.

3.5 Blood samples and sera collection

Use of human samples in this study was approved by University of Malaya Medical Centre Medical Ethics Committee (MEC Ref. No: 817.18) (Appendix 1). Malaria blood samples were collected from patients who were admitted to University Malaya Medical Centre (UMMC), Kuala Lumpur, Malaysia from July 2008 to December 2012. Patient samples infected with malaria were confirmed by microscopic examination, nested PCR based on *Plasmodium SSU rRNA* genes (Singh *et al.*, 1999; Singh *et al.*, 2004) (Appendix 2) and BinaxNOW® malaria rapid diagnostic test (Alere Inc., U.K.) (Appendix 3). Non-malarial parasitic infections were confirmed by commercial ELISA tests. Patient sera were categorized as follow: (A) *P. knowlesi* human malaria (B) non-knowlesi human malaria (*P. falciparum, P. vivax, P. ovale*) (C) non-malarial parasitic infection (filariasis, amoebiasis, cysticercosis, toxoplasmosis, toxocarasis) and (D) healthy donor.

3.6 Extraction of *P. knowlesi* DNA

Plasmodium knowlesi DNA was extracted from knowlesi-infected patient blood using commercialised DNeasy® blood & tissue kit (Qiagen, Hilden, Germany) with the protocol provided. Proteinase K, 20 µl, was pipetted into a 1.5 ml microcentrifuge tube. Patient blood, 100 µl and 1X PBS, 100 µl were added into the tube. Buffer AL, 200 µl was added. The sample was mixed by vortexing, and incubated at 56℃ for 10 min. Absolute ethanol, 200 µl was added to the

sample and mixed thoroughly by vortexing to yield a homogeneous solution. The mixture was pipetted into the DNeasy Mini spin column placed in a 2 ml collection tube (provided in the kit). The mixture was centrifuged at 8000 rpm for 1 min. The flow-through and collection tube were discarded and the DNeasy Mini spin column was placed in a new 2 ml collection tube. Buffer AW1, 500 µl was added and the mixture was centrifuged at 8000 rpm for 1 min. The flow-through and collection tube were discarded and the DNeasy Mini spin column was placed in a new 2 ml collection tube. Buffer AW2, 500 µl was added and the mixture was centrifuged at 14000 rpm for 3 min to dry the DNeasy membrane. The flow-through and collection tube were discarded. The DNeasy Mini spin column was placed in a clean 1.5 ml microcentrifuge tube. Buffer AE, 100 µl was pipetted directly onto the DNeasy membrane and incubated at room temperature for 1 min, and then centrifuged at 8000 rpm for 1 min for elution of DNA.

3.7 PCR of *pkMSP-1$_{33}$* and *pkMSP-1$_{42}$* genes

The PCR for amplification of *pkMSP-1$_{33}$* and *pkMSP-1$_{42}$* genes was carried out using the following reagents:

ddH_2O	15.3	µl
10X PCR buffer (20 mM $MgCl_2$)	2.5	µl
10 mM dNTPs(2.5 mM each)	2.0	µl
pkMSP-1_{33}_F /pkMSP-1_{42}_F primer (10 µM)	0.5	µl
pkMSP-1_{33}_R/ pkMSP-1_{42}_R primer (10 µM)	0.5	µl
i-Taq^{TM} DNA polymerase (5 U/ µl)	0.2	µl
DNA template/ddH_2O*	4.0	µl
Total volume	25.0	µl

* *P. knowlesi* DNA template was added into the sample reaction PCR tube, while ddH_2O was added into the negative control PCR tube.

For *pkMSP-1*$_{33}$, PCR amplification was initiated with initial denaturing step at 95 ℃ for 4 min (step 1), followed by 35 cycles of denaturation at 95 ℃ for 30 seconds, annealing at 55 ℃ for 30 seconds, and elongation at 72 ℃ for 40 seconds (step 2). A final elongation step at 72 ℃ for 10 min (step 3) was added to the last cycle and the reaction was hold at 4 ℃ (step 4).

PCR conditions of *pkMSP-1*$_{42}$ were identical to PCR conditions of *pkMSP-1*$_{33}$, except the elongation time at 72 ℃ in step 2 was 1 min 15 seconds.

3.8 Agarose gel electrophoresis

3.8.1 Preparation of agarose gel

Agarose gel, 1.5% was used for electrophoresis. Electrophoresis-grade agarose powder, 0.38 g was dissolved in 25 ml of 1X TAE buffer. Agarose was melted in microwave oven. Melted gel was cooled to 50 ℃ under running tap water. SYBR® safe DNA gel stain, 1 µl was added to the cooled gel and the gel was poured onto a casting tray and gel comb was inserted. The gel was allowed to harden.

3.8.2 PCR products loading and gel electrophoresis

The harden gel was placed in the electrophoresis tank and gel comb was removed. Sufficient 1X TAE was added into the tank until the gel was completely been covered by buffer. Generuler™ 1kb DNA ladder was loaded into one of the well for PCR product size estimation. PCR products were loaded into wells and electrophoresis was run at 100 V for 25 min. Gel was visualized

using Molecular Imager® Gel Doc™ XR+ system (Bio-Rad Laboratories, U.S.A.).

3.9 Cloning of PCR products into pCR® 2.1-TOPO® vector

3.9.1 Purification of PCR products

PCR products were purified using commercialised QIAquick® gel extraction kit (Qiagen, Hilden, Germany) with the protocol provided. Agarose gel electrophoresis was performed on PCR products using 0.8% agarose gel. The target fragments with the expected size were excised from gel and put into 1.5 ml microcentrifuge tubes. The gel slices were weighed and three volume of Buffer QG was added to one volume of gel (100 mg ~ 100 µl). The mixtures were incubated at 50 ℃ for 10 min until the gel slices were completely dissolved. The tubes were vortexed every 2-3 min to help the dissolving of gels. The samples were pipetted into the QIAquick spin columns placed in 2 ml collection tubes (provided in the kit). The samples were centrifuged at 13000 rpm for 1 min. The flow-through was discarded and the QIAquick columns were placed back into the same collection tubes. Buffer QG, 500 µl was added and the mixtures were centrifuged at 13000 rpm for 1 min. The flow-through was discarded and the QIAquick columns were placed back into the same collection tubes. Buffer PE, 750 µl was added and the mixtures were centrifuged at 13000 rpm for 1 min for washing purpose. The flow-through was discarded and the QIAquick columns were placed back into the same collection tubes. The columns were centrifuged once more at 13000 rpm for 1 min in the same collection tubes to remove residual wash buffer. The QIAquick spin columns were placed in clean 1.5 ml microcentrifuge tubes. Buffer EB, 30 µl was pipetted to the centre of the QIAquick spin columns and incubated at room

temperature for 1 min, and then centrifuged at 13000 rpm for 1 min for elution of DNA.

3.9.2 Ligation of PCR products into pCR® 2.1-TOPO® vector

The purified PCR amplified fragments were cloned into pCR® 2.1-TOPO® vector using commercialised TOPO® TA cloning® kit (Invitrogen Corp., U.S.A.). The ligation mixtures were carried out using the following reagents:

Salt solution	1.0	µl
pCR® 2.1-TOPO® vector	1.0	µl
purified PCR products	4.0	µl
Total volume	6.0	µl

The ligation reactions were mixed gently and incubated at room temperature for 5 min.

3.9.3 Transformation into competent *E. coli* TOP10F' cells

Ligation mixtures, 5 µl were added to vials of One Shot® Chemically Competent *E. coli* TOP10F' strain (provided in the kit) and mixed gently. The mixtures were incubated on ice for 30 min. The cells were heat-shocked at 42 ℃ for 30 seconds without shaking. The tubes were immediately transferred to ice. S.O.C. medium (provided in the kit), 250 µl was added. The tubes were shaked with 250 rpm at 37 ℃ for 1 hour. Transformation products, 50 µl were spread on pre-warmed LB plates containing 100 µg/ml ampicillin and incubated overnight at 37 ℃.

3.9.4 Colony PCR for selection of positive recombinant clones

Colony PCR for selection of positive recombinant clones was carried out using the following reagents:

ddH_2O	19.3	µl
10X PCR buffer (20 mM $MgCl_2$)	2.5	µl
10 mM dNTPs(2.5 mM each)	2.0	µl
M13 forward primer (10 µM)	0.5	µl
M13 reverse primer (10 µM)	0.5	µl
i-Taq^{TM} DNA polymerase (5 U/ µl)	0.2	µl
Total volume	25.0	µl

Colonies on the transformation plates were picked by using tips and dipped into the sample reaction PCR tubes, while no colony was chosen for negative control tube.

For colony PCR of *pkMSP-1*$_{33}$, PCR amplification was initiated with initial denaturing step at 95 ℃ for 4 min (step 1), followed by 35 cycles of denaturation at 95 ℃ for 30 seconds, annealing at 50 ℃ for 30 seconds, and elongation at 72 ℃ for 1 min (step 2). A final elongation step at 72 ℃ for 10 min (step 3) was added to the last cycle and the reaction was hold at 4 ℃ (step 4).

Colony PCR conditions of *pkMSP-1*$_{42}$ were identical to colony PCR conditions of *pkMSP-1*$_{33}$, except the elongation time at 72 ℃ in step 2 was 1 min 30 seconds.

Positive recombinant TOPO-*pkMSP-1*$_{33}$ and TOPO-*pkMSP-1*$_{42}$ clones were selected for plasmids extraction.

3.10 Plasmids extraction of positive recombinant clones

Plasmids of the selected positive recombinant clones were extracted using commercialised QIAprep® spin Miniprep kit (Qiagen, Hilden, Germany) with the protocol provided. Selected clones were grew overnight in 5 ml of LB broth containing 100 µg/ml ampicillin at 37℃ with shaking speed 250 rpm. Cultures were centrifuged at 5000 rpm for 10 min. The supernatants were discarded and the pelleted bacterial cells were resuspended in 250 µl Buffer P1 and transferred into 1.5 ml microcentrifuge tubes. Buffer P2, 250 µl was added and mixed thoroughly by inverting the tubes 4-6 times until the solutions became viscous. Buffer N3, 350 µl was added and mixed immediately and thoroughly by inverting the tube 4-6 times until the solutions became cloudy. The samples were centrifuged at 13000 rpm for 10 min. The supernatants were pipetted into QIAprep spin columns placed in 2 ml collection tubes (provided in the kit). The samples were centrifuged at 13000 rpm for 1 min. The flow-through was discarded and the QIAprep columns were placed back into the same collection tubes. Buffer PB, 500 µl was added and the mixtures were centrifuged at 13000 rpm for 1 min. The flow-through was discarded and the QIAprep columns were placed back into the same collection tubes. Buffer PE, 750 µl was added and the mixtures were centrifuged at 13000 rpm for 1 min for washing purpose. The flow-through was discarded and the QIAprep columns were placed back into the same collection tubes. The columns were centrifuged once more at 13000 rpm for 1 min in the same collection tubes to remove residual wash buffer. The QIAprep spin columns were placed in clean 1.5 ml microcentrifuge tubes. Buffer EB, 50 µl was pipetted to the centre of the QIAprep spin columns and incubated at room temperature for 1 min, and then centrifuged at 13000 rpm for 1 min for elution of plasmid DNA.

3.11 Cloning of target fragments into pRSET A vector

3.11.1 Digestion of TOPO-*pkMSP-1*$_{33}$ and TOPO-*pkMSP-1*$_{42}$ plasmids with RE

RE *Sac*I and *Bam*HI were used to digest the extracted TOPO-*pkMSP-1*$_{33}$ and TOPO-*pkMSP-1*$_{42}$ plasmids respectively, using the following reagents:

Plasmid DNA	34.0	µl
RE *Sac*I/*Bam*HI	2.0	µl
10X RE buffer	4.0	µl
Total volume	40.0	µl

The digestion mixture was incubated at 37 ℃ for 3 hours.

3.11.2 Digestion and dephosphorylation of expression vector pRSET A

For *pkMSP-1*$_{33}$, pRSET A plasmid was digested with RE *Sac*I. For *pkMSP-1*$_{42}$, RE *Bam*HI was used to digest the pRSET A plasmid. Digestion of pRSET A plasmids was carried out as mentioned in section 3.11.1. These digested pRSET A were dephosphorylated by CIAP to prevent plasmid self-ligation. Dephosphorylation was carried out with the following reagents:

Digested pRSET A plasmid DNA	38.0	µl
10X CIAP buffer	4.5	µl
CIAP	0.5	µl
ddH_2O	2.0	µl
Total volume	45.0	µl

The mixtures were incubated at 37 ℃ for 30 min. Then, the reactions were terminated by incubation at 85 ℃ for 15 min.

3.11.3 Purification of digested target fragments and pRSET A plasmids

Agarose gel electrophoresis was performed on digested recombinant TOPO-*pkMSP-1*$_{33}$, TOPO-*pkMSP-1*$_{42}$ and pRSET A plasmids using 0.8% agarose gel. The digested target fragments *pkMSP-1*$_{33}$, *pkMSP-1*$_{42}$ and pRSET A with expected size were excised from gel and purified using QIAquick® gel extraction kit as mentioned in section 3.9.1.

3.11.4 Ligation of purified target fragments into pRSET A vector

Ligation of purified target fragments *pkMSP-1*$_{33}$ into pRSET A vector was carried out with the following reagents:

*Sac*I-digested pRSET A vector	2.0	µl
*Sac*I-digested *pkMSP-1*$_{33}$	6.0	µl
T4 ligase	1.0	µl
10X ligation buffer	1.0	µl
Total volume	10.0	µl

Ligation of *pkMSP-1*$_{42}$ into pRSET A vector was done with following reagents:

*Bam*HI-digested pRSET A vector	2.0	µl
*Bam*HI-digested *pkMSP-1*$_{42}$	6.0	µl
T4 ligase	1.0	µl
10X ligation buffer	1.0	µl
Total volume	10.0	µl

Both of the ligation mixtures were incubated at 4 ℃ overnight.

3.11.5 Transformation into propagation and maintenance host *E. coli* TOP10F' cells

Ligation mixtures, 10 µl were added to vials of 100 µl chemically competent *E. coli* TOP10F' strain and mixed gently. The mixtures were incubated on ice for 30 min. The cells were heat-shocked at 42 ℃ for 45 seconds without shaking. The tubes were immediately transferred to ice. LB broth, 1 ml was added. The tubes were shaked with 250 rpm at 37 ℃ for 1 hour. The tubes were centrifuged at 10000 rpm for 1 min. The supernatants were discarded and the pelleted bacterial cells were resuspend in 200 µl LB broth. Transformation products, 100 µl were spread on pre-warmed LB plates containing 100 µg/ml ampicillin and incubated overnight at 37 ℃.

3.11.6 Directional PCR for selection of positive recombinant clones

Directional PCR was performed to select positive recombinant clones with sense orientation of cloned fragment. PCR was carried out using the same protocol as mentioned in section 3.9.4, by using pkMSP-1_{33} forward primer and T7 terminator primer for *pkMSP-1_{33}*, while pkMSP-1_{42} forward primer and T7 terminator primer for *pkMSP-1_{42}*.

3.11.7 Plasmids extraction of positive recombinant clones

Plasmids of the selected positive recombinant clones were extracted from *E. coli* TOP10F' cells using commercialised QIAprep® spin Miniprep kit as mentioned in section 3.10.

3.11.8 Transformation into expression host *E. coli* BL21 (DE3)pLysS cells

Extracted recombinant plasmids, 1 µl was added to vials of 100 µl chemically competent *E. coli* BL21 (DE3)pLysS strain and mixed gently. Transformation was carried out as mentioned in section 3.11.5. Transformation products, 100 µl were spread on pre-warmed LB plates containing 100 µg/ml ampicillin and 34 µg/ml chloramphenicol. The plates were incubated overnight at 37 ℃.

3.11.9 Directional PCR for selection of positive recombinant clones

Directional PCR was performed to select positive recombinant clones with sense orientation of cloned fragment. PCR was carried out using the same protocol as mentioned in section 3.11.6.

3.12 Confirmation of inserted *pkMSP-1$_{33}$* and *pkMSP-1$_{42}$* nucleotide and deduced amino acid sequences by sequence analysis

Nucleotide sequences of the recombinant plasmid TOPO-*pkMSP-1$_{33}$*, pRSET A-*pkMSP-1$_{33}$*, TOPO-*pkMSP-1$_{42}$* and pRSET A-*pkMSP-1$_{42}$* were confirmed by sequencing services from company (Bioneer Corp., Korea). The amino acid sequences of insert fragments were deduced from the nucleotide sequences. Basic Local Alignment Search Tool (BLAST) was used to compare these nucleotide and deduced amino acid sequences to previously published *P. knowlesi MSP-1$_{33}$* and *MSP-1$_{42}$* nucleotide and protein sequences in National Center for Biotechnology Information (NCBI) database in order to confirm their identity.

3.13 Expression of recombinant pkMSP-1_{33} and pkMSP-1_{42} in *E. coli* expression system

3.13.1 Small scale protein expression

Single recombinant BL21 (DE3)pLysS colony for both pkMSP-1_{33} and pkMSP-1_{42} was inoculated and propagated overnight in LB broth containing ampicillin (100 µg/ml) and chloramphenicol (34 µg/ml) at 37℃ with shaking. The overnight cultures were diluted with LB broth to optical density (OD) at 600 nm = 0.1 with final volume of 10 ml, and the cultures were allowed to grow to OD_{600} of 0.4 to 0.6. The cultures were induced with 1 mM IPTG and grew at 37℃ with shaking speed 250 rpm. Cell culture fragments (1 ml) were collected before induction and every two hours after induction up to four hours after induction. The cells were harvested by centrifugation at 5000 × g for 10 min. Non-recombinant clone (pRSET A only) was used as negative control.

3.13.2 Larger scale protein expression

Scale-up protein expression was performed to produce larger amount of recombinant pkMSP-1_{33} and pkMSP-1_{42}. Recombinant proteins were expressed in volume of 50 ml with expression conditions as mentioned in section 3.13.1.

3.14 Analysis of expressed pkMSP-1_{33} and pkMSP-1_{42}

3.14.1 SDS-PAGE

Samples were run under denaturing conditions. Pellets were resuspended in 25 µl PBS and 25 µl of 2X sample buffer was added. Samples were boiled for 15 min. Samples of each time point were analysed using SDS-PAGE by loading 5 µl of the boiled samples into different wells on a 12% SDS-PAGE gel. Electrophoresis was carried out by 120 V for 75 min. After electrophoresis, the

gel was stained with Coomassie Brilliant Blue staining solution for four hours, and destained with destaining solution overnight. The recombinant protein bands with expected size on the gel were identified. The optimal time point with the highest band intensity was determined.

3.14.2 Western Blot assay

The proteins were separated by electrophoresis. The SDS-PAGE gel and blot papers were soaked in transfer buffer for 10 min before electroblotting. PVDF membrane (Bio-Rad Laboratories, U.S.A.) was soaked in absolute methanol for 5 min prior soak in transfer buffer. The Trans-Blot® SD *Semi-Dry* Electrophoretic Transfer Cell Unit (Bio-Rad Laboratories, U.S.A.) was used in transblotting. Transblotting of proteins from gel onto PVDF membrane was done by 15V for 40 min. The membrane was blocked overnight in TBS containing 5% (w/v) skimmed milk at 4℃. The membrane was washed three times with 0.2% (v/v) TBS-T and then probed with anti-Xpress™ monoclonal antibody (Invitrogen Corp., U.S.A., 1:5000 dilution) in TBS containing 2.5% (w/v) skimmed milk for one hour with constant shaking at room temperature. After three additional washes, the membrane was treated with biotin-labelled goat anti-mouse IgG (KPL Inc., U.S.A., 1:2500 dilution) in TBS containing 2.5% (w/v) skimmed milk for one hour at room temperature. The membrane was washed three times, and followed by incubation of streptavidin-alkaline phosphatase (Invitrogen Corp., U.S.A., 1:2500 dilution) in TBS containing 2.5% (w/v) skimmed milk for one hour at room temperature. Finally, the membrane was washed three times and the protein bands were revealed by the chromogenic substrate NBT/BCIP (Sigma Chemical Co., U.S.A.). The colour on membrane was allowed to develop at room temperature in dark. The membrane was washed

with ddH_2O, dried and photographed. The recombinant protein bands with expected size were identified.

3.15 Purification of pkMSP-1_{33} and pkMSP-1_{42}

Expressed pkMSP-1_{33} and pkMSP-1_{42} were affinity-purified by using ProBond^{TM} purification system (Invitrogen Corp., U.S.A.) in hybrid condition.

3.15.1 Preparation of bacterial cell lysates

Guanidinium lysis buffer (pH 7.8) was equilibrated to 37 ℃. Bacteria cells were harvested from 50 ml cultures by centrifugation at 5000 × g for 10 min. The supernatants were removed and cell pellets were resuspended in 8 ml guanidinium lysis buffer. The cells were rocked for 10 min at room temperature to ensure thorough cell lysis. Then, the turbid cell lysates were sonicated on ice at high intensity until the lysates turned into translucent solutions. The lysates were centrifuged at 3,000 × g for 15 min to pellet the cellular debris. The supernatants were transferred to new tubes.

3.15.2 Preparation of polypropylene columns

Purification polypropylene columns (Qiagen, Hilden, Germany) were prepared under denaturing condition. Nickel-NTA agarose resin (Qiagen, Hilden, Germany) was resuspended in its bottle by inverting and gently tapping the bottle repeatedly, and 2 ml of resin was pipetted into each purification polypropylene column. The resin was allowed to settle completely by gravity for 10 min. The supernatants were aspirated gently. Sterile distilled water, 6 ml was added into the columns and resin was resuspended by inverting the columns. The resin was allowed to settle by gravity and the supernatants were aspirated

gently. Denaturing binding buffer (pH 7.8), 6 ml was added into the columns and resin was resuspended by inverting the columns. The resin was allowed to settle by gravity and the supernatants were aspirated gently. Then, another 6 ml of denaturing binding buffer was added and resin was resuspended. The resin was allowed to settle by gravity and the supernatants were aspirated gently.

3.15.3 Purification procedure

pkMSP-1_{33} and pkMSP-1_{42} cell lysates, 8 ml each, were added to the prepared polypropylene columns. The lysates were allowed to bind on resin for 15 min at room temperature with gentle agitation to keep the resin suspended in the lysate solutions. Resin was allowed to settle by gravity and the supernatants were aspirated carefully. The columns were washed with 4 ml denaturing binding buffer (pH 7.8) by resuspending the resin and rocking for 2 min. The resin was allowed to settle by gravity and the supernatants were aspirated carefully. The columns were washed twice with denaturing binding buffer. Then, the columns were washed with 4 ml denaturing wash buffer (pH 6.0) by resuspending the resin and rocking for 2 min. The resin was allowed to settle by gravity and the supernatants were aspirated carefully. The columns were washed twice with denaturing wash buffer. Next, the columns were washed with 8 ml native wash buffer (pH 8.0) by resuspending the resin and rocking for 2 min. The resin was allowed to settle by gravity and the supernatants were aspirated carefully. The columns were washed with native wash buffer for a total of four washes. Finally, the columns were clamped in a vertical position and the caps on the lower end of the columns were snapped off. The purified proteins were eluted with 6 ml native elution buffer (pH 8.0) and stored at -80 ℃.

3.16 Dialysis of purified pkMSP-1_{33} and pkMSP-1_{42}

Dialysis was performed on purified pkMSP-1_{33} and pkMSP-1_{42} using SnakeSkin dialysis tubing, 10K MWCO (Thermo Scientific, U.S.A.). Tris-EDTA dialysis buffer, 1000 ml was poured into each beaker and pre-cold on ice. Dialysis membranes with required length were cut from the packaging tube. One end of the membranes was briefly dipped into dialysis buffer and a knot was tightly tied in the wetted end of the tubings. Purified proteins, 3 ml were added into the tubings from the open end. A knot was securely tied in the open end of tubings. The filled dialysis tubings were floated on the dialysis buffer and the proteins were dialysed for four hours. The external dialysis buffer was exchanged with new dialysis buffer and the proteins were dialysed overnight. External buffer was exchanged again with new dialysis buffer and the proteins were allowed to dialyse for another four hours. Nick was made at one end of the dialysis tubings and the dialysed proteins were pipetted out. Dialysis buffer was stirred on ice using stirrer throughout the whole dialysis process.

3.17 Analysis and evaluation of purified pkMSP-1_{33} and pkMSP-1_{42}

3.17.1 SDS-PAGE

Purified proteins, 25 µl were added to 25 µl 2X sample buffer. Samples were boiled for 5 min and analysed using SDS-PAGE by loading 15 µl of the boiled samples into different wells on a 12% SDS-PAGE gel. Electrophoresis was carried out using the same protocol as mentioned in section 3.14.1.

3.17.2 Western Blot assay

Purified proteins were separated using electrophoresis by loading 15 µl of the boiled samples into different wells on a 12% SDS-PAGE gel. Western

Blot assay for purified proteins was carried out using the same protocol as mentioned in section 3.14.2.

3.18 Quantification of concentration of purified pkMSP-1_{33} and pkMSP-1_{42}

The concentration of the purified pkMSP-1_{33} and pkMSP-1_{42} was determined by using Quick Start™ Bradford protein assay (Bio-Rad Laboratories, U.S.A.). BSA was used as standard. BSA with stock concentration of 2.0 mg/ml was diluted into concentrations of 1.5 mg/ml, 1.0 mg/ml, 0.75 mg/ml, 0.5 mg/ml, 0.25 mg/ml, and 0.125 mg/ml, while water was used as blank (0 mg/ml). The 1X dye reagent was removed from 4 ℃ storage and warmed to ambient temperature. The 1X dye reagent was inverted for a few times before use. BSA standards and purified protein samples, 5 µl were pipetted into separate microplate wells. The 1X dye reagent, 250 µl was added into each microplate well and mixed well by using microplate mixer. The mixtures were incubated at room temperature for 5 min. The absorbance of the standards and samples at wavelength of 595 nm was measured using microplate reader Infinite® M200 PRO NanoQuant (Tecan Group Ltd., Switzerland). Standards and samples were run in duplicates. The average reading of blank values was subtracted from the average reading of standard and sample values. A standard curve was generated by plotting the absorbance of standard BSA at 595 nm (Y axis) versus their concentration in mg/ml (X axis).The concentration of purified pkMSP-1_{33} and pkMSP-1_{42} was determined using the standard curve.

3.19 Evaluation of purified pkMSP-1_{33} and pkMSP-1_{42} in Western Blot assays using patient sera

The purified pkMSP-1_{33} was tested in Western Blot using sera of patients infected with: (A) *P. knowlesi* (n = 31); (B) non-knowlesi human *Plasmodium* species which include *P. falciparum* (n = 11), *P. vivax* (n = 16), and *P. ovale* (n = 1); (C) non-malarial parasitic infections which include filariasis (n = 4), amoebiasis (n = 16), cysticercosis (n = 12), toxoplasmosis (n = 17), toxocarasis (n = 3); and (D) healthy donor (n = 65). Total of 176 serum samples were used. PVDF membrane strips containing 70 ng of blotted purified pkMSP-1_{33} were incubated with different serum samples (1:250 dilution) for two hours at room temperature, followed by incubation with biotin-labelled goat anti-human IgM + IgG + 1gA (1:2500 dilution) for one hour, streptavidin-alkaline phosphatase (1:2500 dilution) for one hour, and finally NBT/BCIP substrate for development of colour.

The purified pkMSP-1_{42} was evaluated with patient sera of same categories as pkMSP-1_{33}. A total of 189 serum samples were used, which include: (A) *P. knowlesi* (n = 38); (B) non-knowlesi human *Plasmodium* species [*P. falciparum* (n = 13), *P. vivax* (n = 15), and *P. ovale* (n = 1)]; (C) non-malarial parasitic infections [filariasis (n = 4), amoebiasis (n = 16), cysticercosis (n = 13), toxoplasmosis (n = 11), toxocarasis (n = 3)]; and (D) healthy donor (n =75). The Western Blot assay for pkMSP-1_{42} was carried out as for pkMSP-1_{33}.

3.20 Evaluation of purified pkMSP-1_{33} and pkMSP-1_{42} in ELISA using patient sera

The same patient sera used in Western Blot assay for pkMSP-1_{33} (n = 176) and pkMSP-1_{42} (n = 189) were used in ELISA. Purified pkMSP-1_{33} and

pkMSP-1_{42} with concentration of 10 µg/ml were coated on Nunc MaxiSorp® flat-bottom 96 well microtitre plates (Thermo Scientific, U.S.A.) using 0.05 M sodium bicarbonate buffer (pH 9.6) and incubated overnight at 4 ℃. The wells were washed three times with 0.1% (v/v) PBS-T. Blocking buffer 1% (w/v) BSA/PBS, 100 µl was added into each well and incubated for two hours at 37 ℃. The wells were then washed three times. Patient serum (1:80 dilution) in 1% (w/v) BSA/PBS was separately added into each well and incubated for one hour at 37 ℃. After five time washes, HRP-labelled goat anti-human IgM + IgG + IgA (1:2500 dilution) was added and followed with one hour incubation at 37 ℃. The wells were washed five times and incubated with TMB (Amresco Inc., U.S.A.) for 30 min in dark. The reaction was stopped by adding 2 N sulphuric acid stop solution. The absorbance of samples at wavelength of 450 nm was measured using microplate reader. Samples were run in duplicates. The cut-off value was set at $M_N + 2\sigma$ of the healthy donor serum group, where M_N is the mean absorbance and σ is the standard deviation. Samples with absorbance value higher than $M_N + 2\sigma$ were considered positive.

3.21 Immunogenicity tests of purified pkMSP-1_{42} using mouse model

Use of experimental animals and experiment procedures in this study were approved by University of Malaya Institutional Animal Care And Use Committee (PAR/28/09/2011/CFW) (Appendix 4).

3.21.1 Mice injection

Six to eight week old female BALB/c mice were used for immunization (pkMSP-1_{42}-immunized group and negative control group, n = 5 per group). Purified pkMSP-1_{42}, 30 µg, was mixed with adjuvant in a volume of 1:1 ratio

and the mixture was injected into each mouse in a total volume of 100 µl. Complete Freund's Adjuvant (CFA) (Sigma Chemical Co., U.S.A.) was used in the prime boost and Incomplete Freund's Adjuvant (IFA) (Sigma Chemical Co., U.S.A.) was used in the subsequent boosters. Booster was given on day 14 and 21 post-immunization. All injections were given subcutaneously. Mice in the negative control group were injected with purified non-recombinant protein pRSET A.

3.21.2 Measurement of cytokine levels in mice

3.21.2.1 Purification of mouse spleen cells

Mice were sacrificed 10 days after second booster (day 31 post-immunization) by cervical dislocation and placed on a dissection board. The mouse belly was wiped with alcohol and a vertical incision was performed with surgical scissors through the mouse belly. The mouse spleen was removed and transferred into a 50 ml centrifuge tube containing 5 ml complete RPMI 1640 medium. The spleen was put inside a 70 µm nylon mesh cell strainer (Becton, Dickinson and Co., U.S.A.) which placed in a petri dish under the hood. The spleen was mashed over the cell strainer by using syringe plunger. Complete RPMI 1640 medium, 5 ml was added into the petri dish. The solution was transferred into a 50 ml centrifuge tube. The remaining spleen cells left in the petri dish were collected by rinsing 5 ml of complete RPMI 1640 medium. The solution was centrifuged at 1500 rpm for 7 min. The supernatant was removed and discarded. The pellet was resuspended with 5 ml of ACK lysis buffer and incubated at room temperature for 5 min. The solution was brought to 25 ml with complete RPMI 1640 medium and the tube was shaken while the medium was added. The solution was centrifuged at 1500 rpm for 7 min. The supernatant

was removed and discarded. The pellet was resuspended with 10 ml of complete RPMI 1640 medium and centrifuged at 1500 rpm for 7 min. The supernatant was discarded and the pellet was resuspended with 10 ml of complete RPMI 1640 medium.

3.21.2.2 Quantification of live spleen cells

The live spleen cells were counted by dye exclusion method using Fluka® Trypan blue stain (Sigma Chemical Co., U.S.A.) with volume of 1:1 ratio. Haemocytometer was used for cell counting. Live cells in each of the four 0.1 mm^3 corner square were counted (Figure 3.1). The cells touching the top or left borders were counted while the cells touching the bottom or right borders were not counted. Amount of live cells per ml was determined using the following equation:

Cells/ml = N X dilution factor X 10^4

Note: N, average cell count per corner square; Dilution factor = 2

3.21.2.3 Culture of spleen cells and collection of spleen cell supernatants

Spleen cells were grown in tissue culture grade flat-bottom 96 well microtitre plates (TPP, Trasadingen, Switzerland), with a total of 2 X 10^5 cells in final volume of 100 µl culture medium per well. Purified pkMSP-1_{42}, 30 µg/ml was added as stimulator. Lymphocyte mitogen ConA (Merck KGaA, Germany), 5 µg/ml was used as positive control, while negative control was performed with cells growth without any stimulator. The plates were placed in 5% carbon dioxide (CO_2) incubator at 37℃ and cells were allowed to grow for 65 hours. The plates were then centrifuged at 2000 rpm for 20 min. Cell supernatants were collected and used in mouse cytokine IL-2, IL-4, IL-10 and IFN-γ assays.

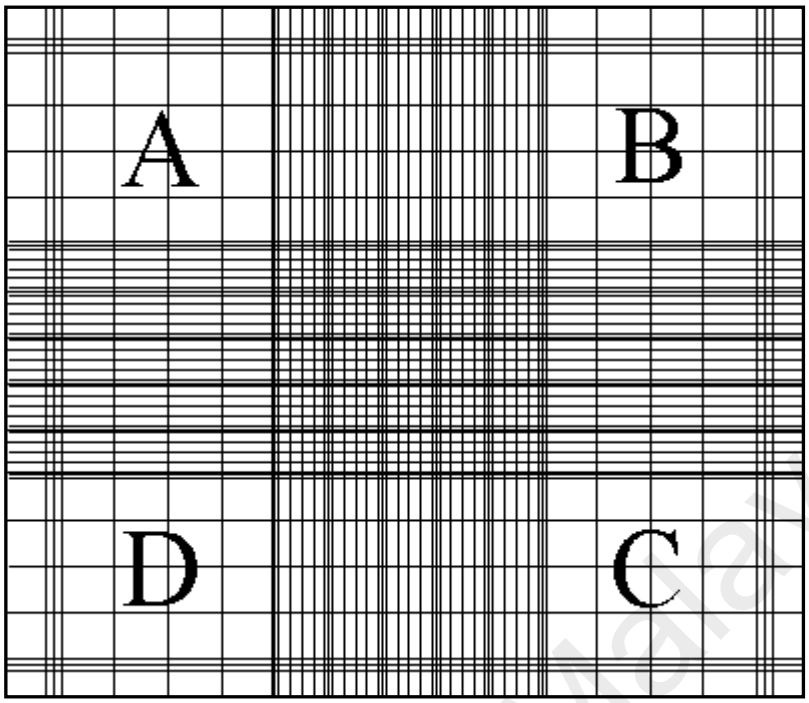

Figure 3.1. Haemocytometer grid. Live spleen cells were counted in all four 0.1 mm^3 corner squares labelled A thru D.

The total cell count in four squares = A + B + C + D

N = Average cell count per corner square = $\frac{A + B + C + D}{4}$

3.21.2.4 Mouse IL-2 ELISA

Mouse IL-2 in culture supernatants was quantified by using commercialised mouse IL-2 ELISA kit (Thermo Scientific, U.S.A.) with protocol provided. Samples and reagents were equilibrated to room temperature before used. Lyophilized standard was reconstituted with complete RPMI 1640 medium and mixed by gently inverting the vial. Complete RPMI 1640 medium was used to prepare standard curve dilutions, from stock concentration of 850 pg/ml into 170 pg/ml, 34 pg/ml and 0 pg/ml. Plate Reagent, 50 µl was added to all wells. Reconstituted standards or test samples, 50 µl were separately added into each well. Standards and samples were run in duplicates. Plate was covered with adhesive plate cover and incubated for two hours at 37℃ in a humidified incubator. Plate was washed five times with Wash Buffer. Prepared Conjugate Reagent, 100 µl was added to each well. Plate was covered with a new adhesive cover and incubated for one hour at 37℃ in a humidified incubator. Plate was washed five times with Wash Buffer. TMB Substrate Solution, 100 µl was added into each well. Colour reaction was allowed to develop at room temperature in the dark for 30 min. The reaction was stopped by adding 100 µl of Stop Solution to each well. Absorbance of the samples at wavelength 450 nm was measured using microplate reader. Standard curve was generated by plotting the average absorbance obtained for each standard concentration on the vertical (Y) axis versus the corresponding IL-2 concentration (pg/ml) in the horizontal (X) axis. The IL-2 amount in each sample was determined by interpolating from the absorbance value (Y axis) to IL-2 concentration (X axis) using the standard curve. Mann-Whitney statistical test was performed to assess the significance level of IL-2 concentration among pRSET A-immunized mice group and pkMSP-1_{42}-immunized mice group.

3.21.2.5 Mouse IL-4 ELISA

Mouse IL-4 in culture supernatants was quantified by using commercialised mouse IL-4 ELISA kit (Thermo Scientific, U.S.A.) with protocol provided. Samples and reagents were equilibrated to room temperature before used. Lyophilized standard was reconstituted with complete RPMI 1640 medium and mixed by gently inverting the vial. Complete RPMI 1640 medium was used to prepare standard curve dilutions, from stock concentration of 375 pg/ml into 75 pg/ml, 15 pg/ml and 0 pg/ml. Plate Reagent, 50 µl was added to all wells. Reconstituted standards or test samples, 50 µl were separately added into each well. Standards and samples were run in duplicates. Plate was covered with adhesive plate cover and incubated for two hours at 37℃ in a humidified incubator. Plate was washed five times with Wash Buffer. Prediluted Conjugate Reagent, 100 µl was added to each well. Plate was covered with a new adhesive cover and incubated one hour at 37℃ in a humidified incubator. Plate was washed five times with Wash Buffer. TMB Substrate Solution, 100 µl was added into each well. Colour reaction was allowed to develop at room temperature in the dark for 30 min. The reaction was stopped by adding 100 µl of Stop Solution to each well. Absorbance of the samples at wavelength 450 nm was measured using microplate reader. Standard curve was generated by plotting the average absorbance obtained for each standard concentration on the vertical (Y) axis versus the corresponding IL-4 concentration (pg/ml) in the horizontal (X) axis. The IL-4 amount in each sample was determined by interpolating from the absorbance value (Y axis) to IL-4 concentration (X axis) using the standard curve. Mann-Whitney statistical test was performed to assess the significance level of IL-4 concentration among pRSET A-immunized mice group and pkMSP-1_{42}-immunized mice group.

3.21.2.6 Mouse IL-10 ELISA

Mouse IL-10 in culture supernatants was quantified by using commercialised mouse IL-10 ELISA kit (Thermo Scientific, U.S.A.) with protocol provided. Samples and reagents were equilibrated to room temperature before used. Lyophilized standard was reconstituted with ultrapure water and mixed by gently inverting the vial. Complete RPMI 1640 medium was used to prepare standard curve dilutions, from stock concentration of 3000 pg/ml into 1000 pg/ml, 333 pg/ml, 111 pg/ml, 37 pg/ml and 0 pg/ml. Assay Buffer, 50 µl was added to all wells. Reconstituted standards or test samples, 50 µl were separately added into each well. Standards and samples were run in duplicates. Plate was covered with adhesive plate cover and incubated for three hours at room temperature. Plate was washed three times with Wash Buffer. Biotinylated Antibody Reagent, 50 µl was added to each well. Plate was covered with a new adhesive cover and incubated one hour at room temperature. Plate was washed three times with Wash Buffer. Prepared streptavidin-HRP Solution, 100 µl was added to each well. Plate was covered with new adhesive plate cover and incubated for 30 min at room temperature. Plate was washed three times with Wash Buffer. TMB Substrate Solution, 100 µl was added into each well. Colour reaction was allowed to develop at room temperature in the dark for 30 min. The reaction was stopped by adding 100 µl of Stop Solution to each well. Absorbance of the samples at wavelength 450 nm was measured using microplate reader. Standard curve was generated by plotting the average absorbance obtained for each standard concentration on the vertical (Y) axis versus the corresponding IL-10 concentration (pg/ml) in the horizontal (X) axis. The IL-10 amount in each sample was determined by interpolating from the absorbance value (Y axis) to IL-10 concentration (X axis) using the standard

curve. Mann-Whitney statistical test was performed to assess the significance level of IL-10 concentration among pRSET A-immunized mice group and pkMSP-1_{42}-immunized mice group.

3.21.2.7 Mouse IFN-γ ELISA

Mouse IFN-γ in culture supernatants was quantified by using commercialised mouse IFN-γ ELISA kit (Thermo Scientific, U.S.A.) with protocol provided. Samples and reagents were equilibrated to room temperature before used. Lyophilized standard was reconstituted with ultrapure water and mixed by gently inverting the vial. Complete RPMI 1640 medium was used to prepare standard curve dilutions, from stock concentration of 9000 pg/ml into 3000 pg/ml, 1000 pg/ml, 333 pg/ml, 111 pg/ml, 37 pg/ml and 0 pg/ml. Reconstituted standards or test samples, 50 µl were separately added into each well. Standards and samples were run in duplicates. Plate was covered with adhesive plate cover and incubated for two hours at room temperature. Biotinylated Antibody Reagent, 50 µl was added to all wells without washing. Plate was covered with a new adhesive cover and incubated one hour at room temperature. Plate was washed three times with Wash Buffer. Prepared streptavidin-HRP Solution, 100 µl was added to each well. Plate was covered with a new adhesive cover and incubated 30 min at room temperature. Plate was washed three times with Wash Buffer. TMB Substrate Solution, 100 µl was added into each well. Colour reaction was allowed to develop at room temperature in the dark for 30 min. The reaction was stopped by adding 100 µl of Stop Solution to each well. Absorbance of the samples at wavelength 450 nm was measured using microplate reader. Standard curve was generated by plotting the average absorbance obtained for each standard concentration on the vertical

(Y) axis versus the corresponding IFN-γ concentration (pg/ml) in the horizontal (X) axis. The mouse IFN-γ amount in each sample was determined by interpolating from the absorbance value (Y axis) to IFN-γ concentration (X axis) using the standard curve. Mann-Whitney statistical test was performed to assess the significance level of IFN-γ concentration among pRSET A-immunized mice group and pkMSP-1_{42}-immunized mice group.

3.21.3 Characterization of raised antibodies in mice

3.21.3.1 Collection of immunized mice sera

Blood of each mouse was collected at day 0, 7, 14, 21 and 31 post-immunization. Approximately 80 µl of blood was collected from each mouse by tail bleeding. The bloods were stored overnight at 4 ℃. Bloods were centrifuged at 3000 rpm for 20 min. Sera were pipetted into new tubes and stored at -20 ℃.

3.21.3.2 Detection of anti-pkMSP-1_{42} antibodies in mice sera using Western Blot assays

Antibody responses in immunized mice towards pkMSP-1_{42} at different time points were analysed. PVDF membrane strips containing 1 µg of blotted purified pkMSP-1_{42} were incubated with mice sera collected at different points (1:250 dilution) for two hours at room temperature, followed by incubation with biotin-labelled goat anti-mouse IgM + IgG + 1gA (1:2500 dilution) for one hour, streptavidin-alkaline phosphatase (1:2500 dilution) for one hour, and finally NBT/BCIP substrate for development of colour.

3.21.3.3 Measurement of IgM and IgG level in mice sera using ELISA

HRP-labelled goat anti-mouse IgM and IgG were used to determine the IgM and IgG level in pkMSP-1_{42}-immunized mice sera respectively. Purified pkMSP-1_{42} with concentration of 10 µg/ml were coated on microtitre plate and mice serum collected at different points (1:200 dilution) was separately added into each well and incubated for one hour, followed by incubation with HRP-labelled goat anti-mouse antibodies (1:2500 dilution) for one hour. The wells were incubated with TMB for 30 min in dark and the reaction was stopped by adding 2 N sulphuric acid stop solution. The absorbance of samples at wavelength of 450 nm was measured using microplate reader. Samples were run in duplicates. The cut-off value was set at $M_N + 2\sigma$ of the negative control group (pRSET A-immunized mice group).

3.21.3.4 Determination of IgG isotype distribution

HRP-labelled anti-mouse IgG1, IgG2a, IgG2b and IgG3 were used for determination of IgG subclass distribution in pkMSP-1_{42}-immunized mice sera. Purified pkMSP-1_{42} with concentration of 10 µg/ml were coated on microtitre plate and mice serum collected at day 31 post-immunization (1:200 dilution) was separately added into each well and incubated for one hour. The wells were separately incubated with HRP-labelled anti-mouse IgG subtypes (1:2500 dilution) for one hour, followed by incubation with TMB for 30 min in dark. The reaction was stopped by adding 2 N sulphuric acid stop solution and the absorbance of samples at wavelength of 450 nm was measured using microplate reader. Samples were run in duplicates. The cut-off value was set at $M_N + 2\sigma$ of the negative control group.

3.21.3.5 Determination of endpoint titre of mice sera

Serial dilution was performed on the pkMSP-1_{42}-immunized mice sera collected at day 31 post-immunization (1:400, 1:800, 1:1600, 1:3200, 1:6400, 1:12800, 1:25600, 1:51200, 1:102400, 1:204800, 1:409600 and 1:819200 dilution). ELISA was carried out as mentioned in section 3.21.3.4, by incubation of serial-diluted mice sera followed by HRP-labelled anti-mouse IgM + IgG + IgA (1:2500 dilution).

3.21.3.6 Determination of reactivity of immunized mice sera against *P. knowlesi* parasites using IFA

Anti-pkMSP-1_{42} antibodies in pkMSP-1_{42}-immunized mice sera were tested for their ability to recognise the *P. knowlesi* protein. Thin blood smear was prepared by using knowlesi-infected patient blood. The smear was fixed with an acetone-methanol mixture (9:1, v/v) for 15 min at -20 ℃ and washed with 1X PBS. The smear was further rinsed with ddH_2O to prevent salt crystal formation. Area of smear that was required for the experiment (area of non-overlapping single erythrocyte layer) was circled at the back of the slide. Blocking buffer 3% (w/v) BSA/PBS was added to the circled spot on smear for one hour at room temperature. Immunized mice sera collected at day 31 post-immunization (1:100 dilution) were added to the circled spot and incubated for one hour at 37 ℃ in a humidified incubator. Smear was briefly washed with ddH_2O, followed by three washes with 1X PBS. The smear was incubated with FITC-labelled anti-mouse IgM + IgG (KPL Inc., U.S.A., 1:1000 dilution) in 3% (w/v) BSA/PBS for one hour at 37 ℃ in a dark humidified incubator. The smear was carefully rinsed with ddH_2O for three times. DAPI/Antifade solution (Merck Millipore Corp., U.S.A., 1:200 dilution) was added to the spot and incubated for 15 min at room

temperature in dark condition. After three rinses with ddH_2O, the smear was mounted with cover slip using Calbiochem® FluorSave™ reagent (Merck Millipore Corp., U.S.A.) and kept at 4℃ overnight in dark condition. The slide was examined under fluorescence microscope BX51-FL-CCD (Olympus, Japan).

3.22 Identification and characterization of potential epitopes on *P. knowlesi* MSP-1_{42} by using pkMSP-1_{42}-immunized mice sera and synthetic peptide library

Epitope mapping of antibody responses to *P. knowelsi* MSP-1_{42} in pkMSP-1_{42}-immunized mice sera was carried out using synthetic peptide library. BALB/c mice were immunized with non-recombinant protein pRSET A and pkMSP-1_{42} as described in section 3.21.1 (n = 16 for each group). An overlapping peptide library which consist of 36 peptides (18-mer each, 9-mer overlapping) covered the entire *P. knowlesi* MSP-1_{42} protein sequence was synthesised by Genscript Inc. (U.S.A.). Peptide 1-36, 10 µg/ml each, was coated on Nunc MaxiSorp® flat-bottom 96 well plate with 0.05 M sodium bicarbonate buffer, pH 9.6 at 4℃ overnight. Mice serum collected at day 31 post-immunization (1:100 dilution) was separately added to each well and detected by HRP-labelled anti-mouse IgM + IgG + IgA (1:2500 dilution) with TMB as substrate. Mice sera from negative control group were used to determine the cut-off value. Reactivity strength of pkMSP-1_{42}-immunized mice sera towards each peptide was analysed with Mann-Whitney statistical analysis and categorised into the following groups; negative reactivity = below cut-off, low reactivity = higher than cut-off, moderate reactivity = cut-off + 0.5 OD, high reactivity = cut-off + 1.0 OD. The peptides which have significant higher reactivity with

pkMSP-1_{42}-immunized mice sera compared to negative control mice sera were identified as potential epitopes.

3.23 Identification and characterization of potential epitopes on *P. knowlesi* MSP-1_{42} by using purified pkMSP-1_{42}-immunized mice sera and phage display library

3.23.1 Affinity purification of anti-pkMSP-1_{42} antibodies

pkMSP-1_{42}-immunized mice sera used in section 3.22 were affinity purified. Purified pkMSP-1_{42}, 50 µg/ml was coated on Nunc MaxiSorp® flat-bottom 96 well microtitre plates (Thermo Scientific, U.S.A.) using 0.05 M sodium bicarbonate buffer (pH 9.6) and incubated overnight at 4 ℃. Mice sera collected at day 31 post-immunization (undiluted) were added into wells and incubated three hours at room temperature. The unbound sera were discarded by pouring off and slapping plate face down onto a clean paper towel. The wells were washed five times with 0.1% (v/v) PBS-T. The bound sera were eluted by incubation of wells with elution buffer 0.2 M Glycine-HCl in 1 mg/ml BSA (pH 2.2) for 20 min at room temperature. The eluate was neutralised with 1 M Tris-HCl (pH 9.1).

3.23.2 Titre of phage

Single colony of *E. coli* ER2738 host strain was inoculated and propagated in 10 ml LB broth containing tetracycline (20 µg/ml). The culture was incubated at 37 ℃ with vigorous shaking until mid-log phase (OD_{600} ~ 0.5). TOP agar was melted in microwave and dispensed 3 ml into sterile culture tubes, one per expected phage dilution. The tubes were maintained at 45 ℃. LB agar plates containing IPTG/X-gal, one plate per expected dilution, were pre-warmed

at 37℃ until ready for use. Serial dilutions of phage, 10 to 10^3 fold, were prepared in LB broth. The suggested dilution ranges for unamplified panning eluates and amplified phage culture supernatants were 10^1-10^4 and 10^8-10^{11}, respectively. ER2738 culture, 200 µl was dispensed into microcentrifuge tubes, one for each phage dilution. Each phage dilution, 10 µl was added into each tube. The microcentrifuge tubes were briefly vortexed and incubated for 5 min at room temperature. The infected cells, one infection at a time, were transferred to the culture tubes containing TOP agar. The culture tubes were quickly vortexed and the cultures were immediately poured onto a pre-warmed LB agar plates containing IPTG/X-gal. Plates were gently tilted and rotated to spread TOP agar evenly. The plates were allowed to cool for 5 min and incubated overnight at 37℃. Plaques on plates that have approximately 100 plaques were counted. Each count was multiplied by the dilution factor for that plate in order to get the phage titre in plaque forming units (pfu) per 10 µl.

3.23.3 Surface panning (Direct target coating)

The simplest method of affinity partitioning (panning) of phage display could be carried out by directly coating a plastic surface with the target of interest, passing the pool of phage over the target-coated surface, discard the unbound phage, and finally elute the bound phage with suitable elution buffer. This direct target coating method was chosen in the present study to identify the potential epitopes on *P. knowlesi* MSP-1_{42} by using purified pkMSP-1_{42}-immunized mice sera and phage display library. Ph.D.-12 premade random phage display library (New England Biolabs, U.S.A.) was used in the present study for panning of phage towards the affinity-purified anti-pkMSP-1_{42} antibodies.

Affinity-purified anti-pkMSP-1_{42} antibody (1:200 dilution) was coated on Nunc MaxiSorp® flat-bottom 96 well microtitre plate (Thermo Scientific, U.S.A.) using 0.1 M sodium bicarbonate buffer (pH 8.6) and incubated overnight at 4 ℃. For tittering, single colony of *E. coli* ER2738 host strain was inoculated and propagated in 10 ml LB broth containing tetracycline (20 µg/ml). For amplifying the eluted phage, single colony of *E. coli* ER2738 host strain was inoculated in 20 ml of LB broth containing tetracycline (20 µg/ml) in a 250 ml Erlenmeyer flask. Both cultures were incubated at 37 ℃ with vigorous shaking. The tittering culture was allowed to grow to OD_{600} of 0.5, while the amplifying culture was carefully monitored to avoid grow beyond early-log phase (OD_{600} 0.01 to 0.05). The target coating solution was discarded and residual solution was removed by firmly slapped the plate faces down onto a clean paper towel. Blocking buffer 1% (w/v) BSA/TBS, 400 µl was added into well and incubated for four hours at room temperature. Blocking buffer was discarded and well was washed six times with 0.5% (v/v) TBS-T by swirling. Phage library with a total 2 X 10^{11} phage in 0.1% BSA/TBS was added into well and incubated overnight at 4 ℃. Unbound phage were discarded and the well was washed 15 times with 0.5% (v/v) TBS-T, followed by five time washes with TBS. Bound phage were eluted by adding elution buffer 0.2 M Glycine-HCl in 1 mg/ml BSA (pH 2.2) into well and the plate was gently rocked for 12 min at room temperature to disrupt the binding interactions among bound phage and coated target. The eluate was pipetted into a microcentrifuge tube and neutralised with 1 M Tris-HCl (pH 9.1).

Small amount of the eluate (~1 µl) was tittered as described in section 3.23.2. The rest of the eluate was amplified by adding the eluate to the 20 ml amplifying culture in 250 ml Erlenmeyer flask and incubated for 4.5 hours at

37 ℃ with vigorous shaking. The culture was transferred to a centrifuge tube and centrifuged at 12,000 × g for 10 min at 4 ℃. The upper 80% of the supernatant was transferred to a fresh tube and 1/6 volume of 20% (w/v) PEG/2.5 M NaCl was added into the tube. The phage was allowed to precipitate overnight at 4 ℃. The PEG precipitation was centrifuged at 12000 × g for 15 min at 4 ℃ and the supernatant was completely discarded. The white finger print sized-phage pellet was resuspended in 1 ml of TBS. The suspension was transferred to a microcentrifuge tube and centrifuged at 14000 rpm for 5 min at 4 ℃. The supernatant was transferred to a fresh microcentrifuge tube and 1/6 volume of 20% (w/v) PEG/2.5 M NaCl was added for reprecipitation. The tube was incubated on ice for one hour and the tube was centrifuged at 14000 rpm for 10 min at 4 ℃. The supernatant was completely discarded and the pellet was resuspended in 200 µl of TBS. The tube was centrifuged for 1 min to pellet any remaining insoluble material. The supernatant, which was the amplified eluate, was transferred to a fresh tube. The amplified eluate was tittered as described in section 3.23.2. Equal volume of sterile glycerol was added to the amplified eluate and stored at -20 ℃.

A plate was coated for the second round of panning as mentioned above. Blue plaques on the tittering plates of amplified eluate were counted and the phage titre was determined. The phage titre was used to calculate an input volume corresponding to the input titre in first round of panning (2 X 10^{11} phage). Second round of panning was carried out by using the calculated amount of the first round amplified eluate as input phage. The second round amplified eluate was tittered and used as input phage in third round of panning. A total of three rounds of panning were performed.

3.23.4 Plaque amplification for ELISA and nucleotide sequencing

A single colony of *E. coli* ER2738 host strain was inoculated in 10 ml of LB broth containing tetracycline (20 µg/ml) and incubated overnight at 37 ℃ with constant shaking. The overnight culture was diluted 1:100 in LB broth. Diluted culture, 1 ml was dispensed into culture tubes, one for each clone to be characterized. Unamplified eluate from final round of panning was tittered. Blue plaques from the tittering plate with less than 100 plaques were stabbed by using pipette tips and transferred to tubes containing the diluted culture. Well-separated plaques were picked to ensure that each plaque contains only a single DNA sequence. Tubes were incubated for 4.5 hours at 37 ℃ with vigorous shaking. The cultures were transferred to microcentrifuge tubes and centrifuged at 14000 rpm for 20 min at 4 ℃. The supernatants (amplified phage), 200 µl and 500 µl respectively, were transferred to separate fresh tubes. For the 200 µl supernatants, a 1/6 volume of 20% (w/v) PEG/2.5 M NaCl was added. The phage was allowed to precipitate overnight at 4 ℃. The tubes were centrifuged at 14000 rpm for 20 min at 4 ℃. The supernatants were discarded and the pellets were resuspended in 200 µl PBS. The suspensions were used in ELISA in section 3.23.5. The 500 µl supernatants were stored at 4 ℃ for DNA extraction in section 3.23.6.

3.23.5 Determination of binding avidity of amplified phage towards anti-pkMSP-1_{42} antibodies using ELISA

ELISA was performed to screen several hundred individual phage clones in order to determine their binding avidity towards anti-pkMSP-1_{42} antibodies. pkMSP-1_{42}-immunized mice serum (1:200 dilution) was coated on Nunc MaxiSorp® flat-bottom 96 well microtitre plate (Thermo Scientific, U.S.A.)

using 0.1 M sodium bicarbonate buffer (pH 8.6) and incubated overnight at 4 ℃. Amplified phage clones were separately added into each well and incubated for one hour, followed by incubation with HRP-labelled anti-M13 pIII monoclonal antibody (New England Biolabs, U.S.A., 1:2500 dilution) for one hour at 37 ℃. The wells were incubated with TMB for 30 min in dark and the reaction was stopped by adding 2 N sulphuric acid stop solution. The absorbance of samples at wavelength of 450 nm was measured using microplate reader. The phage clones with high absorbance reading (approximately three to four times higher than background absorbance reading) were chosen and the DNA of the selected phage clones was extracted.

3.23.6 DNA extraction of selected phage clones

The 500 µl amplified phage clones in section 3.23.4 were used for phage DNA extraction. A volume of 200 µl of 20% (w/v) PEG/2.5 M NaCl was added to the tubes and the tubes were inverted several times to mix. After incubation of 20 min at room temperature, the tubes were centrifuged at 14000 rpm for 10 min at 4 ℃ and the supernatants were completely discarded. The pellets were resuspended thoroughly in 100 µl of iodide buffer and the tubes were vigorously tapped. Absolute ethanol, 250 µl was added to the tubes followed by incubation of 20 min at room temperature to precipitate the single-stranded phage DNA. The tubes were centrifuged at 14000 rpm for 10 min at 4 ℃ and the supernatants were discarded. The pellets were washed with 500 µl of 70% cold ethanol (stored at -20 ℃) and tubes were centrifuged at 14000 rpm for 10 min at 4 ℃. The supernatants were discarded and the pellets were briefly dried under vacuum. The pellets were resuspended in 30 µl of TE buffer.

3.23.7 DNA sequence analysis of extracted phage DNA

Nucleotide sequences of the each extracted phage clone were confirmed by sequencing services from company (MyTACG Bioscience Enterprise, Malaysia) by using -96 gIII sequencing primer. The amino acid sequences of the library dodecapeptide inserts were deduced from the nucleotide sequences (Appendix 5). These amino acid sequences were assessed for homology to the primary sequence of *P. knowlesi* MSP-1_{42} by using BioEdit Sequence Alignment Editor.

3.24 Evaluation and characterization of identified potential epitopes using mouse model

Potential epitopes identified by synthetic peptide library and by random phage display library were compared. Out of these potential epitopes, two of the most prominent epitopes were evaluated and characterized in mouse model. Peptides which represent the potential epitopes were synthesised large scale by Genscript Inc. (U.S.A.).

3.24.1 Mice injection

Six to eight week old female BALB/c mice were used for immunization (n = 5 per group). Synthetic peptides, 50 µg, were mixed with adjuvant in a volume of 1:1 ratio and the mixture was injected into each mouse by using intraperitoneal route of administration. Complete Freund's Adjuvant (Sigma Chemical Co., U.S.A.) was used in the prime boost and Incomplete Freund's Adjuvant (Sigma Chemical Co., U.S.A.) was used in the subsequent boosters. Booster was given on day 14, 28, and 42 post-immunization. Mice in negative control group were injected with PBS.

3.24.2 Measurement of cytokine levels in peptide-immunized mice

3.24.2.1 Purification and quantification of mouse spleen cells

Mice were sacrificed 10 days after third booster (day 52 post-immunization) as mentioned in section 3.21.2.1, and the spleen cells were quantified as mentioned in section 3.21.2.2.

3.24.2.2 Culture of spleen cells and collection of spleen cell supernatants

Spleen cells were grown in tissue culture grade flat-bottom 96 well microtitre plates (TPP, Trasadingen, Switzerland). Purified pkMSP-1_{42} and peptides, 25 µg/ml and 50 µg/ml respectively, were separately added into each well as stimulator. Cell supernatants were then collected as mentioned in section 3.21.2.3.

3.24.2.3 Mouse cytokine ELISA

Mouse IL-2, IL-4, IL-10 and IFN-γ in culture supernatants were quantified by using commercialised mouse cytokine ELISA kits (Thermo Scientific, U.S.A.) as mentioned in sections 3.21.2.4 to 3.21.2.7.

3.24.3 Characterization of raised antibodies in peptide-immunized mice

3.24.3.1 Collection of peptide-immunized mice sera

Blood of each mouse was collected at day 0, 14, 28, 42 and 52 post-immunization as mentioned in section 3.21.3.1.

3.24.3.2 Detection of anti-peptide antibodies in mice sera using Western Blot assays

Antibody responses in peptide-immunized mice towards pkMSP-1_{42} were analysed. PVDF membrane strips containing 2 µg of blotted purified pkMSP-1_{42} were incubated with mice sera collected before injection and day 52 post-immunization as mentioned in section 3.21.3.2.

3.24.3.3 Determination of IgG isotype distribution

IgG subclass distribution of peptide-immunized mice sera (collected at day 52 post-immunization, 1:200 dilution) was determined as mentioned in section 3.21.3.4.

3.24.3.4 Determination of reactivity of peptide-immunized mice sera against *P. knowlesi* parasites using IFA

Raised anti-peptide antibodies in peptide-immunized mice sera were tested for their ability to recognise the *P. knowlesi* protein in IFA as mentioned in section 3.21.3.6.

CHAPTER 4: RESULTS

4.1 PCR of *pkMSP-1$_{33}$* and *pkMSP-1$_{42}$* genes

Plasmodium knowlesi DNA was extracted from knowlesi-infected patient blood. *pkMSP-1$_{33}$* and *pkMSP-1$_{42}$* genes were amplified by PCR with the extracted DNA as template.

For *pkMSP-1$_{33}$*, RE *Sac*I cut site GAGCTC was incorporated into the amplified fragments during PCR amplification by using pkMSP-1$_{33}$ forward and reverse primers which contained *Sac*I cut site sequence at the 5'- ends.

For *pkMSP-1$_{42}$*, RE *Bam*HI cut site GGATCC was incorporated into the amplified fragments during PCR amplification.

Agarose gel electrophoresis was performed on the PCR products to determine the size of the amplified fragments. Figure 4.1 showed the (a) amplified *pkMSP-1$_{33}$* fragment with the expected size of 705 base pairs (bp) and (b) amplified *pkMSP-1$_{42}$* fragment with the expected size of 984 bp.

4.2 Cloning of PCR products into pCR® 2.1-TOPO® vector

4.2.1 Ligation of PCR products to pCR® 2.1-TOPO® vector

PCR products were ligated to pCR® 2.1-TOPO® vector by using commercialised TOPO® TA cloning® kit (Invitrogen Corp., U.S.A.). *Taq* DNA polymerase used in PCR has a nontemplate-dependent terminal transferase activity that adds a single deoxyadenosine (A) overhangs to the 3' ends of PCR products. Hence, the linearized pCR® 2.1-TOPO® vector which has a single overhang 3'-deoxythymidine (T) residue facilitates the ligation of PCR products to the vector efficiently through A-T complementary pairing (Appendix 6).

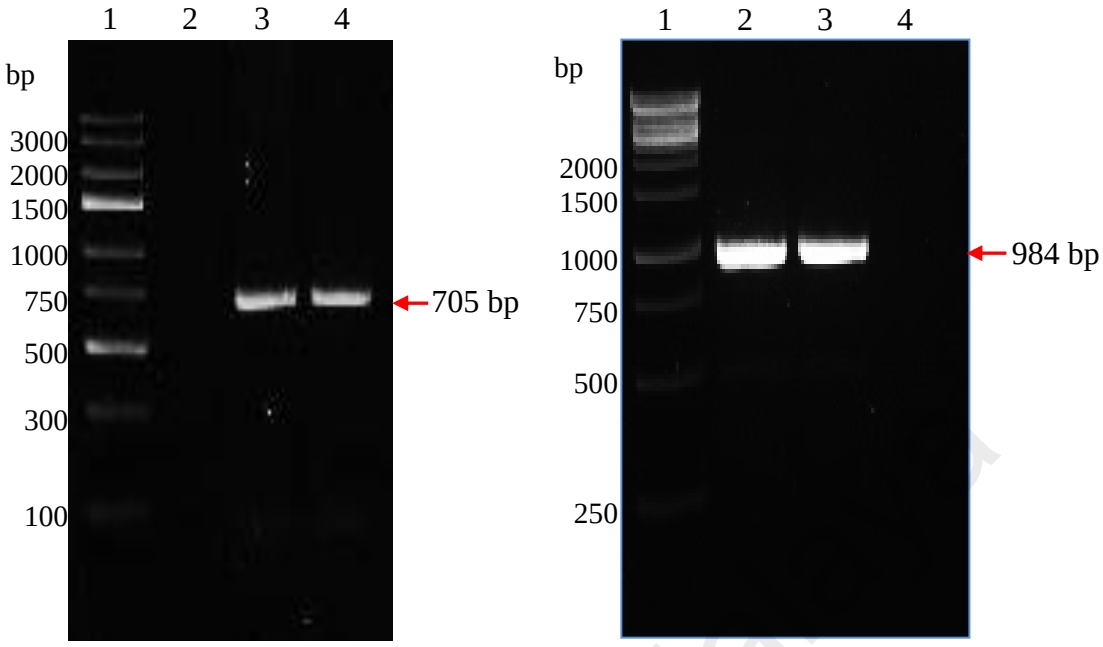

(a) (b)

Figure 4.1. Agarose gel electrophoresis of PCR products for (a) *pkMSP-1*$_{33}$ and (b) *pkMSP-1*$_{42}$ gene amplification respectively. (a) PCR of *pkMSP-1*$_{33}$ gene by using genomic DNA of *P. knowlesi* (extracted from knowlesi-infected patient bloods) generated a single bright band with the expected size of 705 bp (lanes 3 and 4, arrow). (b) PCR of *pkMSP-1*$_{42}$ gene by using genomic DNA of *P. knowlesi* generated a single bright band with the expected size of 984 bp (lanes 2 and 3, arrow). No band was observed for non-template negative control [lane 2 in (a) and lane 4 in (b)]. Lane 1 in both panels serves as DNA ladder.

Transformation into competent *E. coli* TOP 10F' cells was carried out and the cells were incubated overnight at 37 ℃. Approximately 80 colonies were growth on the incubated ampicillin plates.

4.2.2 Colony PCR for selection of positive recombinant clones

Four colonies on the transformation plates were chosen and colony PCR was performed by using M13 forward and M13 reverse primers. Agarose gel electrophoresis was performed on the PCR products to determine the size of the amplified fragments. Figure 4.2 showed the positive recombinant clones of (a) TOPO-*pkMSP-1*$_{33}$ with the expected size of ~1 kb (705 bp of *pkMSP-1*$_{33}$ plus ~300 bp of vector) and (b) TOPO-*pkMSP-1*$_{42}$ with the expected size of ~1.3 kb (984 bp of *pkMSP-1*$_{42}$ plus ~300 bp of vector). Non-recombinant clones (without inserted fragment) give a size of ~300 bp.

4.3 Cloning of target fragment into pRSET A

4.3.1 Digestion of recombinant TOPO-*pkMSP-1*$_{33}$, TOPO-*pkMSP-1*$_{42}$ and pRSET A plasmids with RE

The plasmids of positive TOPO-*pkMSP-1*$_{33}$ and TOPO-*pkMSP-1*$_{42}$ were extracted using QIAprep® spin Miniprep kit (Qiagen, Hilden, Germany).

The extracted TOPO-*pkMSP-1*$_{33}$ and pRSET A plasmids were digested with RE *Sac*I. The digested recombinant TOPO-*pkMSP-1*$_{33}$ plasmid generated a 3.9 kb TOPO plasmid and a ~700 bp inserted fragment, while digested pRSET A generated a linearized plasmid with a size of 2.9 kb (Figure 4.3a).

RE *Bam*HI was used to digest recombinant TOPO-*pkMSP-1*$_{42}$ and pRSET A plasmids. The digested recombinant TOPO-*pkMSP-1*$_{42}$ plasmid generated a

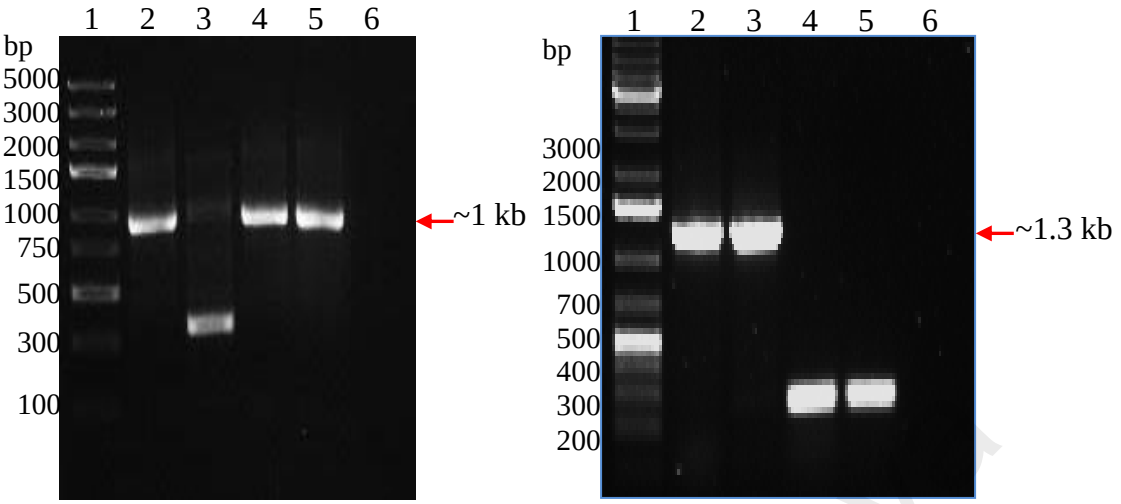

(a) (b)

Figure 4.2. Agarose gel electrophoresis of PCR products for selection of positive recombinant (a) TOPO-*pkMSP-1*$_{33}$ and (b) TOPO-*pkMSP-1*$_{42}$ respectively in TOP10F' cells. (a) PCR of the clones with insertion of DNA fragment generated expected PCR band of ~1 kb (lanes 2, 4 and 5, arrow). (b) PCR of the clones with insertion of DNA fragment generated expected PCR band of ~1.3 kb (lanes 2 and 3, arrow). PCR of the clones without insertion of DNA fragment generated expected PCR band of ~300 bp [lane 3 in (a) and lanes 4 and 5 in (b)]. No band was observed for non-template negative control (lane 6 in both panels). Lane 1 in both panels serves as DNA ladder.

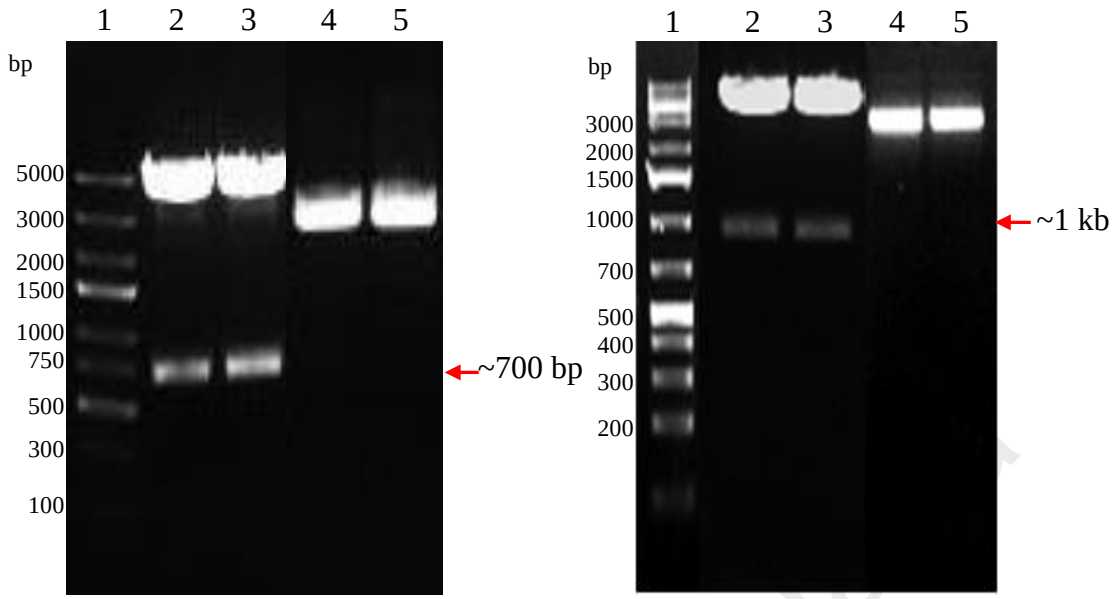

(a) (b)

Figure 4.3. Restriction digestion of pRSET A plasmid with (a) recombinant TOPO-*pkMSP-1*$_{33}$ plasmid and (b) recombinant TOPO-*pkMSP-1*$_{42}$ plasmid respectively. (a) Digested TOPO-*pkMSP-1*$_{33}$ plasmid generated a 3.9 kb TOPO plasmid and a ~700 bp *pkMSP-1*$_{33}$ target fragment (lanes 2 and 3, arrow). (b) Digested TOPO-*pkMSP-1*$_{42}$ plasmid generated a TOPO plasmid and a ~1 kb *pkMSP-1*$_{42}$ target fragment (lanes 2 and 3, arrow). Lanes 4 and 5 in both panels showed digested pRSET A plasmid with a size of 2.9 kb. Lane 1 in both panels serves as DNA ladder.

3.9 kb TOPO plasmid and a ~1 kb inserted fragment, while digested pRSET A had a size of 2.9 kb (Figure 4.3b).

Agarose gel electrophoresis was performed on digested recombinant TOPO-*pkMSP-1*$_{33}$, TOPO-*pkMSP-1*$_{42}$ and pRSET A plasmids using 0.8% agarose gel. The target fragments and pRSET A plasmid were excised from gel and purified using QIAquick® gel extraction kit (Qiagen, Hilden, Germany).

4.3.2 Directional PCR and selection of positive recombinant clones

Purified target fragments were ligated to pRSET A vector and transformed into propagation and maintenance host *E. coli* TOP10F' cells. Five colonies on the transformation plates were chosen and directional PCR was performed to check the orientation of the cloned fragments.

For selection of positive recombinant pRSET A-*pkMSP-1*$_{33}$, pkMSP-1$_{33}$ forward primer and T7 terminator primer were used, while pkMSP-1$_{42}$ forward primer and T7 terminator primer were used to select positive recombinant pRSET A-*pkMSP-1*$_{42}$.

Figure 4.4 showed the agarose gel electrophoresis of the PCR products, which the (a) positive recombinant pRSET A-*pkMSP-1*$_{33}$ clones with insert in the sense orientation showed a size of ~850 bp (705 bp of *pkMSP-1*$_{33}$ plus ~150 bp of vector), while (b) positive recombinant pRSET A-*pkMSP-1*$_{42}$ clones with insert in the sense orientation showed a size of ~1.15 kb (984 bp of *pkMSP-1*$_{42}$ plus ~150 bp of vector). No amplification was detected for non-recombinant clones or clones with insert in the antisense orientation.

The plasmids of positive recombinant clones were extracted and transformed into expression host *E. coli* BL21 (DE3)pLysS cells. Five colonies

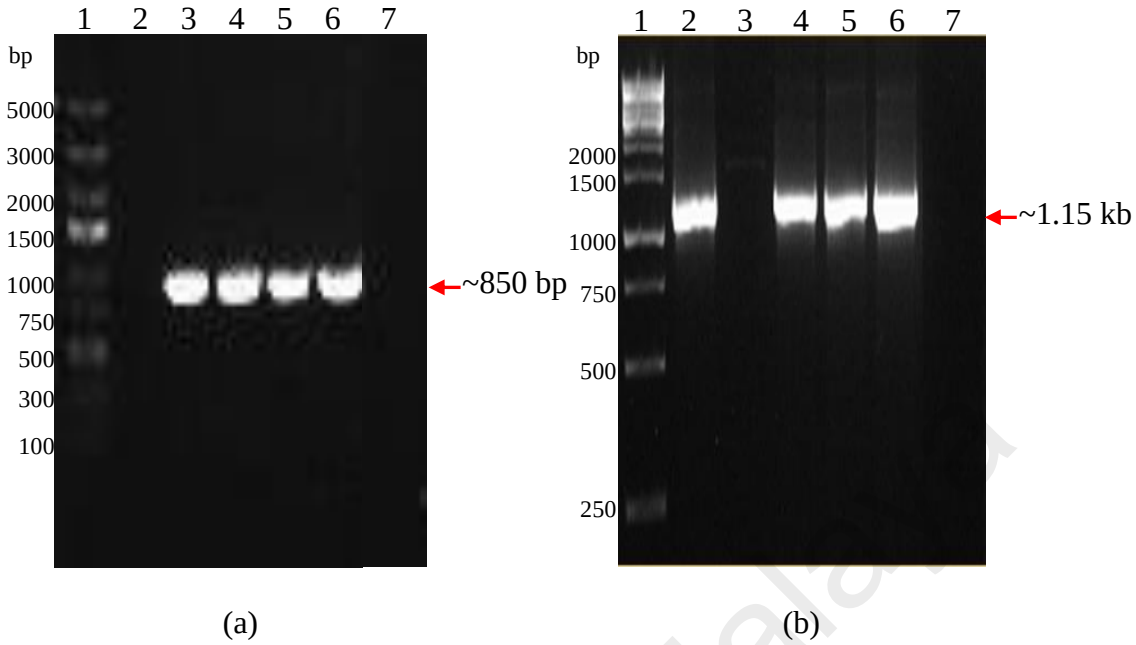

(a) (b)

Figure 4.4. Agarose gel electrophoresis of PCR products for selection of positive recombinant (a) pRSET A-*pkMSP-1*$_{33}$ and (b) pRSET A-*pkMSP-1*$_{42}$ respectively in TOP10F' cells. (a) PCR of the clones with insert in the sense orientation generated expected PCR band of ~850 bp (lanes 3 to 6, arrow). (b) PCR of the clones with insert in the sense orientation generated expected PCR band of ~1.15 kb (lanes 2, 4 to 6, arrow). As expected PCR of the clones with insert in the antisense orientation showed no band [lane 2 in (a) and lane 3 in (b)]. No band was observed in non-template negative control (lane 7 in both panels). Lane 1 in both panels represents the DNA ladder.

were chosen from the transformation plates and directional PCR was performed as mentioned above. Figure 4.5 demonstrated that all colonies selected were positive recombinant clones with insert in the sense orientation which have size of ~850 bp for (a) recombinant pRSET A-*pkMSP-1*$_{33}$ and size of ~1.15 kb for (b) pRSET A-*pkMSP-1*$_{42}$.

4.4 Confirmation of nucleotide and amino acid sequences of inserted fragments

Nucleotide sequencing for recombinant TOPO-*pkMSP-1*$_{33}$, pRSET A-*pkMSP-1*$_{33}$, TOPO-*pkMSP-1*$_{42}$ and pRSET A-*pkMSP-1*$_{42}$ plasmids was done by sequencing services from company. The nucleotide sequences of inserted fragments were analysed (Appendix 7) and BLAST was used to compare the nucleotide sequences with previously published *P. knowlesi MSP-1*$_{33}$ and *MSP-1*$_{42}$ gene sequences. The identity of the inserted fragments was confirmed as *P. knowlesi MSP-1*$_{33}$ and *MSP-1*$_{42}$, which both the nucleotide sequences were 99% identical to the GenBank *P. knowlesi* strain H *MSP-1* reference sequence (Accession number: XM_002258546) (Appendix 8). The amino acid sequences of inserted fragments were deduced by using software Gene Runner (Appendix 9) and BLAST results indicated that both the deduced pkMSP-1$_{33}$ and pkMSP-1$_{42}$ protein sequences also had an identity of 99% to the GenPept *P. knowlesi* strain H MSP-1 reference sequence (Accession number: XM_002258582) (Appendix 10).

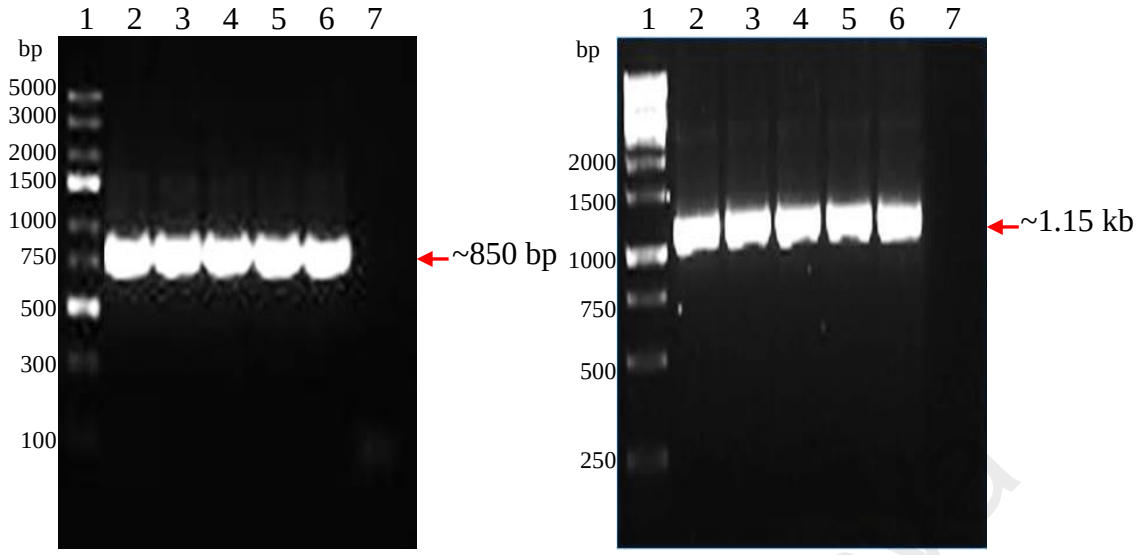

(a) (b)

Figure 4.5. Agarose gel electrophoresis of PCR products for selection of positive recombinant (a) pRSET A-*pkMSP-1*$_{33}$ and (b) pRSET A-*pkMSP-1*$_{42}$ respectively in BL21 (DE3)pLysS cells. (a) PCR of the clones with insert in the sense orientation generated expected PCR band of ~850 bp (lanes 2 to 6, arrow). (b) PCR of the clones with insert in the sense orientation generated expected PCR band of ~1.15 kb (lanes 2 to 6, arrow). No band was observed in non-template negative control (lane 7 in both panels). Lane 1 in both panels represents the DNA ladder.

4.5 Protein expression of recombinant pkMSP-1_{33} and pkMSP-1_{42} in *E. coli* expression system

Culture sample fragments (1 ml) were collected before IPTG induction and every two hours after induction up to four hours. Protein samples from different time points were electrophoresed on 12% SDS-PAGE gels. The gels were then stained with Coomassie Brilliant Blue and destained with destaining solution. The separated proteins also electrophorectically transferred onto PVDF membrane and analysed in Western Blot assays by using anti-Xpress™ monoclonal antibody which specifically detect the Xpress leader peptide (-Asp-Leu-Tyr-Asp-Asp-Asp-Asp-Lys-) in pRSET vector. Figure 4.6 and 4.7 indicated the protein expressions of (a) recombinant pkMSP-1_{33} and (b) recombinant pkMSP-1_{42}, with molecular mass of ~28 kDa and ~42 kDa, respectively. Protein expression could be observed two hours after induction, and the band intensity did not increase at four hours after induction. Therefore, both the recombinant pkMSP-1_{33} and pkMSP-1_{42} could be expressed optimally after two hours of induction with 1 mM IPTG at 37℃ with constant shaking speed of 250 rpm. The same band was not observed in the negative control pRSET A clone.

4.6 Purification and dialysis of recombinant pkMSP-1_{33} and pkMSP-1_{42}

Protein purification was done by using ProBond™ purification system. The purified and dialysed proteins were electrophoresed on SDS-PAGE gel and analysed with Western Blot assays. The purified (a) pkMSP-1_{33} and (b) pkMSP-1_{42} showed a distinct band of ~28 kDa and ~42 kDa respectively, which was absent in the purified pRSET A (Figure 4.8 and 4.9).

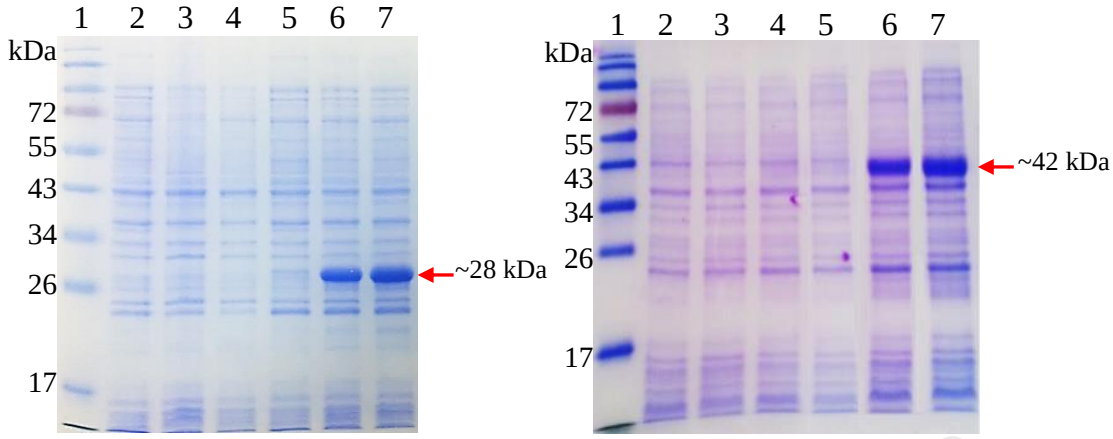

(a) (b)

Figure 4.6. Coomassie brilliant blue-stained SDS gel of protein expression the recombinant clones. Panel (a) represents recombinant pkMSP-1_{33}. Lanes 2, 3 and 4 represent pRSET A at 0, 2 and 4 hours after IPTG induction respectively; lanes 5, 6 and 7 represent recombinant pkMSP-1_{33} at 0, 2 and 4 hours after induction respectively. The pkMSP-1_{33} with a size of ~28 kDa was detected after two hours (arrow). Panel (b) represents recombinant pkMSP-1_{42}. Lanes 2, 3 and 4 represent pRSET A at 0, 2 and 4 hours after IPTG induction respectively; lanes 5, 6 and 7 represent recombinant pkMSP-1_{42} at 0, 2 and 4 hours after induction respectively. The pkMSP-1_{42} with a size of ~42 kDa was detected after two hours (arrow). Lane 1 in both panels was Bio-Rad Prestained Broad Range Protein Marker.

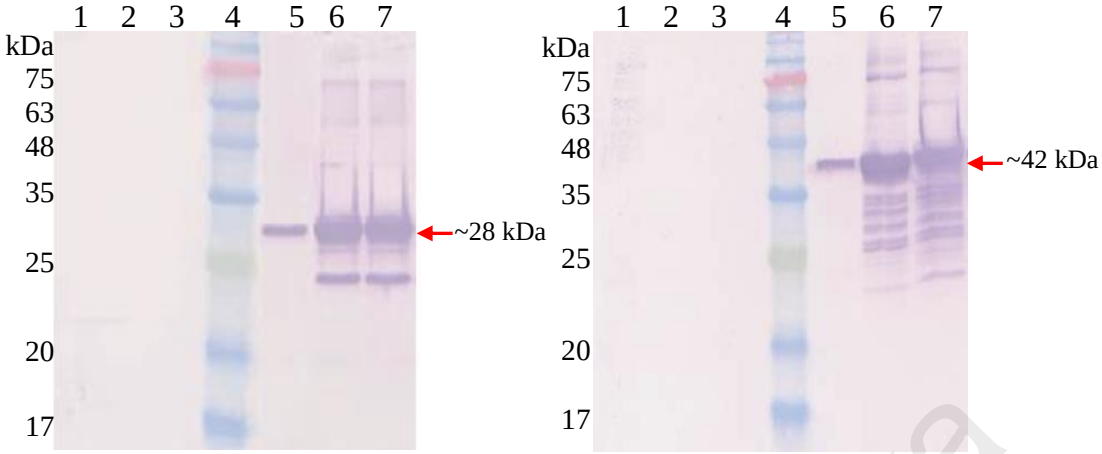

(a) (b)

Figure 4.7. Western Blot assay of protein expression of the recombinant clones. Panel (a) represents recombinant pkMSP-1_{33} probed with anti-Xpress™ antibody. Lanes 1, 2 and 3 represent pRSET A at 0, 2 and 4 hours after IPTG induction respectively; lanes 5, 6 and 7 represent recombinant pkMSP-1_{33} at 0, 2 and 4 hours after induction respectively. The ~28 kDa pkMSP-1_{33} was detected after two hours (arrow). Panel (b) represents recombinant pkMSP-1_{42} probed with anti-Xpress™ antibody. Lanes 1, 2 and 3 represent pRSET A at 0, 2 and 4 hours after IPTG induction respectively; lanes 5, 6 and 7 represent recombinant pkMSP-1_{42} at 0, 2 and 4 hours after induction respectively. The ~42 kDa pkMSP-1_{42} was detected after two hours (arrow). Lane 4 in both panels was Bio-Rad Prestained Broad Range Protein Marker.

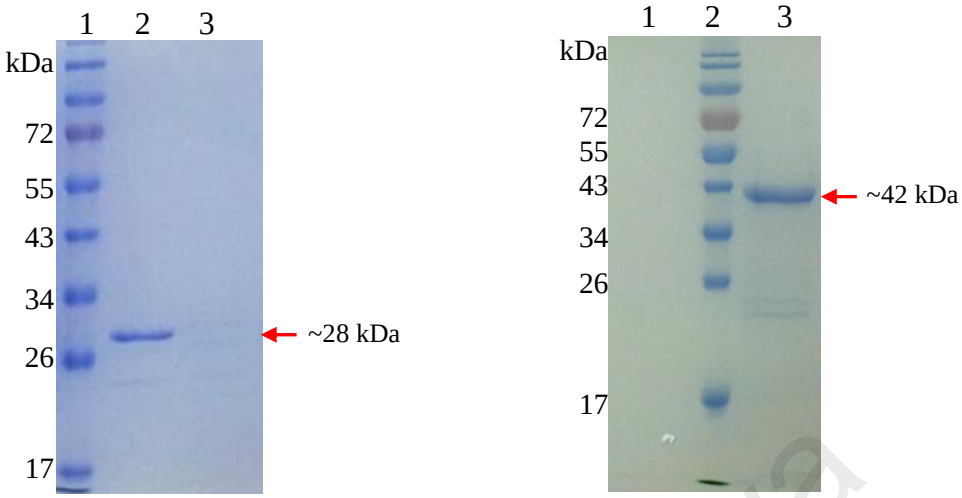

(a) (b)

Figure 4.8. Coomassie brilliant blue-stained SDS gel of (a) purified pkMSP-1_{33} and (b) purified pkMSP-1_{42}. (a) A distinct band of ~28 kDa was detected in purified pkMSP-1_{33} clone (lane 2, arrow), but absent in purified pRSET A clone (lane 3). (b) A thick band with size of ~42 kDa was observed in purified pkMSP-1_{42} clone (lane 3, arrow), which was not detected in purified pRSET A clone (lane 1). Lane 1 in (a) and lane 2 in (b) was Bio-Rad Prestained Broad Range Protein Marker.

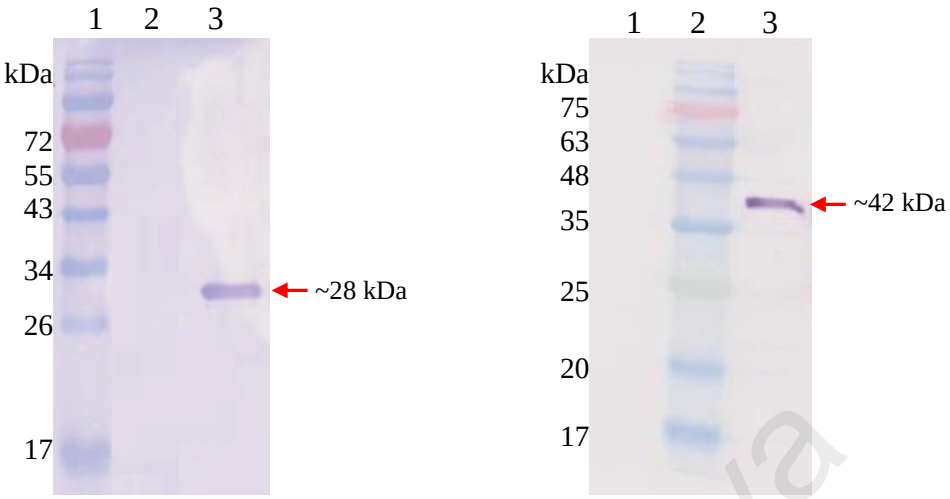

(a) (b)

Figure 4.9. Western Blot assay of (a) purified pkMSP-1_{33} and (b) purified pkMSP-1_{42} probed with anti-Xpress™ antibody. (a) A distinct band of ~28 kDa was detected in purified pkMSP-1_{33} clone (lane 3, arrow), but absent in purified pRSET A clone (lane 2). (b) A thick band with size of ~42 kDa was observed in purified pkMSP-1_{42} clone (lane 3, arrow), which was not detected in purified pRSET A clone (lane 1). Lane 1 in (a) and lane 2 in (b) was Bio-Rad Prestained Broad Range Protein Marker.

4.7 Quantification of concentration of purified pkMSP-1_{33} and pkMSP-1_{42}

Bradford protein assay was used to determine the concentration of the purified pkMSP-1_{33} and pkMSP-1_{42}. This assay is simple and accurate for determination of protein concentration in solution. The Coomassie brilliant blue G-250 dye, which was the 1X dye reagent used in the assay, binds to protein and the colour of dye changes. The dye was predominantly in the doubly protonated red cationic form when under acidic conditions, and it was converted to stable unprotonated blue form when it bound to proteins. This blue protein-dye form in the assay was then detected at wavelength 595 nm using microplate reader. Standard curve was generated by plotting the absorbance of standard BSA at 595 nm (Y axis) versus their concentration in mg/ml (X axis) (Appendix 11). The concentration of purified pkMSP-1_{33} and pkMSP-1_{42} was determined by interpolating from the pkMSP-1_{33} and pkMSP-1_{42} absorbance value (Y axis) to concentration (X axis) using the standard curve. The concentration of purified pkMSP-1_{33} obtained was ranged from 0.3 mg/ml to 1.0 mg/ml, while for pkMSP-1_{42} was 0.3 mg/ml to 1.2 mg/ml.

4.8 Evaluation of purified pkMSP-1_{33} and pkMSP-1_{42} in Western Blot assays and ELISA using patient sera

The purified pkMSP-1_{33} was evaluated in Western Blot assays and ELISA by using patient sera of categories: (A) *P. knowlesi* (B) non-knowlesi human malaria (C) non-malarial parasitic infections and (D) healthy donor. In Western Blot assays (Figure 4.10), the purified pkMSP-1_{33} was able to detect all *P. knowlesi* infection, which resembles 100% sensitivity towards knowlesi infection (31/31). Results indicated that 96.4% of the 28 samples of *P. vivax, P.*

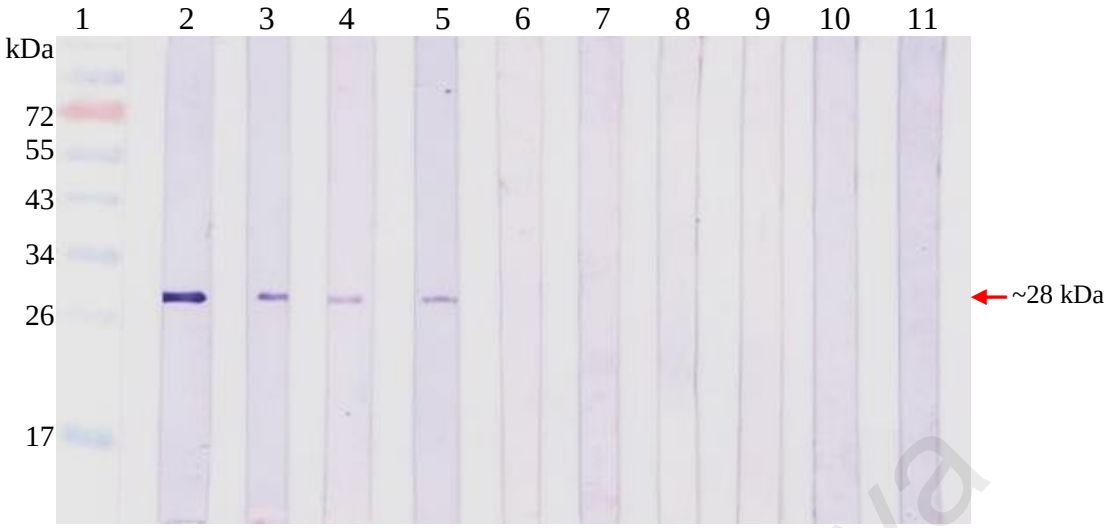

Figure 4.10. Western Blot assays of pkMSP-1_{33} probed with patient sera infected by *P. knowlesi*, non-knowlesi human malaria, non-malarial parasites and healthy donor. Each Western Blot strip which contained 70 ng of the purified pkMSP-1_{33} was tested with serum from each category. Selected samples from each category are shown. pkMSP-1_{33} reacted with sera of patients infected with malaria: *P. knowlesi* (lanes 2 and 3), *P. falciparum* (lane 4), *P. vivax* (lane 5) (arrow). Lanes 6 to10 contained sera of patients infected with non-malarial parasites: filariasis (lane 6), amoebiasis (lane 7), toxoplasmosis (lane 8), cysticercosis (lane 9), toxocarasis (lane 10). Lane 11 contained healthy donor serum which served as negative control. Lane 1 contained Bio-Rad Prestained Broad Range Protein Marker.

falciparum and *P. ovale* (non-knowlesi malarial infection) reacted with pkMSP-1_{33} (27/28). Hence, the overall sensitivity of pkMSP-1_{33} for detection of malarial infection was 98.3% (58/59). Only three sera samples among 117 non-*Plasmodium* and healthy donor sera reacted with pkMSP-1_{33}. The specificity was then determined as 97.4% (114/117). In ELISA, the sensitivity of pkMSP-1_{33} towards knowlesi infection and non-knowlesi malarial infection was 80.7% (25/31) and 71.4% (20/28) respectively, with the overall sensitivity for malarial detection 76.3% (45/59). There are six samples of non-*Plasmodium* parasitic infection sera and healthy donor sera that reacted with recombinant pkMSP-1_{33}, which lead to the specificity of 94.9% (111/117). Evaluation of pkMSP-1_{33} with patient sera by using Western Blot assays and ELISA is summarised in Table 4.1.

The pkMSP-1_{42} was evaluated with patient sera of same categories as pkMSP-1_{33}. In Western Blot assays (Figure 4.11), pkMSP-1_{42} reacted with 86.8% (33/38) of knowlesi malaria serum samples and 96.6% (28/29) of non-knowlesi malaria serum samples. Therefore, the overall sensitivity of pkMSP-1_{42} for malarial detection was 91.0% (61/67). Three of the 122 non-*Plasmodium* parasitic infection and healthy donor sera reacted with pkMSP-1_{42}, giving a specificity of 97.5% (119/122). In ELISA, pkMSP-1_{42} reacted with 34 of 38 knowlesi malaria serum samples, thus giving sensitivity of 89.5% for knowlesi malaria detection (34/38). A total of 93.1% (27/29) of non-knowlesi malaria serum samples reacted with pkMSP-1_{42}. Therefore, the overall sensitivity for detection of malarial infection was 91.0% (61/67). The specificity of ELISA was 92.6% (113/122). Table 4.2 represented the evaluation of pkMSP-1_{42} with patient sera by using Western Blot assays and ELISA.

Table 4.1. Evaluation of purified pkMSP-1_{33} with patient sera in Western Blot assays and ELISA

Human Sera Group	Number of Sera	Western Blot		ELISA	
		Positive (No.)	Negative (No.)	Positive (No.)	Negative (No.)
A. *Plasmodium knowlesi*	31	31	0	25	6
B. Non-knowlesi human malaria					
i. *P. vivax*	16	16	0	11	5
ii. *P. falciparum*	11	10	1	9	2
iii. *P. ovale*	1	1	0	0	1
C. Non-malarial parasitic infection					
i. Filariasis	4	1	3	1	3
ii. Amoebiasis	16	1	15	3	13
iii. Cysticercosis	12	0	12	0	12
iv. Toxoplasmosis	17	1	16	2	15
v. Toxocarasis	3	0	3	0	3
D. Healthy donor	65	0	65	0	65

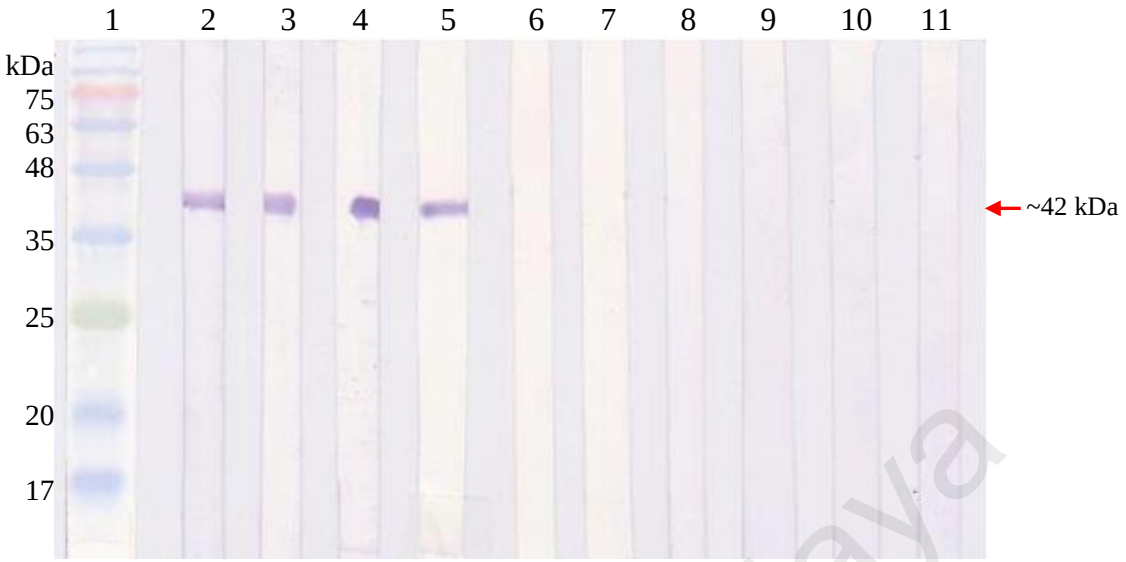

Figure 4.11. Western Blot assays of pkMSP-1_{42} probed with patient sera infected by *P. knowlesi*, non-knowlesi human malaria, non-malarial parasites and healthy donor. Each Western Blot strip which contained 60 ng of the purified pkMSP-1_{42} was tested with serum from each category. Selected samples from each category are shown. pkMSP-1_{42} reacted with sera of patients infected with malaria: *P. knowlesi* (lanes 2 and 3), *P. falciparum* (lane 4), *P. vivax* (lane 5) (arrow). Lanes 6 to10 contained sera of patients infected with non-malarial parasites: filariasis (lane 6), amoebiasis (lane 7), toxoplasmosis (lane 8), cysticercosis (lane 9), toxocarasis (lane 10). Lane 11 contained healthy donor serum which served as negative control. Lane 1 contained Bio-Rad Prestained Broad Range Protein Marker.

Table 4.2. Evaluation of pkMSP-1_{42} with patient sera in Western Blot assays and ELISA

Human sera group	Number of sera	Western Blot		ELISA	
		Positive (No.)	Negative (No.)	Positive (No.)	Negative (No.)
A. *P. knowlesi*	38	33	5	34	4
B. Non-knowlesi human malaria					
i. *P. vivax*	15	14	1	14	1
ii. *P. falciparum*	13	13	0	12	1
iii. *P. ovale*	1	1	0	1	0
C. Non-malarial parasitic infection					
i. Filariasis	4	1	3	0	4
ii. Amoebiasis	16	2	14	4	2
iii. Cysticercosis	13	0	13	2	11
iv. Toxoplasmosis	11	0	11	1	10
v. Toxocarasis	3	0	3	1	2
D. Healthy donor	75	0	75	1	74

Table 4.3 summarised the sensitivity and specificity of purified pkMSP-1_{33} and pkMSP-1_{42} for detection of malarial infection in Western Blot assays and ELISA.

4.9 Immunogenicity tests of purified pkMSP-1_{42} using mouse model

4.9.1 Measurement of cytokine levels in mice

4.9.1.1 Mouse IL-2 ELISA

Mouse IL-2 in culture supernatants was quantified by using commercialised mouse IL-2 ELISA kit (Thermo Scientific, U.S.A.) with protocol provided. Standard curve was generated by plotting the average absorbance obtained at 450 nm for each standard concentration on the Y axis versus the corresponding IL-2 concentration (pg/ml) in the X axis (Appendix 12). The IL-2 amount in each sample was determined by interpolating from the sample absorbance value (Y axis) to IL-2 concentration (X axis) using the standard curve. From the results, IL-2 of pRSET A-immunized mice group had a value of [75.8 (60.0-86.1)] pg/ml, while pkMSP-1_{42}-immunized mice group was [280.0 (268.1-287.0)] pg/ml. Mann-Whitney statistical test was performed and the IL-2 level of pkMSP-1_{42}-immunized mice group was significantly higher than those of the negative control group, with a *P* value of 0.008 (Figure 4.12).

4.9.1.2 Mouse IL-4 ELISA

Mouse IL-4 in culture supernatants was quantified by using commercialised mouse IL-4 ELISA kit (Thermo Scientific, U.S.A.) with protocol provided. Standard curve was generated by plotting the average absorbance obtained at 450 nm for each standard concentration on the Y axis

Table 4.3. Sensitivity and specificity of pkMSP-1_{33} and pkMSP-1_{42} for detection of malarial infection in Western Blot assays and ELISA

Antigen	Assay	Sensitivity (%)			Specificity (%)
		knowlesi infection	Non-knowlesi malarial infection	Overall	
pkMSP-1_{33}	Western Blot	100.0	96.4	98.3	97.4
	ELISA	80.7	71.4	76.3	94.9
pkMSP-1_{42}	Western Blot	86.8	96.6	91.0	97.5
	ELISA	89.5	93.1	91.0	92.6

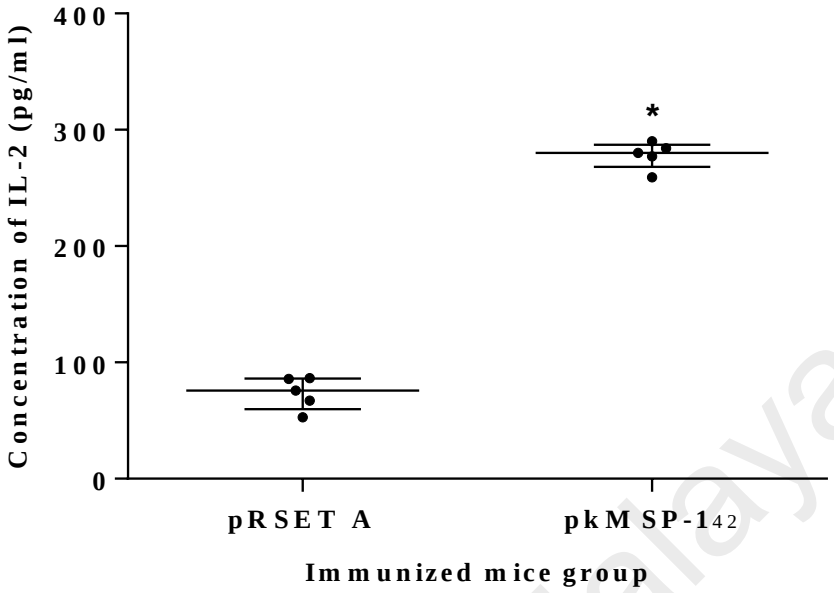

Figure 4.12. Level of cytokine IL-2 in pRSET A-immunized mice group and pkMSP-1_{42}-immunized mice group. Data shown were median with interquartile range in each group (n = 5). Level of IL-2 in pkMSP-1_{42}-immunized mice group was significantly higher compared to pRSET A-immunized mice group. Note: *$P < 0.05$.

versus the corresponding IL-4 concentration (pg/ml) in the X axis (Appendix 13). The IL-4 amount in each sample was determined by interpolating from the sample absorbance value (Y axis) to IL-4 concentration (X axis) using the standard curve. From the results, IL-4 of pRSET A-immunized mice group had a value of [3.4 (0.7-6.8)] pg/ml, while pkMSP-1_{42}-immunized mice group was [91.0 (56.6-146.2)] pg/ml. Mann-Whitney statistical test was performed and the IL-4 level of pkMSP-1_{42}-immunized mice group was significantly higher than those of the negative control group, with a *P* value of 0.008 (Figure 4.13).

4.9.1.3 Mouse IL-10 ELISA

Mouse IL-10 in culture supernatants was quantified by using commercialised mouse IL-10 ELISA kit (Thermo Scientific, U.S.A.) with protocol provided. Standard curve was generated by plotting the average absorbance obtained at 450 nm for each standard concentration on the Y axis versus the corresponding IL-10 concentration (pg/ml) in the X axis (Appendix 14). The IL-10 amount in each sample was determined by interpolating from the sample absorbance value (Y axis) to IL-10 concentration (X axis) using the standard curve. From the results, IL-10 of pRSET A-immunized mice group had a value of [89.9 (82.9-131.8)] pg/ml, while pkMSP-1_{42}-immunized mice group was [156.7 (136.8-250.8)] pg/ml. Mann-Whitney statistical test was performed and the IL-10 level of pkMSP-1_{42}-immunized mice group was significantly higher than those of the negative control group, with a *P* value of 0.016 (Figure 4.14).

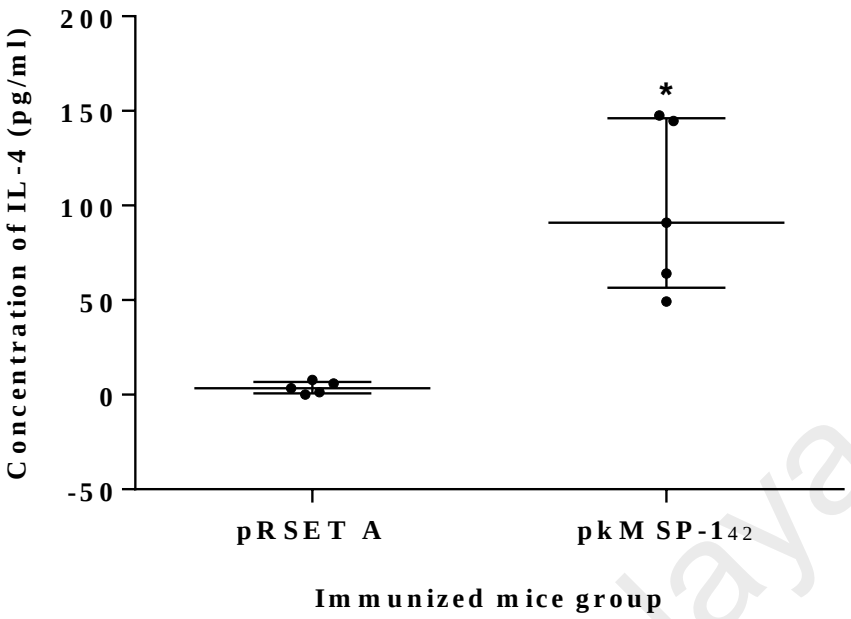

Figure 4.13. Level of cytokine IL-4 in pRSET A-immunized mice group and pkMSP-1_{42}-immunized mice group. Data shown were median with interquartile range in each group (n = 5). Level of IL-4 in pkMSP-1_{42}-immunized mice group was significantly higher compared to pRSET A-immunized mice group. Note: *$P < 0.05$.

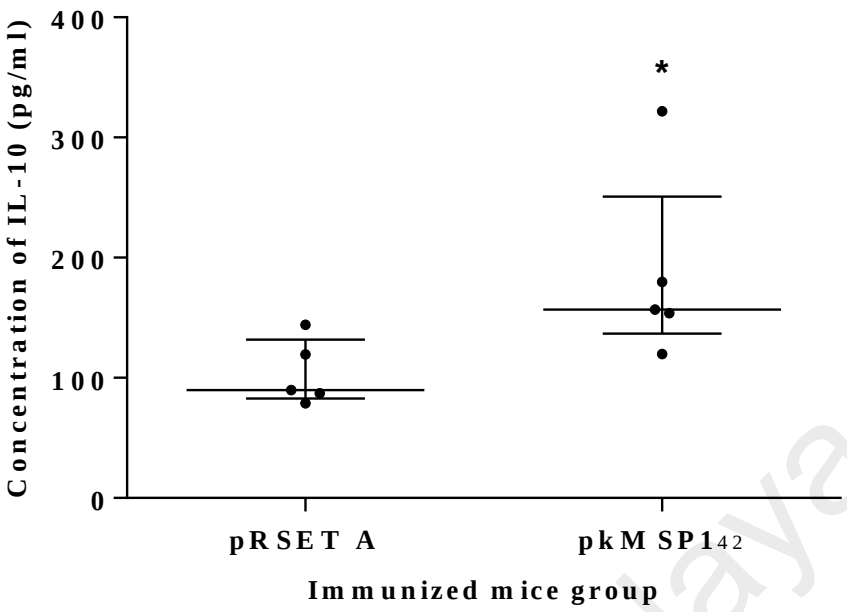

Figure 4.14. Level of cytokine IL-10 in pRSET A-immunized mice group and pkMSP-1_{42}-immunized mice group. Data shown were median with interquartile range in each group (n = 5). Level of IL-10 in pkMSP-1_{42}-immunized mice group was significantly higher compared to pRSET A-immunized mice group. Note: *$P < 0.05$.

4.9.1.4 Mouse IFN-γ ELISA

Mouse IFN-γ in culture supernatants was quantified by using commercialised mouse IFN-γ ELISA kit (Thermo Scientific, U.S.A.) with protocol provided. Standard curve was generated by plotting the average absorbance obtained at 450 nm for each standard concentration on the Y axis versus the corresponding IFN-γ concentration (pg/ml) in the X axis (Appendix 15). The IFN-γ amount in each sample was determined by interpolating from the sample absorbance value (Y axis) to IFN-γ concentration (X axis) using the standard curve. From the results, IFN-γ of pRSET A-immunized mice group had a value of [165.7 (0.0-411.9)] pg/ml, while pkMSP-1_{42}-immunized mice group was [2262.0 (1515.0-2437.0)] pg/ml. Mann-Whitney statistical test was performed and the IFN-γ level of pkMSP-1_{42}-immunized mice group was significantly higher than those of the negative control group, with a *P* value of 0.008 (Figure 4.15). Cytokine profiles of pRSET A-immunized mice and pkMSP-1_{42}-immunized mice were summarised in Table 4.4.

4.9.2 Characterization of raised antibodies in mice

4.9.2.1 Detection of anti-pkMSP-1_{42} antibodies in mice sera using Western Blot assays

Antibody responses in mice towards pkMSP-1_{42} at different time points were analysed. Immunized mice sera at different time point were collected and evaluated using Western Blot assays. Western Blot strips showed that antibodies against pkMSP-1_{42} were detected one week after prime boost. Purified pkMSP-1_{42} reacted with pkMSP-1_{42}-immunized mice sera at day 7, 14, 21 and 31 post-immunization, while no reactivity was observed in the negative control mice sera throughout the whole immunization period (Figure 4.16).

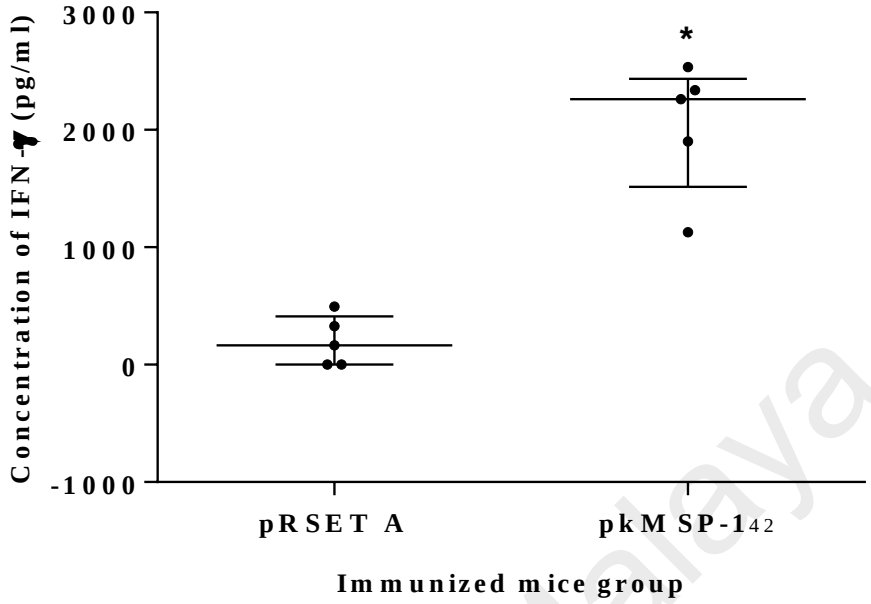

Figure 4.15. Level of cytokine IFN-γ in pRSET A-immunized mice group and pkMSP-1_{42}-immunized mice group. Data shown were median with interquartile range in each group (n = 5). Level of IFN-γ in pkMSP-1_{42}-immunized mice group was significantly higher compared to pRSET A-immunized mice group. Note: **P* < 0.05.

Table 4.4. Cytokine profiles of pRSET A-immunized mice and pkMSP-1_{42}-immunized mice

Antigen	IL-2	IL-4	IL-10	IFN-γ
pRSET A	75.8 (60.0-86.1)	3.4 (0.7-6.8)	89.9 (82.9-131.8)	165.7 (0.0-411.9)
pkMSP-1_{42}	280.0 (268.1-287.0)*	91.0 (56.6-146.2)*	156.7 (136.8-250.8)*	2262.0 (1515.0-2437.0)*
	P = 0.008	P = 0.008	P = 0.016	P = 0.008

Note: Values shown were median (interquartile range). IL-2, interleukin-2; IL-4, interleukin-4; IL-10, interleukin-10; IFN-γ, interferon-gamma.

Concentration of cytokines in pg/ml. * $P < 0.05$.

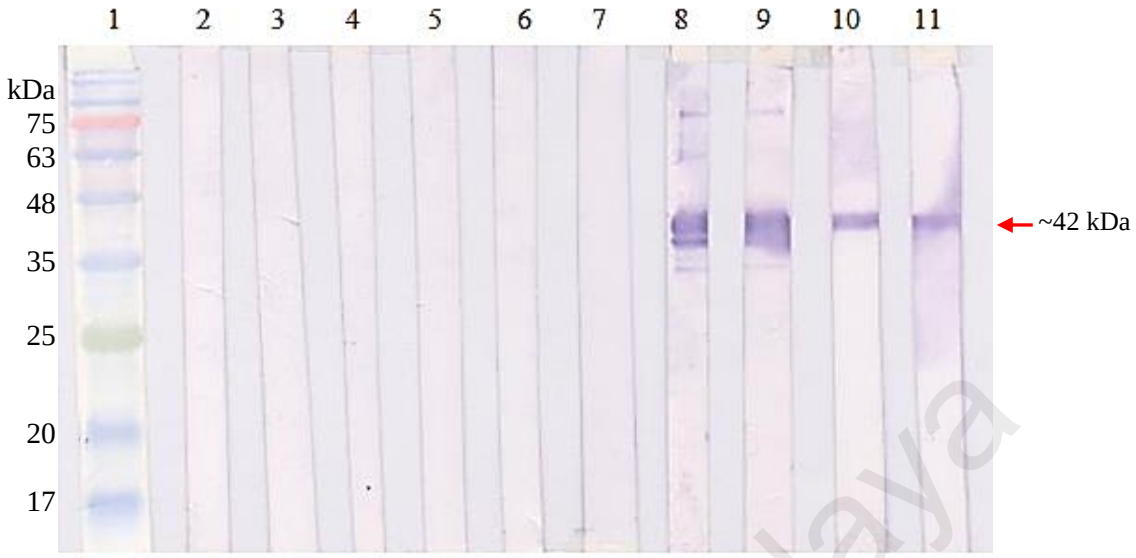

Figure 4.16. Western Blot assays of pkMSP-1_{42} probed with pRSET A-immunized mice sera and pkMSP-1_{42}-immunized mice sera collected at different time point. Lanes 2 to 6 contained sera of mice injected with non-recombinant protein pRSET A at day 0, 7, 14, 21 and 31 post-immunization respectively; lanes 7 to 11 contained sera of mice injected with purified pkMSP-1_{42} at day 0, 7, 14, 21 and 31 post-immunization respectively. Lane 1 contained Bio-Rad Prestained Broad Range Protein Marker. Anti-pkMSP-1_{42} antibodies were detected in pkMSP-1_{42}-immunized mice one week after prime boost and throughout the whole immunization period (arrow) but not in pRSET A-immunized mice.

4.9.2.2 Measurement of IgM and IgG level in mice sera using ELISA

Level of IgM and IgG in pkMSP-1_{42}-immunized mice sera was measured by ELISA. Results indicated that both IgM and IgG were detected in sera one week after prime boost. IgM level slightly decreased from day 14 until day 31 post-immunization. IgG level was relatively lower than IgM at first week after prime boost, yet high response was detected at day 14 post-immunization and continued to rise until day 31 post-immunization (Figure 4.17).

4.9.2.3 Determination of IgG isotype distribution

IgG isotype distribution in pkMSP-1_{42}-immunized mice sera was determined by ELISA. The predominant IgG isotype in mice sera was IgG1. The IgG2b level was slightly lower than the IgG1 level, followed by IgG3, while IgG2a was the least-detected IgG isotype in the mice sera (Figure 4.18).

4.9.2.4 Determination of endpoint titre of mice sera

Endpoint titre of antibodies in pkMSP-1_{42}-immunized mice sera was determined by ELISA. High antibody response towards pkMPS-1_{42} was observed, with the endpoint titre ranging between 1:204,800 and 1:819,200.

4.9.2.5 Determination of reactivity of immunized mice sera against *P. knowlesi* parasites using IFA

Anti-pkMSP-1_{42} antibodies were tested for their ability to recognise the *P. knowlesi* protein by using thin blood smear of *P. knowlesi*-infected patient blood. DAPI is a fluorescent stain that binds to DNA. DAPI has an absorption maximum at a wavelength of 358 nm (ultraviolet) and emission

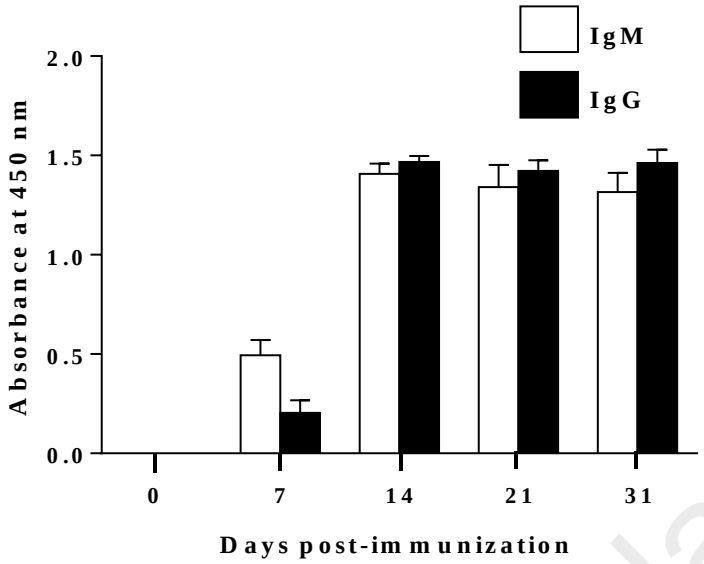

Figure 4.17. IgM and IgG levels in pkMSP-1_{42}-immunized mice. pkMSP-1_{42}-immunized mice sera with 1:200 dilution were used. Data shown were median with interquartile range. Both IgM and IgG were detected one week after prime boost and the levels increased few folds two weeks after prime boost. Both IgM and IgG levels were maintained at high level until day 31 post-immunization.

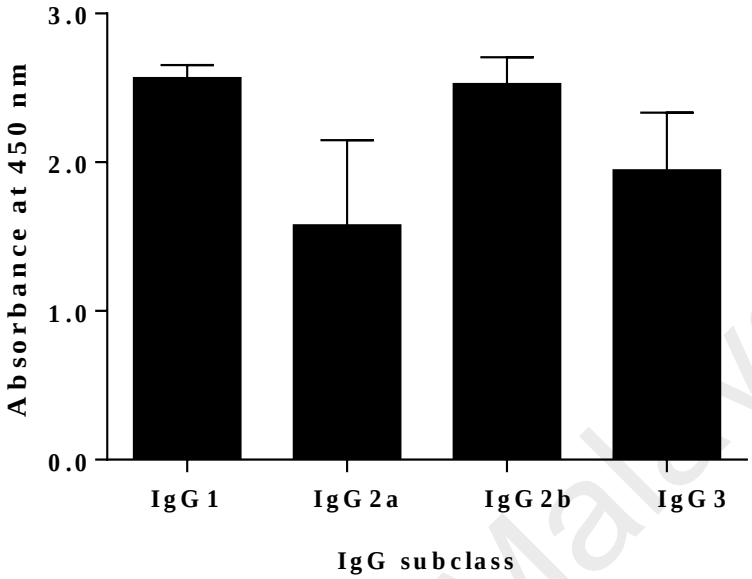

Figure 4.18. IgG isotype-specific antibody levels in pkMSP-1_{42}-immunized mice. pkMSP-1_{42}-immunized mice sera with 1:200 dilution were used. Data shown were median with interquartile range. The IgG isotype distribution in pkMSP-1_{42}-immunized mice was IgG1 > IgG2b > IgG3 > IgG2a.

maximum at 461 nm (blue) when bound to double-stranded DNA. In fluorescence microscopy, DAPI is excited with ultraviolet light and is detected through a blue/cyan filter. FITC is a derivative of fluorescein, which is widely used as a fluorescent tracer in fluorescent microscopy. The absorbance peak of FITC is at 495 nm (blue), while its emission peak is at 519 nm (green). Hence, fluorescent green colour will be detected under FITC filter. In the present study, DAPI stain was used as an indicator of *P. knowlesi* blood stage parasites, as the nuclei of parasites showed bright blue fluorescence under DAPI filter. Fluorescence microscopy result indicated that recombinant pkMSP-1_{42} resembles the parasite protein as antibodies raised against pkMSP-1_{42} were able to recognise *P. knowlesi* blood stage parasites in IFA. Parasites probed with pkMSP-1_{42}-immunized mice sera exhibited bright green fluorescence under FITC filter, while no recognition was found using pRSET A-immunized mice sera (Figure 4.19).

4.10 Identification and characterization of potential epitopes on *P. knowlesi* MSP-1_{42} by using pkMSP-1_{42}-immunized mice sera and synthetic peptide library

Epitope mapping of antibody responses using pkMSP-1_{42}-immunized mice sera was done with synthetic peptide library which consists of all potential epitopes in *P. knowlesi* MSP-1_{42}. Figure 4.20 demonstrated the reactivity of pkMSP-1_{42}-immunized mice sera (n = 16) towards each peptide. Reactivity strength of each serum towards each peptide was categorized into four groups: Negative, low, moderate and high reactivity, based on their value of absorbance at 450 nm. Mann-Whitney test was performed and pkMSP-1_{42}-immunized mice

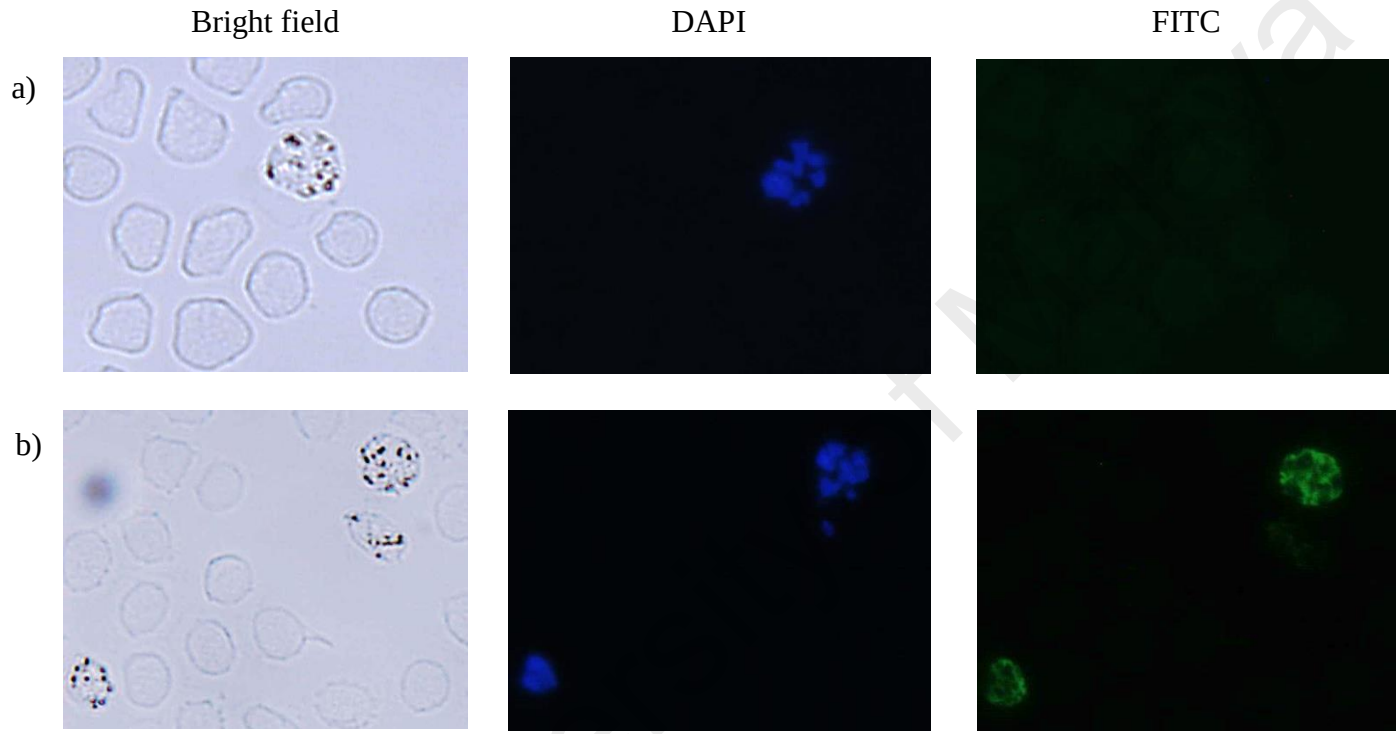

Figure 4.19. Fluorescence microscopy examination of *P. knowlesi*-positive blood smear probed with (a) pRSET A-immunized mice sera and (b) pkMSP-1_{42}-immunized mice sera in IFA. Bright blue fluorescence was observed in both sets of experiment under DAPI filter indicated the presence and location of *P. knowlesi* blood stage parasites. Anti-pkMSP-1_{42} antibodies were able to recognise *P. knowlesi* blood stage parasites as green fluorescence was observed only in smear probed with pkMSP-1_{42}-immunized mice sera but not in smear probed with pRSET A-immunized mice sera under FITC filter.

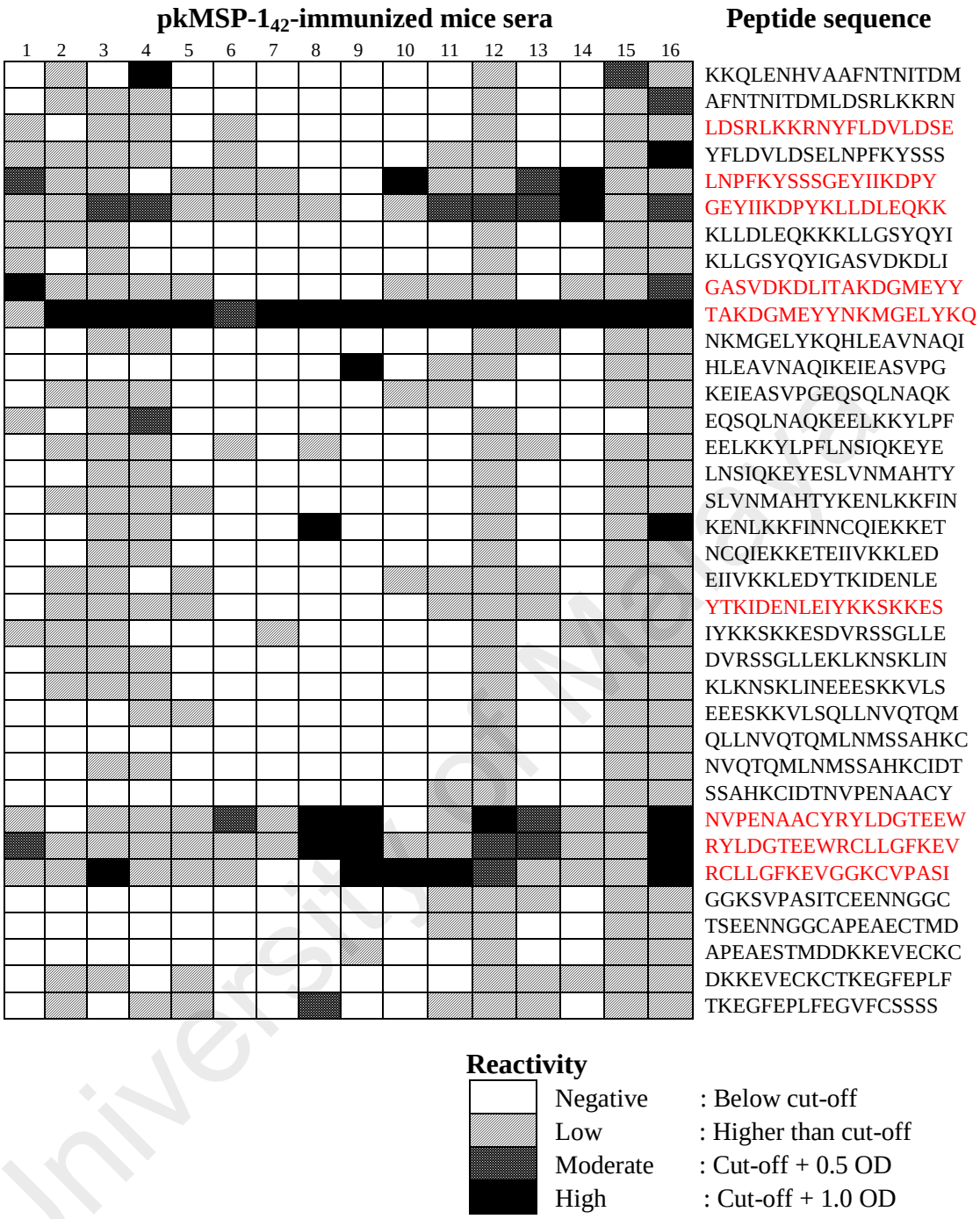

Figure 4.20. Reactivity of pkMSP-1$_{42}$-immunized mice sera with peptide library. Reactivity of each serum with individual peptides was shown as shaded box. The strength of reactivity was represented by the depth of shading. The sequences of each peptide representing *P. knowlesi* MSP-1$_{42}$ were indicated down the right hand side of the figure. A total of nine peptides (letter in red colour) had significant higher reactivity with pkMSP-1$_{42}$-immunized mice sera compared to negative control mice sera.

sera were found to have a significant higher reactivity towards nine peptides of 36 peptides in the peptide library, compared to negative control mice sera (Table 4.5). These nine peptides could be categorised into four groups based on the position of peptides in the primary sequence of *P. knowlesi* MSP-1_{42}.

4.11 Identification and characterization of potential epitopes on *P. knowlesi* MSP-1_{42} by using purified pkMSP-1_{42}-immunized mice sera and phage display library

Three rounds of panning were carried out using affinity purified anti-pkMSP-1_{42} antibodies coated-microtitre plates. Background levels of approximately 10^3 phage were recovered from wells with coating buffer only (negative control). After the final round of panning with anti-pkMSP-1_{42} antibodies, the amount of phage eluted were approximately 130 times higher than the background phage level. The titre of unamplified phage and amplified phage in three rounds of panning was summarised in Table 4.6.

Several hundred individual phage clones from the final round of panning were screened in ELISA in order to determine their binding avidity towards anti-pkMSP-1_{42} antibodies. The phage clones with absorbance reading approximately three to four times higher than` background (wells without presence of phage) were considered positive clones. The nucleotide sequence of 63 positive clones was analysed and some of the clones carried the same peptide. For instance, SNLSWPANMKHP and TWHHSYFNSVRV were sequenced 23 times and 22 times, respectively. A total of 14 different peptides were isolated and these peptides could be categorised into four groups that had homology with different regions of *P. knowlesi* MSP-1_{42} (Table 4.7). Most of the peptides (eight

Table 4.5. Identified potential epitopes on *P. knowlesi* MSP-1_{42} by using synthetic peptide library

Group		Sequence		*P* value
Group 1				
pkMSP-1_{42}	15	LDSRLKKRNYFLDVLDSELNPFKYSSSGEYIIKDPYKLLDLEQKK	59	
P3		LDSRLKKRNYFLDVLDSE		0.0424
P5		LNPFKYSSSGEYIIKDPY		< 0.0001
P6		GEYIIKDPYKLLDLEQKK		< 0.0001
Group 2				
pkMSP-1_{42}	69	GASVDKDLITAKDGMEYYKKMGELYKQ	95	
P9		GASVDKDLITAKDGMEYY		0.0034
P10		TAKDGMEYYNKMGELYKQ		< 0.0001
Group 3				
pkMSP-1_{42}	177	YTKIDENLEIYKKSKKES	194	
P21		YTKIDENLEIYKKSKKES		0.0287
Group 4				
pkMSP-1_{42}	243	NVPENAACYRYLDGTEEWRCLLGFKEVGGKCVPASI	278	
P29		NVPENAACYRYLDGTEEW		0.0037
P30		RYLDGTEEWRCLLGFKEV		0.0009
P31		RCLLGFKEVGGKCVPASI		< 0.0001

Note: P, Peptide

Table 4.6. Titre of unamplified phage and amplified phage in three rounds of panning

Round of panning	Anti-pkMSP-1_{42} antibodies		Coating buffer (Negative)	
	Unamplified phage (pfu/µl)	Amplified phage (pfu/µl)	Unamplified phage (pfu/µl)	Amplified phage (pfu/µl)
First	3.0×10^3	1.8×10^{12}	4.0×10^3	3.5×10^{12}
Second	2.0×10^2	1.7×10^{10}	9.5×10^2	6.3×10^9
Third	2.6×10^5	3.7×10^{10}	2.0×10^3	3.0×10^{10}

Table 4.7. Alignment of *P. knowlesi* MSP-1_{42} sequence with deduced amino acid sequences of phage dodecapeptide inserts

Group	Sequence	Number sequenced
Group 1		
MSP-1_{42}	240 IDTNVPENAACYRYLDGTEEWRCLLGFKEVGGKCVPASITCEENNGGCAP 289	
1	VE**T**--**P**T----L**RY**----SH**W**Q	1
2	ATT**P**NDND----**L**N---R**W**	3
3	SN**L**S----**W**--------------**PA**NMKH--------**P**	23
4	FH-----**E**S**W**--------------**P**S-MSSAA	3
5	**W**N------------A**P**PM**I**NRMST	1
6	T**W**-----**F**EALR---LNTDM	1
7	T**W**HHSY-**F**NS**V**R---**V**	22
8	T**G**HHSY-----**F**NS**V**S---**V**	1
Group 2		
MSP-1_{42}	37 KYSSSGEYIIKDPYKLLDLEQKKKLLGSYQYIGASVDKDLITAKDGMEYYKKM 89	
9	E**YS**ARVQ**Y**L---QFR	1
10	R**DPY**T**L**I----------**QY**LSV	2
11	HA**G**--------------Q**K**D**LL**SAWM	1
12	MVFP**KDG**R**E**--A**K**L	2
Group 3		
MSP-1_{42}	135 IQKEYESLVNMAH 147	
13	VDLDFR**SL**I-LVQ	1
Group 4		
MSP-1_{42}	304 KCTKEGSEPLFEGVFCS 320	
14	NM**T**-----**P**F**FEGV**IFN	1

Note: Letter in bold and red colour represented the exact matches of phage sequences with the *P. knowlesi* MSP-1_{42} sequence. Number sequenced indicated the number of times the dodecapeptide was isolated.

of the 14 peptides) were fall in Group 1, which were homologous to residues 240-289 in *P. knowlesi* MSP-1_{42}. Group 2 contained four peptides that mimic residues 37-89 in *P. knowlesi* MSP-1_{42}. There was only one peptide each in Group 3 and Group 4, with the peptide sequence homology to residues 135-147 and 304-320, respectively.

4.12 Comparison of epitopes identified by synthetic peptide library and by random phage display library

Screening of anti-pkMSP-1_{42} antibodies by using synthetic peptide library and random phage display library isolated nine and 14 peptides, respectively. Group 4 of synthetic peptide library (residues 243-278) and Group 1 of phage display library (residues 240-289) were spanning the same region of *P. knowlesi* MSP-1_{42}, while Group 2 of synthetic peptide library (residues 69-95) fall in the similar region as Group 2 of phage display library (residues 37-89). Therefore, these two regions could be possibly the dominant epitope regions on *P. knowlesi* MSP-1_{42}, as anti-pkMSP-1_{42} antibodies exhibited high reactivity towards peptides in the two regions by using both synthetic peptide library and phage display library epitope mapping techniques. There were some regions identified by synthetic peptide library but not by phage display library, or vice versa. Among the identified potential epitopes, two of the most prominent epitopes (one each from the two dominant epitope regions) were selected for further evaluation using mouse model. Selection was done based on the significance level and the reactivity strength of the anti-pkMSP-1_{42} antibodies against peptides in the two regions, which represented by peptides in Group 2 (Peptide 9 and 10) and Group 4 (Peptide 29, 30, and 31) of synthetic peptide library (Figure 4.21). The two peptides which have the highest absorbance value

and significance level, Peptide 10 (TAKDGMEYYNKMGELYKQ) and Peptide 31 (RCLLGFKEVGGKCVPASI), were chosen.

4.13 Evaluation and characterization of identified epitopes using mouse model

4.13.1 Measurement of cytokine levels in mice

4.13.1.1 Mouse IL-2 ELISA

For the culture supernatants stimulated with purified pkMSP-1_{42}, the IL-2 level of PBS-immunized mice group, P10-immunized mice group and P31-immunized mice was [139.6 (107.4-147.7)] pg/ml, [129.7 (108.3-141.0)] pg/ml and [106.8 (103.7-118.0)] pg/ml, respectively (Figure 4.22a). On the other hand, PBS-immunized mice group had an IL-2 value of [52.5 (10.9-71.2)] pg/ml and [22.7 (6.6-54.7)] pg/ml when stimulated with P10 and P31 respectively. The IL-2 level of P10-immunized mice group was [53.7 (40.2-75.6)] pg/ml and P31-immunized mice group was [270.4 (235.1-386.7)] pg/ml when stimulated with respective peptides. The IL-2 level of P31-immunized mice group was significantly higher than those of the negative control group when stimulated with P31 (Figure 4.22b).

4.13.1.2 Mouse IL-4 ELISA

IL-4 was undetectable in both pkMSP-1_{42}-stimulated and peptide-stimulated culture supernatants of all three immunized mice groups.

4.13.1.3 Mouse IL-10 ELISA

For the culture supernatants stimulated with purified pkMSP-1_{42}, the IL-10 level of PBS-immunized mice group, P10-immunized mice group and P31-

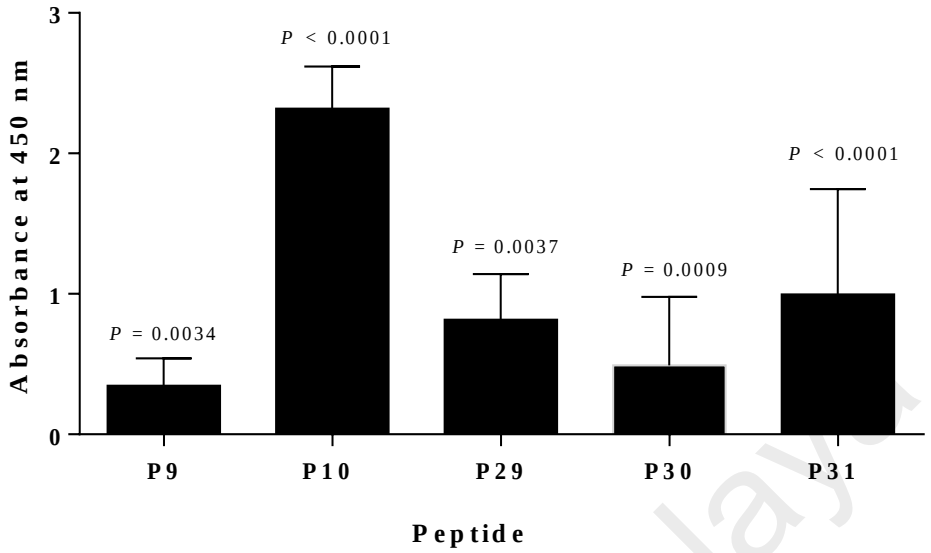

Figure 4.21. Comparison of significance level and reactivity strength of the anti-pkMSP-1_{42} antibodies against five peptides in the two dominant epitope regions on *P. knowlesi* MSP-1_{42}. pkMSP-1_{42}-immunized mice sera with 1:100 dilution were used. Data shown were median with interquartile range. Peptide 10 and Peptide 31 were selected for further evaluation in mouse model as these two peptides have the highest absorbance value and significance level.

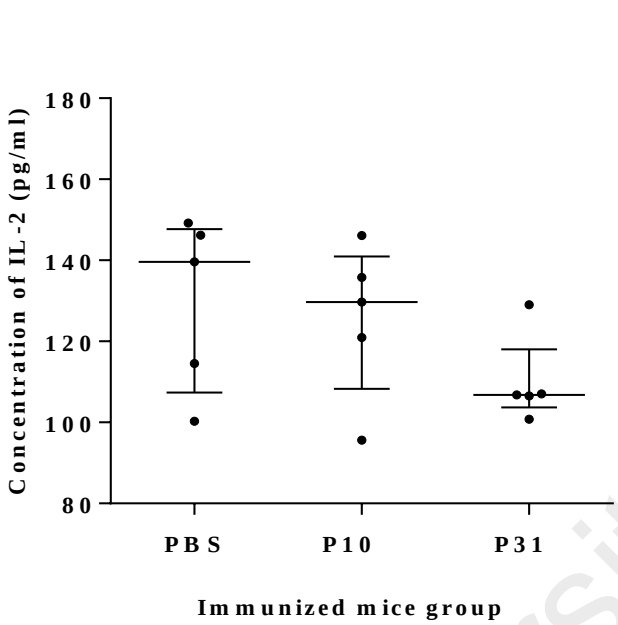

(a)

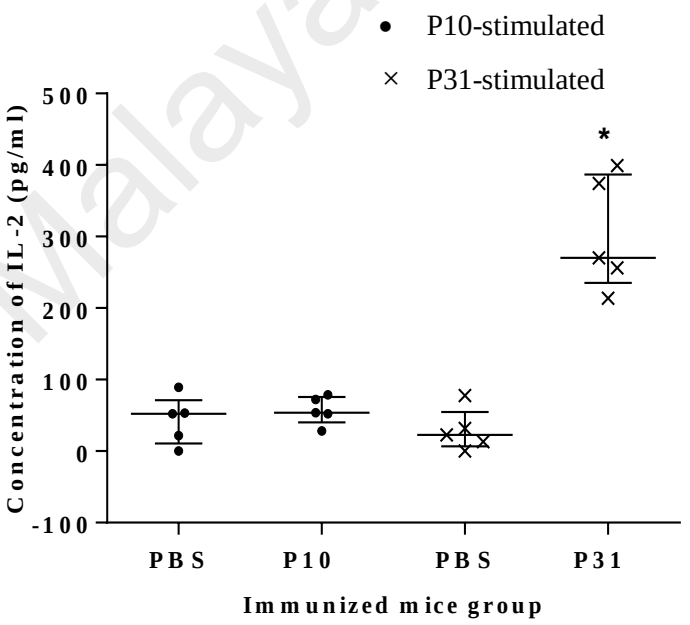

(b)

Figure 4.22. Level of cytokine IL-2 in PBS-immunized, P10-immunized and P31-immunized mice group stimulated with (a) purified pkMSP-1_{42} and (b) peptides. Data shown were median with interquartile range in each group (n = 5). Level of IL-2 in P31-immunized mice group was significantly higher compared to PBS-immunized mice group with stimulation of respective peptide. Note: *$P < 0.05$.

immunized mice was [324.8 (261.0-430.5)] pg/ml, [528.2 (518.6-616.5)] pg/ml and [606.6 (551.6-625.2)] pg/ml, respectively. Both P10-immunized and P31-immunized mice group had a significantly higher level of IL-10 compared to PBS-immunized mice group (Figure 4.23). However, IL-10 was undetectable in peptide-stimulated culture supernatants of all three immunized mice groups.

4.13.1.4 Mouse IFN-γ ELISA

For pkMSP-1_{42}-stimulated culture supernatants, the IFN-γ level of PBS-immunized mice group, P10-immunized mice group and P31-immunized mice group was [1265.0 (591.5-5008.0)] pg/ml, [3083.0 (2039.0-4586.0)] pg/ml and [8153.0 (5713.0-9673.0)] pg/ml, respectively (Figure 4.24a). On the other hand, PBS-immunized mice group had an IFN-γ value of [11.9 (7.5-20.8)] pg/ml and [20.1 (12.9-39.4)] pg/ml when stimulated with P10 and P31 respectively. The IFN-γ level of P10-immunized mice group was [24.9 (14.4-51.1)] pg/ml and P31-immunized mice group was [84.9 (62.0-136.8)] pg/ml with respective peptides stimulation. Significant higher level of IFN-γ was detected in P31-immunized mice group compared to negative control group when stimulated with both pkMSP-1_{42} and P31 (Figure 4.24b). Cytokine profiles of PBS-immunized mice, P10-immunized mice and P31-immunized mice were summarised in Table 4.8.

4.13.2 Characterization of raised antibodies in peptide-immunized mice

4.13.2.1 Detection of anti-peptide antibodies in mice sera using Western Blot assays

Antibody responses in peptide-immunized mice towards pkMSP-1_{42} were analysed. Western Blot strips showed that both P10-injected and P31-

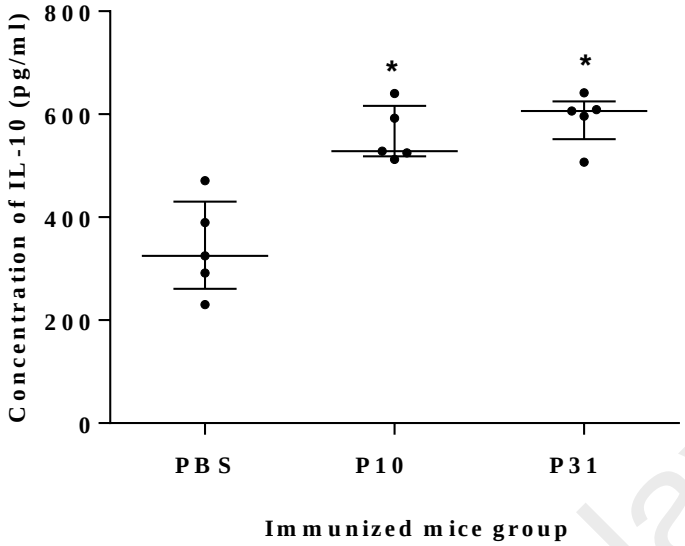

Figure 4.23. Level of cytokine IL-10 in PBS-immunized, P10-immunized and P31-immunized mice group stimulated with purified pkMSP-1_{42}. Data shown were median with interquartile range in each group (n = 5). Level of IL-10 in P10-immunized and P31-immunized mice group was significantly higher compared to PBS-immunized mice group. Note: *$P < 0.05$.

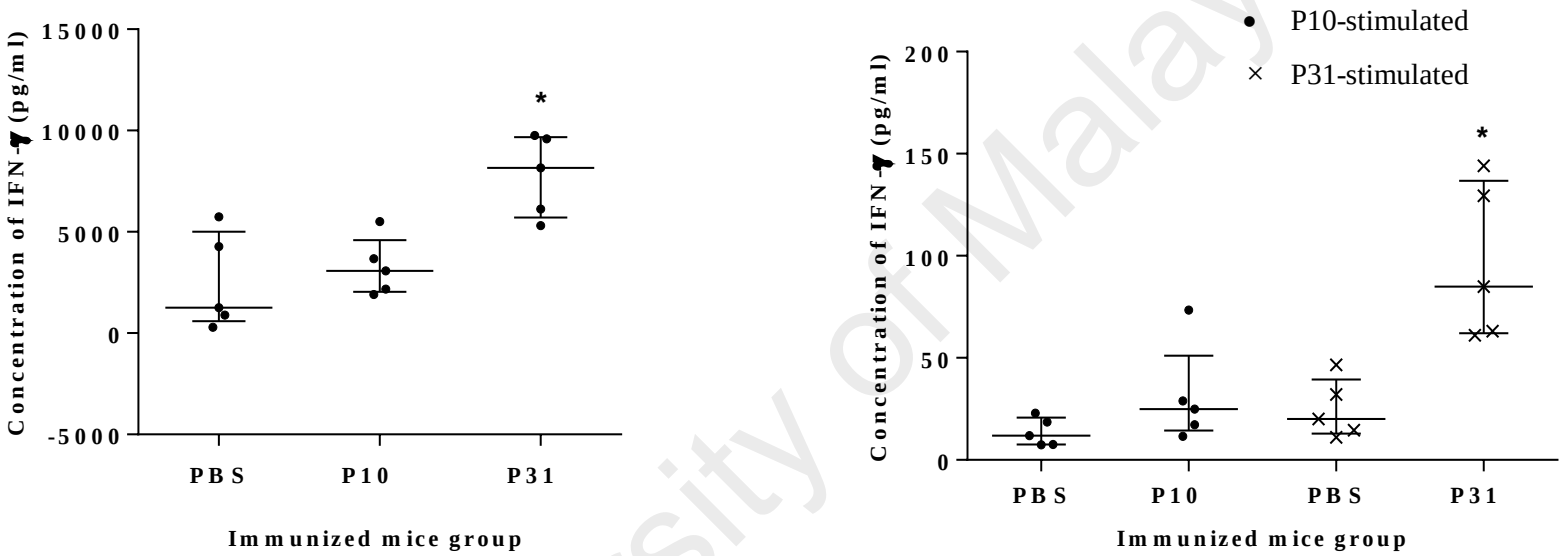

Figure 4.24. Level of cytokine IFN-γ in PBS-immunized, P10-immunized and P31-immunized mice group stimulated with (a) purified pkMSP-1_{42} and (b) peptides. Data shown were median with interquartile range in each group (n = 5). Significant higher level of IFN-γ was detected in P31-immunized mice culture supernatant with both stimulation of pkMSP-1_{42} and P31 compared to PBS-immunized mice group. Note: *$P < 0.05$.

Table 4.8. Cytokine profiles of PBS-immunized, P10-immunized and P31-immunized mice

Stimulator	Immunized Group	IL-2	IL-10	IFN-γ
	PBS	139.6 (107.4-147.7)	324.8 (261.0-430.5)	1265.0 (591.5-5008.0)
pkMSP-1_{42}	P10	129.7 (108.3-141.0)	528.2 (518.6-616.5)* $P = 0.008$	3083.0 (2039.0-4586.0)
	P31	106.8 (103.7-118.0)	606.6 (551.6-625.2)* $P = 0.008$	8153.0 (5713.0-9673.0)* $P = 0.016$
P10	PBS	52.5 (10.9-71.2)	UD	11.9 (7.5-20.8)
	P10	53.7 (40.2-75.6)	UD	24.9 (14.4-51.1)
P31	PBS	22.7 (6.6-54.7)	UD	20.1 (12.9-39.4)
	P31	270.4 (235.1-386.7) * $P = 0.008$	UD	84.9 (62.0-136.8)* $P = 0.008$

Note: Values shown were median (interquartile range). UD, undetectable; IL-2, interleukin-2; IL-10, interleukin-10; IFN-γ, interferon-gamma. Concentration of cytokines in pg/ml. * $P < 0.05$. Interleukin-4 was undetectable in both pkMSP-1_{42}-stimulated and peptide-stimulated culture supernatants of all three immunized mice groups.

injected mice sera collected at day 52 post-immunization were able to recognise and react with pkMSP-1_{42}, while no reactivity was observed in the PBS-immunized mice sera (Figure 4.25).

4.13.2.2 Determination of IgG isotype distribution

IgG isotype distribution in peptide-immunized mice sera was determined by ELISA. The predominant IgG isotype in both groups of peptide-injected mice sera was IgG2b, followed by IgG1, IgG2a and IgG3. The IgG2b and IgG1 level in P31-immunized mice group was relatively higher than in P10-immunized mice group, indicating that P31 was able to induce higher level of immunodominant antibodies in mouse model compared to P10 (Figure 4.26).

4.13.2.3 Determination of reactivity of peptide-immunized mice sera against *P. knowlesi* parasites using IFA

Plasmodium knowlesi-positive thin blood smears were used to test the ability of anti-peptide antibodies to recognise the *P. knowlesi* protein. Fluorescence microscopy result demonstrated that antibodies raised against both P10 and P31 were able to recognise *P. knowlesi* blood stage parasites in IFA. Parasites in thin smear exhibited bright green fluorescence under FITC filter when probed with P10-immunized and P31-immunized mice sera. No recognition was observed using PBS-immunized mice sera (Figure 4.27).

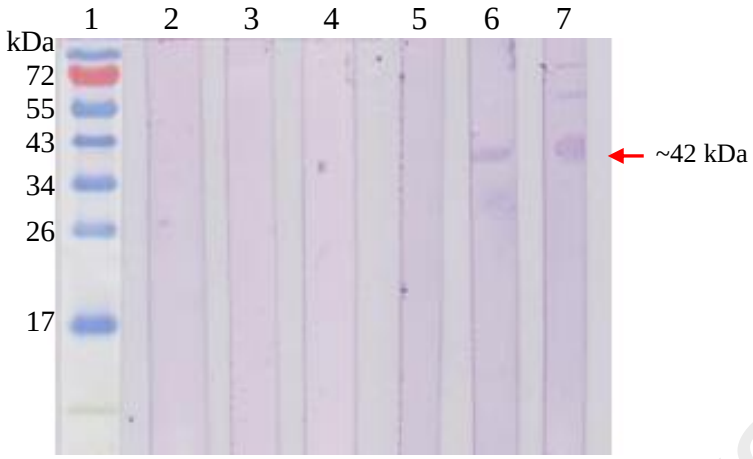

Figure 4.25. Western Blot assays of pkMSP-1_{42} probed with PBS-immunized mice sera, P10-immunized mice sera and P31-immunized mice sera collected at day 0 and 52 post-immunization. Lanes 2 to 4 contained sera of mice at day 0 post-immunization for PBS-immunized, P10-immunized and P31-immunized group respectively; lanes 5 to 7 contained sera of mice at day 52 post-immunization for PBS-immunized, P10-immunized and P31-immunized group respectively. Lane 1 contained Bio-Rad Prestained Broad Range Protein Marker. Both peptide-immunized mice sera were able to recognise and react with pkMSP-1_{42} (arrow) while no reactivity was observed in PBS-immunized mice.

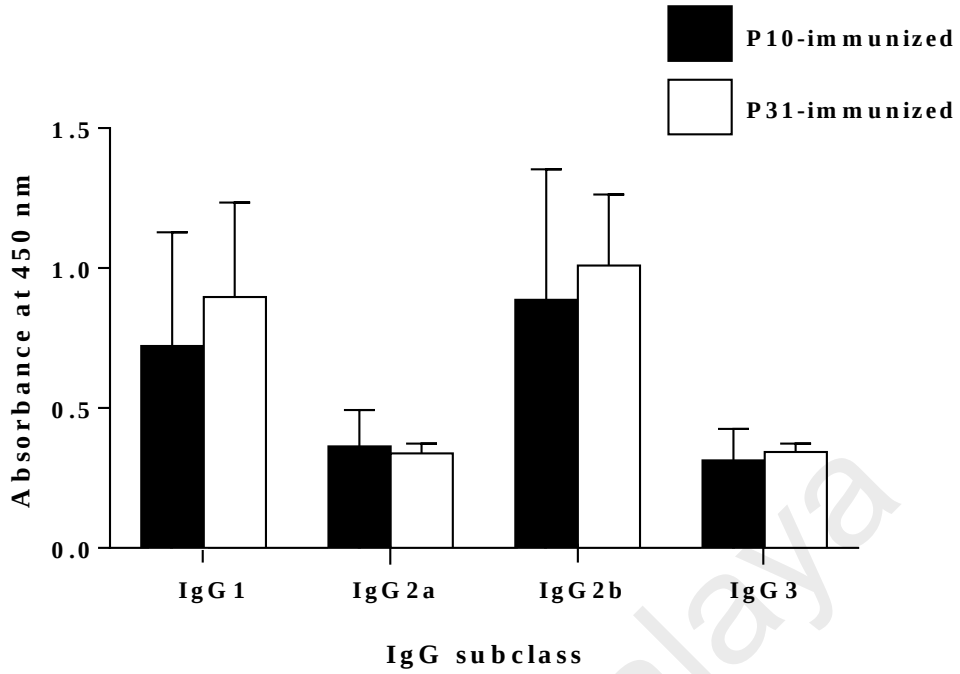

Figure 4.26. IgG isotype-specific antibody levels in peptide-immunized mice. Peptide-immunized mice sera with 1:200 dilution were used. Data shown were median with interquartile range. The IgG isotype distribution in peptide-immunized mice was IgG2b > IgG1 > IgG2a > IgG3.

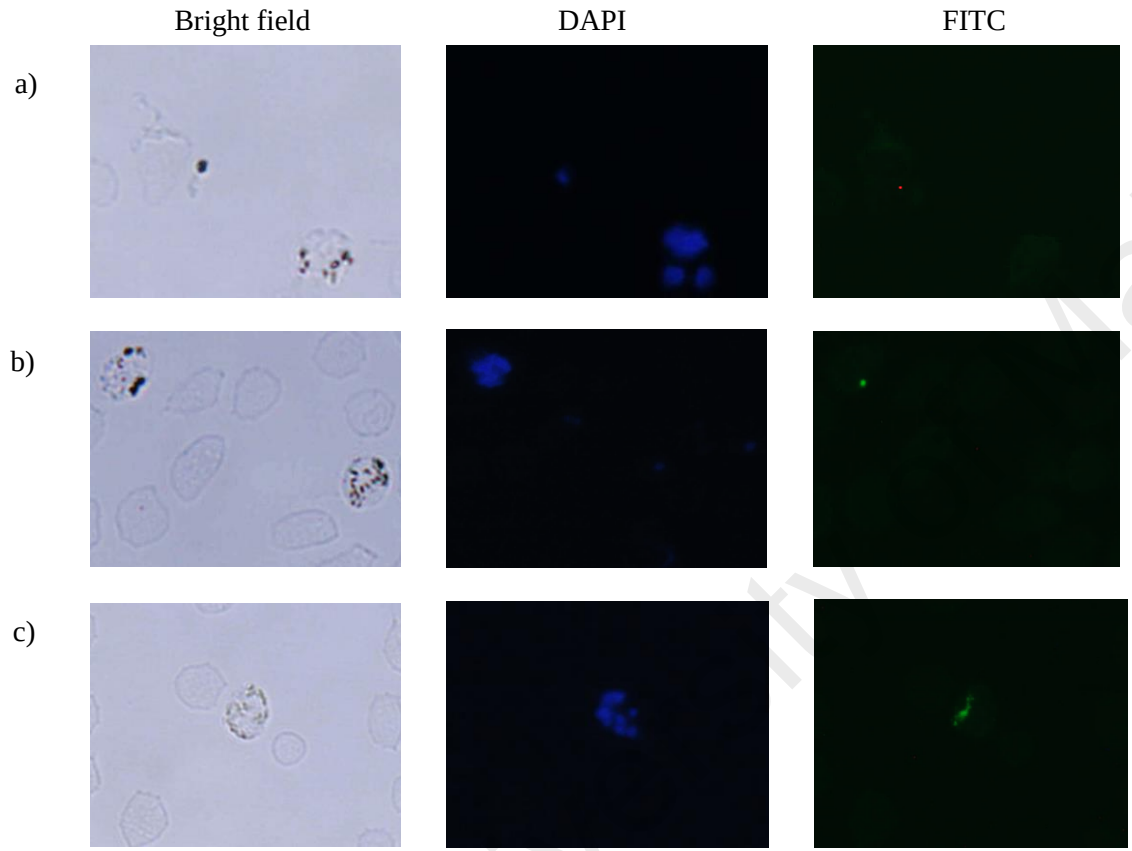

Figure 4.27. Fluorescence microscopy examination of *P. knowlesi*-positive blood smear probed with (a) PBS-immunized (b) P10-immunized and (c) P31-immunized mice sera in IFA. Bright blue fluorescence was observed in all three sets of experiment under DAPI filter indicated the presence and location of *P. knowlesi* blood stage parasites. Anti-P10 and anti-P31 antibodies were able to recognise *P. knowlesi* blood stage parasites as green fluorescence was observed only in smear probed with peptide-immunized mice sera but not in smear probed with PBS-immunized mice sera.

CHAPTER 5: DISCUSSION

5.1 Overview

Plasmodium knowlesi replicates and completes its blood stage cycle in 24 hours, which is one of the shortest period of *Plasmodium* sp. Hence, it can lead to quotidian fever and rapid hyperparasitaemia in human, and could be potentially severe and fatal if it is misdiagnosed as benign malariae-infection or remains untreated (Cox-Singh *et al.*, 2008).

A previous study has shown that protective T cell responses can be induced by epitopes within the dimorphic regions of MSP-1_{33} instead of MSP-1_{42} in *Plasmodium* sp. due to the low prevalence of T-cell responses to MSP-1_{19} (Udhayakumar *et al.*, 1995). On the other hand, MSP-1_{42} of *Plasmodium* sp. has been demonstrated to be immunogenic and able to elicit protective immunity (Tian *et al.*, 1997; Dutta *et al.*, 2005). However, most of the studies on MSP-1_{33} and MSP-1_{42} are still focused on *P. falciparum* and *P. vivax*, while limited literature is available for *P. knowlesi*.

The availability of *P. knowlesi* MSP-1_{33} and MSP-1_{42} proteins is prerequisite for their biochemical and immunological characterization. Difficulties in maintaining long term *in vitro* cultivation of *P. knowlesi* have led to limited supply of live *P. knowlesi*. Moreover, sustainable recovery of sufficient quantities of pure native *P. knowlesi* MSP-1_{33} and MSP-1_{42} from the culture is also a limiting factor. Hence, in this study, recombinant expression technology was used to obtain the continuous supply of *P. knowlesi* MSP-1_{33} and MSP-1_{42}.

Recombinant protein has advantages over native protein. Expression of recombinant protein is rapid, simple and convenient. *Escherichia coli* expression system was chosen in this study due to its safety, simplicity of techniques,

known genetic properties, cost-effectiveness and high efficiency. Foreign DNA can easily be transformed into *E. coli* with well-established genetic manipulation methods. Besides, the *E. coli* system can express large amounts of protein within a few hours as its growth rate is high. MSP-1_{42} is a non-glycosylated protein and this is crucial for its immunogenicity, as a study has demonstrated that glycosylated form of milk-derived MSP-1_{42} secreted by transgenic mice did not confer protection against malaria during *Plasmodium* challenge (Stowers *et al.*, 2002). Therefore, *E. coli* system is a suitable system because of its high efficiency in expressing non-glycosylated proteins (Epp *et al.*, 2003; Singh *et al.*, 2003). Large amounts of native, non-glycosylated recombinant pkMSP-1_{33} and pkMSP-1_{42} can be produced compared to other expression systems using virus, yeast or mammalian cells.

5.2 Selection of pRSET A as expression vector in *E. coli* expression system

The pUC-derived expression vector pRSET A was chosen in this study. This vector is designed for high-level recombinant protein expression and purification in *E. coli*. It contains a polyhistidine tag at the N-terminal, an ATG translation initiation codon, the Xpress™ epitope, and the enterokinase cleavage recognition sequence (Appendix 16). The polyhistidine tag that functions as a metal binding domain in the translated protein facilitates purification of recombinant proteins by immobilized metal affinity chromatography with resin, while the enterokinase cleavage recognition site allows subsequent removal of the purified recombinant protein from the N-terminal fusion peptide. T7 promoter in pRSET A controls the expression of gene of interest. In this study, IPTG was used during protein expression to induce the expression of T7 RNA polymerase which

specifically recognises T7 promoter. When high level of T7 RNA polymerase is produced, it binds to the T7 promoter and transcribes the inserted genes.

5.3 Purification of pkMSP-1_{33} and pkMSP-1_{42}

The recombinant pkMSP-1_{33} and pkMSP-1_{42} were tagged with six tandem histidine residues at the N-terminal. Nickel-NTA agarose resin used in the purification process has high affinity and selectivity towards the His-tagged recombinant proteins. The proteins bound to the resin were then eluted by competition with imidazole in the elution buffer. During protein purification, hybrid condition was chosen for protein purification to preserve the protein structure and activity. In this condition, both pkMSP-1_{33} and pkMSP-1_{42} were solubilised under denaturing buffer, while native buffers were used during the washing and elution steps to refold and re-nature the protein.

Dialysis of purified pkMSP-1_{33} and pkMSP-1_{42} enabled removal of unwanted low molecular weight contaminants such as salts, reducing agents and dyes from sample solutions without significant loss of the purified proteins. The method is based on the diffusion of small molecules from area of high concentration to low concentration through a semi-permeable membrane until equilibrium is reached (usually four to eight hours). SnakeSkin dialysis tubing with 10,000 molecular weight cut-off retains 90% of molecules of 10 kDa or larger during dialysis, while unwanted molecules with smaller size will be dialysed out of the tubing. Dialysis also helps in removing solubilising agents and allows the protein to refold optimally.

5.4 Evaluation of purified pkMSP-1_{33} and pkMSP-1_{42} in Western Blot assays and ELISA using patient sera

Purified proteins were analysed and probed with sera of patients infected with *P. knowlesi* and other parasite species. A total of 176 and 189 sera were used to test the purified pkMSP-1_{33} and pkMSP-1_{42}, respectively, by using Western Blot assays and ELISA.

The sensitivity for pkMSP-1_{33} and specificity for both pkMSP-1_{33} and pkMSP-1_{42} in Western Blot assays was relatively higher than that of ELISA. This discrepancy might be due to the borderline activity of the patient sera in ELISA. In a study comparing ELISA and Western Blotting for human papillomavirus type 16 E7 antibody detection, Suchankova *et al.* (1991) obtained positive results in ELISA yet negative in Western Blot, and they suggested that this situation was apparently associated with the borderline activity of the sera, which some of the OD absorbance values just fall below or above the cut-off value. A similar observation occured in the present study. In fact, some knowlesi and non-knowlesi *Plasmodium* sera had OD absorbance values just below the cut-off value, while OD absorbance values of some non-*Plasmodium* parasitic infection sera were just slightly higher the cut-off value, thus giving false positive or false negative results.

Both pkMSP-1_{33} and pkMSP-1_{42} appeared to have a relatively higher sensitivity and specificity in Western Blot assays compared to ELISA. Nonetheless, there are several advantages of ELISA over Western Blot assays. Optimized ELISA requires smaller volume of serum for each reaction compared to Western Blot assays and this could be very crucial for precious samples. Besides, ELISA can quantitatively determine antibody titre in sera, as the OD absorbance value of the sera directly corresponds to the titre.

The sensitivity of pkMSP-1_{42} for detection of malarial infection was similar with pkMSP-1_{33} in Western Blot (both >90%), but higher compared to pkMSP-1_{33} in ELISA. pkMSP-1_{42} consisted of both MSP-1_{33} and MSP-1_{19} regions. Previous studies showed that human sera from malaria-endemic areas demonstrated strong MSP-1_{19} reactivity (Egan *et al.*, 1996) and MSP-1_{19} fragment consists of several immunodominant B cell epitopes which are important to induce protective anti-MSP-1_{19} antibodies (Hui *et al.*, 1996). Therefore, these epitopes could be recognised by specific anti-MSP-1_{19} antibodies in the sera of malaria-infected patients when pkMSP-1_{42} was used as antigen, but not pkMSP-1_{33}.

In the present study, pkMSP-1_{33} and pkMSP-1_{42} reacted with most of the non-knowlesi malaria sera and this could be explained by serological cross-reactivity. Numerous previous studies have shown that serum cross-reactivity could occur in malaria patients infected with different *Plasmodium* sp. (Diggs & Sadun, 1965; Miller *et al.*, 1980). For instance, sera from patients infected with *P. falciparum* cross-reacted with recombinant *P. vivax* MSP-1 which has a 42% sequence similarity with *P. falciparum* MSP-1 (Kim *et al.*, 2004). Besides, Valderrama-Aguirre *et al.* (2005) also showed that antibodies generated in mice against *P. vivax* MSP-1 fragment, designated as *Pv*200L, recognised and cross-reacted with *P. falciparum* recombinant MSP-1 *Pf*190L fragment, which is the homologue of *Pv*200L, indicating the sharing of B cell epitopes of these two MSP-1 proteins. On the other hand, the *P. vivax* MSP-1_{42} protein, which shares 70% homology with *P. cynomolgi* MSP-1_{42}, has been shown to induce protection during *P. cynomolgi* challenge in rhesus monkey due to their immunological and structural relatedness (Dutta *et al.*, 2005), and antibodies against several antigens of *P. cynomolgi* and *P. vivax* have also been shown to

cross-react (Kamboj *et al.*, 1988; Yang *et al.*, 1994). *Plasmodium knowlesi* MSP-1_{33} has amino acid similarity of 82%, 60% and 70% with MSP-1_{33} of *P. vivax, P. falciparum* and *P. ovale* respectively; while *P. knowlesi* MSP-1_{42} also shares high amino acid similarity with MSP-1_{42} of *P. vivax* (84%), *P. falciparum* (59%) and *Plasmodium ovale* (70%). Hence, *P. knowlesi* MSP-1_{33} and MSP-1_{42} may share certain common B-cell epitopes with these human *Plasmodium* species that lead to cross-reactivity.

Another explanation for the reactivity of pkMSP-1_{33} and pkMSP-1_{42} with non-knowlesi human malaria and non-*Plasmodium* parasitic infection sera is the possibility of previous exposures or infections with *P. knowlesi*. It has been reported that previous infection with *P. vivax* could be one of the reasons for reactivity of recombinant *P. vivax* AMA-1 with *P. falciparum*-infected patient sera (Haghi *et al.*, 2012). Besides, Wipasa *et al.* (2010) demonstrated that antibodies generated against malaria infection were stably maintained over periods of more than five years after the last known malaria infection. Hence, antibodies against *P. knowlesi* could still be detected in Western Blot or ELISA after many years of acute infection.

A few of the malaria infected patient sera did not react with pkMSP-1_{33} and pkMSP-1_{42} in Western blot and/or ELISA and this could be explained by the genetic diversity of MSP-1. *Plasmodium* MSP-1 exhibits extensive sequence diversity among isolates and host immune selective pressure could be one of the reasons that lead to the polymorphism (Tanabe *et al.*, 1987; Putaporntip *et al.*, 2002). *Plasmodium knowlesi* MSP-1 comprises of five conserved and four variable domains. The conserved domains have been reported to undergo nucleotide substitutions and exhibit allelic dimorphism, while three of the four variable domains contain complex repetitive sequence motifs which results in

extensive sequence and size variation. Besides, microheterogeneity comprising amino acid substitutions causing different alleles has been observed in *P. knowlesi* MSP-1_{33} epitopes (Putaporntip *et al.,* 2013). Sequence diversity in these epitopes may alter immunological recognition of the epitopes and hence enhancing parasite survival by evasion of host immune response. Therefore, antibodies in some of the malaria infected patient sera in the present study were not able to detect the variant epitopes on pkMSP-1_{33} and/or pkMSP-1_{42}.

5.5 Immunogenicity tests of pkMSP-1_{42} using mouse model

Sensitivity and specificity obtained for pkMSP-1_{42} in Western Blot assays and ELISA were consistently higher (>90%) as compared to pkMSP-1_{33} which had lower specificity in ELISA (<80%). On top of that, the MSP-1_{42}, which contains the MSP-1_{33} and MSP-1_{19} regions, consists of immunodominant T cell and B cell epitopes. Therefore, MSP-1_{42} should be considered as a more prominent candidate for malaria vaccine as it is able to elicit both cell mediated and humoral responses. Hence, in the present study, immunogenicity of pkMSP-1_{42} was evaluated using mouse model and potential epitopes on *P. knowlesi* MSP-1_{42} were identified.

High IFN-γ and IL-2 levels in pkMSP-1_{42}-immunized mice group indicated that Th1-driven immune response had been stimulated. IFN-γ secretion is a hallmark of Th1 cells and a key molecule in human anti-malarial host defense. It enhances microbicidal activities of macrophages for killing malarial blood stage parasites by reactive oxygen and nitrogen intermediates, and induces macrophages to secrete monokines such as IL-1, IL-6 and TNFα (Clark & Hunt, 1983; Winkler *et al.,* 1998). IFN-γ is produced in primary *P. knowlesi* infection in rhesus macaques (Praba-Egge *et al.*, 2002). IL-2 is an autocrine growth factor

which is secreted mainly by activated CD4 T helper cells and is essential for proliferation, survival and differentiation of clonal T cells into effector and memory T cells. IL-2 also promotes the functional properties of natural killer cells, B cells and macrophages.

On the other hand, the high level of IL-4, IL-10 and predominant IgG1 production in the pkMSP-1_{42}-immunized mice group showed that Th2 response had also been stimulated. IL-4 secretion is a hallmark for Th2 cells and it promotes cytotoxic T lymphocyte activity, growth of mast cells and IgE production. IL-10 is an anti-inflammatory cytokine which is secreted by activated Th2 cells. It down-regulates the production of pro-inflammatory IFN-γ and limits the potentially harmful inflammatory responses during malarial blood stage parasites infection in mouse (D'Andrea *et al.*, 1993; Linke *et al.*, 1996). A study on *P. knowelsi*-inoculated olive baboons found association between increased levels of IL-4, IL-10, IgM and IgG with increased protection against knowlesi-infection (Mustafa, 2010). Cox-Singh *et al.* (2011) observed increase in the IL-10 level in knowlesi malaria patients with considerable parasitaemia. Therefore, they postulated that this anti-inflammatory cytokine plays a role in modulating the expected immune surge during merozoite reinvasion.

Cytokines produced by each subset promote the polarization process, which Th1 cells-produced cytokines that will down-regulate Th2 response, and *vice versa* (Kidd, 2003). The concentrations of IFN-γ and IL-10 have been noted to increase in *P. vivax*-infected individuals during natural infection (Medina *et al.*, 2011). Therefore, stimulation of Th1 and Th2 subsets upon pkMSP-1_{42} immunization is important as homeostasis between Th1/Th2 cells could achieve a balance regulation between pro-inflammatory and anti-inflammatory actions in the immune response.

Some of the T cell stimulated-cytokines are responsible for IgG response determination. For instance, Th1 cell-secreted IFN-γ is responsible for the production of IgG2a in mice (corresponds to IgG1 in human) (Finkelman *et al.*, 1988); while Th2 cell-secreted IL-4 is associated with IgG1 production in mice (corresponds to IgG4 in human) (Severinson *et al.*, 1987). In the present study, four isotypes of IgG were detected in pkMSP-1_{42}-immunized mice. These IgG isotypes help to activate effector responses in different manners. Murine IgG1 binds to mast cell, subtypes IgG2a and IgG2b play a role in complement binding and antibody opsonization, while IgG3 is responsible for carbohydrate epitope recognition (Hussain *et al.*, 1995). IgG2a is the dominant IgG isotype for modulating murine malaria parasitaemia (White *et al.*, 1991). Besides, anti-pkMSP-1_{42} antibodies were raised in the early period of immunization and were detected at day 7 post-immunization. The level of these antibodies then increased several folds and was maintained at a very high titre until day 31 post-immunization. Moreover, these anti-pkMSP-1_{42} antibodies were shown to recognise the *P. knowlesi* proteins in IFA.

All these findings indicate that pkMSP-1_{42} was highly immunogenic, and could elicit both cell-mediated and humoral immunity. These findings support *P. knowlesi* MSP-1_{42} as a potential blood stage vaccine candidate. Similar results were reported in studies using mice immunized with recombinant *P. falciparum* and *P. vivax* MSP-1_{42} (Dutta *et al.*, 2001; Sachdeva *et al.*, 2004; Sachdeva *et al.*, 2006).

5.6 Identification and characterization of potential epitopes on *P. knowlesi* MSP-1_{42} by using synthetic peptide library

Several methods are available for epitope mapping but their validity and utility vary (Laver *et al.*, 1990; Smith-Gill, 1994). X-ray crystallography, combined with computer algorithm and 3D modelling antigen-antibody complexes, is the most precise method for epitope mapping. However, this method is time consuming, expensive, and technically challenging especially in the preparation of antigen-antibody crystals. Therefore, it is quite impractical to perform this epitope mapping method in the vast majority of cases.

Of the epitope mapping methods available, overlapping synthetic peptide library is one of the most efficient for identification of continuous linear epitopes as these epitopes could be represented by the peptide fragments in the overlapping peptide library (Geysen *et al.*, 1984; Carter & Loomis-Price, 2004). This mapping technique is rapid, cost-effective and practical, in which the linear epitopes could be identified by recognition of a particular antibody through a simple immunoassay. Several studies have successfully applied this technique for the recognition of immunogenic epitopes for use in diagnosis assays, therapeutic agents and vaccine development (Ricchiuti *et al.*, 1994; Corey *et al.*, 1997; Vanniasinkam *et al.*, 2001; Bellucci *et al.*, 2007; Malhotra *et al.*, 2008; Dworschak *et al.*, 2012).

Potential epitopes within the *P. knowlesi* MSP-1_{42}, recognised by antibodies raised against the full length antigen pkMSP-1_{42}, were identified by using overlapping synthetic peptide library which covered the entire *P. knowlesi* MSP-1_{42} protein sequence. Peptides with 18 amino acid residues were used in the study. These long peptides may be partially folded in the solution, therefore would increase the chances to incorporate both linear epitopes and epitopes

which depend on the local secondary protein structure (Corey *et al.,* 1997). Before performing the epitope mapping with synthetic fragments, the reactivity of anti-pkMSP-1_{42} antibodies against the full length pkMSP-1_{42} was confirmed in ELISA before using them against the peptide fragments. Epitopes were then defined by identification of the peptides that had strong binding affinity with anti-pkMSP-1_{42} antibodies. Nine peptides reacted significantly with pkMSP-1_{42}-immunized mice sera, which comprised four regions on *P. knowlesi* MSP-1_{42} (residues 15-59, 69-95, 177-194, and 243-278).

Most of the nine peptides were consecutive overlapping peptides (for instance, P5 and P6; P9 and P10; P29, P30 and P31). Several previous studies hypothesised that three to six adjacent amino acid residues in a linear epitope are sufficient for contact with antibodies and contribute the greatest part of interaction energy (Geysen *et al.,* 1987; Laver *et al.,* 1990). In the present study, the consecutive peptides consist of nine overlapping amino acid residues. Hence, the immunodominant amino acid residues that were responsible for contact with anti-pkMSP-1_{42} antibodies could be located in the overlapping portion of these peptides and thus led to high reactivity in both consecutive peptides.

5.7 Identification and characterization of potential epitopes on *P. knowlesi* MSP-1_{42} by using random phage display library

Phage library, which consists of millions of phage displaying peptides with randomised sequences, is another efficient approach for mapping antibody epitopes. Peptides with high affinity towards the paratopes on the antibodies can be recognised and isolated from the library (Bottger & Bottger, 2009). This method has been used to identify immunogenic epitopes and binding hot spots

on *Plasmodium* sp. proteins (Coley *et al.*, 2001; Casey *et al.*, 2004; Harris *et al.*, 2005).

The Ph.D.-12 premade random phage display library used in the present study was designed based on the M13 phage vector. M13 is a filamentous bacteriophage coated by approximately 2700 copies of major coat protein pVIII. Five copies each of minor coat protein pIII and pVI cap the other end of the virus particle. pIII is responsible for particle stability and phage infectivity, and it mediates the phage attachment to the receptor at the tip of the F pilus of host *E. coli* (Russel *et al*., 1997). The M13KE phage in the Ph.D.-12 premade random phage display library was modified by fusing the peptides to the pIII at N-terminal via the flexible linker Gly-Gly-Gly-Ser. The peptide inserts bind to the F pilus of the *E. coli* and are displayed as pentavalent peptides (five copies of peptides) clustered at one end of the virion (Devlin *et al.*, 1990; Scott & Smith, 1990).

M13KE is a non-lytic virus that does not lead to destruction of the host during phage production. Therefore, simple phage purification steps during panning (in the present study, PEG precipitation method was used) would be sufficient to separate the phage from almost all other contaminants such as cell debris and proteins. This is an important advantage over other phage display systems using lytic bacteriophages T4, T7 and λ phage, as tedious and time consuming phage purification steps are required to remove cellular proteins, especially proteases that may degrade the target protein during panning.

The displayed peptides are rather short in this premade library, with only 12 amino acid residues. Hence, the phage infectivity would not be significantly affected even though all five copies of pIII are carrying the displayed peptides. The phage with displayed peptides longer than 20 to 30 amino acid residues

would lead to deleterious effect on the phage infectivity (Cwirla *et al.*, 1990). Furthermore, compared to the Ph.D.-7 premade random phage display library which consists of randomised linear 7-mer peptides, the 12-mer peptides are longer and stand a higher chance of folding into structural elements such as short helices and β-turn (Corey *et al.*, 1997). This can be useful for selection of structure dependent-conformational epitopes.

The infectivity of library phage M13KE could be relatively lower than the environment wild type M13 phage due to the display of foreign peptides on library phage. Theoretically, the enrichment of eluted phage with peptides that strongly bind to the target would reach to an optimum level after the second or third round of panning. Once this point is reached, further round of panning would favour the growth of wild type phage that has growth advantage over the library phage. Contamination from environment wild type phage can easily occur, especially during the phage amplification steps. Even an undetectable low level of contamination (less than one part per billion) may lead to wild type phage dominating or completely overtake the phage pool after third or fourth round of panning. Hence, in the present study, three rounds of panning were carried out. Besides, the whole panning process was carried out in clean and sterile conditions.

One of the ways to differentiate library from wild type phage is by using LB agar plates containing X-gal and IPTG for tittering. The library cloning vector M13KE carries the lacZα gene and would yield blue plaques, while environmental wild type phage would typically appear as colourless plaques when plated on LB agar plates containing X-gal and IPTG. Several colourless plaques were observed in the third round panning tittering plates in the present

study. Blue plaques were carefully picked for screening in binding affinity ELISA and sequencing.

A previous study indicated that by using phage display library, critical amino acid residues within an epitope could be recognised by assessing the amino acid sequence of isolated peptides for homology to the primary sequence of the protein antigen (Wang & Yu, 2009). In the present study, seven of the eight peptides that aligned to the *P. knowlesi* MSP-1_{42} sequence at residues 240-289 consisted of a consensus amino acid residue 'W', three peptides with consensus 'F' and three peptides with consensus 'P' that are homologue with the *P. knowlesi* MSP-1_{42} sequence. These three amino acid residues could therefore be the potential immunodominant residues within the epitopes that were highly recognised by anti-pkMSP-1_{42} antibodies.

It was also shown that the isolated peptide sequences could be aligned as discontinuous segments to the *P. knowlesi* MSP-1_{42} sequence. There was a high possibility that anti-pkMSP-1_{42} antibodies recognised and bound to the discontinuous immunodominant amino acid residues on the peptides. Researchers have demonstrated that peptides isolated from phage library functionally resemble discontinuous epitopes. These isolated peptides are usually unrelated to the primary structure of the protein antigen but mimic discontinuous epitopes, particularly in their structure and ability to bind to antibodies, thus given name as mimotopes (Geysen *et al.*, 1986; Youn *et al.*, 2004; Van Nieuwenhove *et al.*, 2012). In the present study, the isolated peptides were more likely to be mimotopes and the critical amino acid residues recognised by anti-pkMSP-1_{42} antibodies were most probably discontinuous on these peptides.

5.8 Comparison of epitopes identified by synthetic peptide library and by random phage display library

Screening of anti-pkMSP-1_{42} antibodies with synthetic peptide library and random phage display library isolated nine and 14 peptides, respectively. Both epitope mapping techniques identified two regions on the *P. knowlesi* MSP-1_{42} (residues 37-95 and residues 240-289) that could be possibly the dominant epitope regions. However, there were some regions identified by synthetic peptide library but not by phage display library, or vice versa. This discrepancy could be solved by screening a larger number of pkMSP-1_{42}-immunized mice sera using synthetic peptide library. The raised polyclonal antibodies were likely to have numerous antibody clones directed towards different epitopes and different level of epitope specificities corresponding to different region on the *P. knowlesi* MSP-1_{42}. Therefore, by increasing the number of screened sera, the possibility of identifying a novel epitope region could be increased. On the other hand, by screening a larger number of phage clones, additional phage peptides with sequence homologue to the extra epitope regions identified by synthetic peptide library could also be isolated (Williams *et al.*, 1998).

5.9 Evaluation and characterization of identified potential epitopes using mouse model

Two of the most prominent peptides (P10 and P31) were evaluated using mouse model. Minimal cytokine responses were induced in P10-immunized mice group. Altough secretion of IL-2 and IFN-γ were detected, the cytokine levels were not up to statistical significance level compared to the negative

control group, indicating that cell mediated immunity was not significantly up-regulated.

On the other hand, P31-immunized mouse splenocytes secreted high level of cytokines, with both the stimulants pkMSP-1_{42} and P31 were able to induce significant cytokine production. A higher concentration of IFN-γ was induced in the P31-immunized group when stimulated with pkMSP-1_{42} than with P31. However, the baseline IFN-γ level in the PBS negative control group was also comparatively higher when stimulated with the full length protein than with the peptide. Besides, high level of IL-10 was also been stimulated by pkMSP-1_{42} but not peptides. This could be due to contamination by cell debris and vector proteins in the purified pkMSP-1_{42}, which were absent in the peptide solution. Nevertheless, high level of IFN-γ and IL-2 levels indicated that T cells in P31-immunized mice were able to recognise and respond against both the full antigen pkMSP-1_{42} and P31, and the cell mediated immune response was dominantly contributed by Th1 cells.

For the antibody characterization, humoral response was induced in both peptide-injected mice groups. Both peptide-immunized mice sera were able to react with pkMSP-1_{42} in ELISA and Western Blot assay, and four of the main IgG isotypes were detected. Besides, antibodies raised against both peptides were able to recognise *P. knowlesi* blood stage parasites in IFA, indicating that P10 and P31 were immunogenic and might correspond to the epitopes that serve as the binding sites for antibodies on the blood stage parasites.

These findings suggest that P31 could serve as a better epitope candidate for further evaluation as a malaria vaccine and a diagnostic reagent compared to P10, due to its ability to recognise the *P. knowlesi* protein, and to elicit both cell mediated and humoral immunity responses.

5.10 Limitations of the study

One of the limitations in the present study is to obtain *in vitro* culture of *P. knowlesi*. Until today, unlike *P. falciparum, in vitro* culture of *P. knowlesi* is still yet to be well-established and long term culture is difficult to maintain. Therefore, further evaluation of the immunoprotectivity of expressed pkMSP-1_{42} and identified epitopes was unable to be carried out with the limited supply of live *P. knowlesi* parasites. Besides, time constraint was another major limitation. Peptide-immunization of mice is a lengthy procedure which requires about two months for each round of experiment. Repetition of experiments for each epitope is time consuming. Hence, only two identified epitopes were chosen and evaluated using mouse model in the present study.

5.11 Future works

Functional assays should be carried out to assess the immunoprotectivity of pkMSP-1_{42} and identified epitopes, provided that *in vitro* culture of *P. knowlesi* could be established. The ability of anti-pkMSP-1_{42} and anti-peptide antibodies to inhibit the invasion of merozoites into erythrocytes should be evaluated by merozoite invasion inhibition assay. Further method for testing the immunoprotectivity of pkMSP-1_{42} and peptide epitope would be animal immunization and challenge with life *P. knowlesi* parasites.

Besides, the identified epitopes in the present study should be further evaluated with site-directed mutagenesis. Residues which are crucial for immunogenicity can be identified and characterized. By substituting particular amino acid residues in the epitope and assessing the substitution's effect on binding strength, it is possible to identify the critical immunodominant amino

acid residues on the epitopes which serve as binding hot spot for antibodies (King *et al.*, 1992; Chilkoti *et al.*, 1995; Conner *et al.*, 2011).

Computational approach is another way to further characterize the identified potential epitopes. Hitherto, crystallography was done only on *P. knowlesi* MSP-1_{19} (Garman *et al.*, 2003), but not on *P. knowlesi* MSP-1_{42}. The 3D modelling for the structure of *P. knowlesi* MSP-1_{42} should be carried out, followed by 3D epitope mapping of the peptides. This may provide crucial information on the location and structure of the peptides on the protein model. Previous studies have reported that linear and conformational epitopes can be determined successfully by using combination method of phage display and computational algorithm (Rowley *et al.*, 2000; Mumey *et al.*, 2003).

CHAPTER 6: CONCLUSION

In the present study, recombinant pkMSP-1_{33} and pkMSP-1_{42} were successfully expressed using *E. coli* expression system and purified by His-tag affinity chromatography. Large amounts of purified proteins could be obtained to facilitate work on the application of *P. knowlesi* MSP-1_{33} and MSP-1_{42} in immunodiagnosis for malarial infections and immunogenicity tests.

High sensitivity and specificity of *E. coli*-expressed pkMSP-1_{33} and pkMSP-1_{42} in immunoassays reveals that these two recombinant proteins could be useful in general serodiagnosis of malarial infections such as determination of prevalence and endemicity of malarial infection in a population, and blood donor screening. It will be particularly useful in seroepidemiological screening in both human and macaque populations in malaria endemic areas such as Sabah and Sarawak, Malaysia.

pkMSP-1_{42} was highly immunogenic. High cytokine levels and reactivity of the raised antibodies against pkMSP-1_{42} indicated that both cell mediated and humoral immune responses were elicited in pkMSP-1_{42}-immunized mice. Therefore, pkMSP-1_{42} can serve as a potential candidate for malaria vaccine design, although further evaluation needs be carried out to validate its potential and limitations.

Potential epitopes within *P. knowlesi* MSP-1_{42} were identified using overlapping synthetic peptide library and phage display library. Nine peptides were isolated through screening of anti-pkMSP-1_{42} antibodies with synthetic peptide library, while 63 phage clones with 14 different peptide sequences were isolated via screening of anti-pkMSP-1_{42} antibodies with random phage display library. Two regions on *P. knowlesi* MSP-1_{42} (residues 37-95 and residues 240-289) were identified as the potential dominant epitope regions since anti-pkMSP-1_{42} antibodies exhibited high reactivity towards peptides in these two regions by using both epitope mapping techniques, and most of the isolated peptides fell within the two regions.

Two of the most prominent peptides (P10 and P31) were evaluated using mouse model. Significant Th1-dominant cell mediated immune response was elicited in P31-immunized mice. On the other hand, both peptide-immunized mice sera reacted with the full-length pkMSP-1_{42} antigen, indicating that humoral response was elicited in both peptide-immunized groups. P10 and P31 were immunogenic and the antibodies raised against both peptides were able to recognise *P. knowlesi* blood stage parasites. In conclusion, P10 and P31 could be the potential epitopes which serve as binding sites for antibodies on *P. knowelsi* parasites. Nevertheless, further evaluations such as immunoprotectivity assays and site-directed mutagenesis studies are needed to validate the potential of these epitopes for use in the development of malaria vaccine, therapeutic agents or diagnostic tools.

BIBLIOGRAPHY

Abd-el-Aziz, G. A., Landau, I., & Miltgen, F. (1975). Description of *Plasmodium aegyptensis* n. sp., presumed parasite of the Muridae *Arvicanthis noloticus* in Upper Egypt. *Annales de Parasitologie Humaine et Comparee, 50*(4), 419-424.

Adda, C. G., Tilley, L., Anders, R. F., & Foley, M. (1999). Isolation of peptides that mimic epitopes on a malarial antigen from random peptide libraries displayed on phage. *Infection and Immunity, 67*(9), 4679-4688.

Ambroggio, X., Jiang, L., Aebig, J., Obiakor, H., Lukszo, J., & Narum, D. L. (2013). The epitope of monoclonal antibodies blocking erythrocyte invasion by *Plasmodium falciparum* map to the dimerization and receptor glycan binding sites of EBA-175. *PloS One, 8*(2), e56326.

Angov, E., Aufiero, B. M., Turgeon, A. M., Van Handenhove, M., Ockenhouse, C. F., Kester, K. E., Walsh, D. S., McBride, J. S., Dubois, M. C., Cohen, J., Haynes, J. D., Eckels, K. H., Heppner, D. G., Ballou, W. R., Diggs, C. L., & Lyon, J. A. (2003). Development and pre-clinical analysis of a *Plasmodium falciparum* Merozoite Surface Protein-1(42) malaria vaccine. *Molecular and Biochemical Parasitology, 128*(2), 195-204.

Atieli, H. E., Zhou, G., Afrane, Y., Lee, M. C., Mwanzo, I., Githeko, A. K., & Yan, G. (2011). Insecticide-treated net (ITN) ownership, usage, and malaria transmission in the highlands of western Kenya. *Parasites & Vectors, 4*, 113.

Barber, B. E., William, T., Jikal, M., Jilip, J., Dhararaj, P., Menon, J., Yeo, T. W., & Anstey, N. M. (2011). *Plasmodium knowlesi* malaria in children. *Emerging Infectious Diseases, 17*(5), 814-820.

Barlow, D. J., Edwards, M. S., & Thornton, J. M. (1986). Continuous and discontinuous protein antigenic determinants. *Nature, 322*(6081), 747-748.

Bellucci, R., Oertelt, S., Gallagher, M., Li, S., Zorn, E., Weller, E., Porcheray, F., Alyea, E. P., Soiffer, R. J., Munshi, N. C., Gershwin, M. E., & Ritz, J. (2007). Differential epitope mapping of antibodies to PDC-E2 in patients with hematologic malignancies after allogeneic hematopoietic stem cell transplantation and primary biliary cirrhosis. *Blood, 109*(5), 2001-2007.

Blackman, M. J., Chappel, J. A., Shai, S., & Holder, A. A. (1993). A conserved parasite serine protease processes the *Plasmodium falciparum* merozoite surface protein-1. *Molecular and Biochemical Parasitology, 62*(1), 103-114.

Blackman, M. J., Dennis, E. D., Hirst, E. M., Kocken, C. H., Scott-Finnigan, T. J., & Thomas, A. W. (1996). *Plasmodium knowlesi*: secondary processing of the malaria merozoite surface protein-1. *Experimental Parasitology, 83*(2), 229-239.

Blackman, M. J., Heidrich, H. G., Donachie, S., McBride, J. S., & Holder, A. A. (1990). A single fragment of a malaria merozoite surface protein remains on the parasite during red cell invasion and is the target of invasion-inhibiting antibodies. *The Journal of Experimental Medicine, 172*(1), 379-382.

Blackman, M. J., & Holder, A. A. (1992). Secondary processing of the *Plasmodium falciparum* merozoite surface protein-1 (MSP1) by a calcium-dependent membrane-bound serine protease: shedding of MSP133 as a noncovalently associated complex with other fragments of the MSP1. *Molecular and Biochemical Parasitology, 50*(2), 307-315.

Blackman, M. J., Ling, I. T., Nicholls, S. C., & Holder, A. A. (1991a). Proteolytic processing of the *Plasmodium falciparum* merozoite surface protein-1 produces a membrane-bound fragment containing two epidermal growth factor-like domains. *Molecular and Biochemical Parasitology, 49*(1), 29-33.

Blackman, M. J., Scott-Finnigan, T. J., Shai, S., & Holder, A. A. (1994). Antibodies inhibit the protease-mediated processing of a malaria merozoite surface protein. *The Journal of Experimental Medicine, 180*(1), 389-393.

Blackman, M. J., Whittle, H., & Holder, A. A. (1991b). Processing of the *Plasmodium falciparum* major merozoite surface protein-1: identification of a 33-kilodalton secondary processing product which is shed prior to erythrocyte invasion. *Molecular and Biochemical Parasitology, 49*(1), 35-44.

Bottger, V., & Bottger, A. (2009). Epitope mapping using phage display peptide libraries. *Methods in Molecular Biology, 524*, 181-201.

Branch, O. H., Udhayakumar, V., Hightower, A. W., Oloo, A. J., Hawley, W. A., Nahlen, B. L., Bloland, P. B., Kaslow, D. C., & Lal, A. A. (1998). A longitudinal investigation of IgG and IgM antibody responses to the merozoite surface protein-1 19-kiloDalton domain of *Plasmodium falciparum* in pregnant women and infants: associations with febrile illness, parasitemia, and anemia. *The American Journal of Tropical Medicine and Hygiene, 58*(2), 211-219.

Bronner, U., Divis, P. C., Farnert, A., & Singh, B. (2009). Swedish traveller with *Plasmodium knowlesi* malaria after visiting Malaysian Borneo. *Malaria Journal, 8*, 15.

Bublil, E. M., Freund, N. T., Mayrose, I., Penn, O., Roitburd-Berman, A., Rubinstein, N. D., Pupko, T., & Gershoni, J. M. (2007). Stepwise prediction of conformational discontinuous B-cell epitopes using the Mapitope algorithm. *Proteins, 68*(1), 294-304.

Bzik, D. J., Fox, B. A., & Gonyer, K. (1993). Expression of *Plasmodium falciparum* lactate dehydrogenase in *Escherichia coli*. *Molecular and Biochemical Parasitology, 59*(1), 155-166.

Calvo-Calle, J. M., Oliveira, G. A., Watta, C. O., Soverow, J., Parra-Lopez, C., & Nardin, E. H. (2006). A linear peptide containing minimal T- and B-cell epitopes of *Plasmodium falciparum* circumsporozoite protein elicits protection against transgenic sporozoite challenge. *Infection and Immunity*, *74*(12), 6929-6939.

Carter, J. M., & Loomis-Price, L. (2004). B cell epitope mapping using synthetic peptides. In J. E. Coligan, B. Bierer, D. H. Margulies, E. M. Shevach & W. Strober (Eds.), *Current protocols in immunology*. New York, NY: John Wiley & Sons.

Casey, J. L., Coley, A. M., Anders, R. F., Murphy, V. J., Humberstone, K. S., Thomas, A. W., & Foley, M. (2004). Antibodies to malaria peptide mimics inhibit *Plasmodium falciparum* invasion of erythrocytes. *Infection and Immunity*, *72*(2), 1126-1134.

Castagnoli, L., Zucconi, A., Quondam, M., Rossi, M., Vaccaro, P., Panni, S., Paoluzi, S., Santonico, E., Dente, L., & Cesareni, G. (2001). Alternative bacteriophage display systems. *Combinatorial Chemistry & High Throughput Screening*, *4*(2), 121-133.

Chang, S. P., Case, S. E., Gosnell, W. L., Hashimoto, A., Kramer, K. J., Tam, L. Q., Hashiro, C. Q., Nikaido, C. M., Gibson, H. L., Lee-Ng, C. T., Barr, P. J., Yokota, B. T., & Hut, G. S. (1996). A recombinant baculovirus 42-kilodalton C-terminal fragment of *Plasmodium falciparum* merozoite surface protein 1 protects *Aotus* monkeys against malaria. *Infection and Immunity*, *64*(1), 253-261.

Centre for Disease Control and Prevention. (2010). In *About Malaria*. Retrieved June 22, 2014, from http://www.cdc.gov/malaria/about/biology/

Chilkoti, A., Tan, P. H., & Stayton, P. S. (1995). Site-directed mutagenesis studies of the high-affinity streptavidin-biotin complex: contributions of tryptophan

residues 79, 108, and 120. *Proceedings of the National Academy of Sciences of the United States of America, 92*(5), 1754-1758.

Chin, W., Contacos, P. G., Coatney, R. G., & Kimbal, H. R. (1965). A naturally acquired quotidian- type malaria in man transferable to monkeys. *Science, 149*, 865.

Chin, W., Contacos, P. G., Collins, W. E., Jeter, M. H., & Alpert, E. (1968). Experimental mosquito-transmission of *Plasmodium knowlesi* to man and monkey. *The American Journal of Tropical Medicine and Hygiene, 17*(3), 355-358.

Chootong, P., Ntumngia, F. B., VanBuskirk, K. M., Xainli, J., Cole-Tobian, J. L., Campbell, C. O., Fraser, T. S., King, C. L., & Adams, J. H. (2010). Mapping epitopes of the *Plasmodium vivax* Duffy binding protein with naturally acquired inhibitory antibodies. *Infection and Immunity, 78*(3), 1089-1095.

Clark, I. A., & Hunt, N. H. (1983). Evidence for reactive oxygen intermediates causing hemolysis and parasite death in malaria. *Infection and Immunity, 39*(1), 1-6.

Coatney, G. R., Chin, W., Contacos, P. G., & King, H. K. (1966). *Plasmodium inui*, a quartan-type malaria parasite of Old World monkeys transmissible to man. *Journal of Parasitology, 52*(4), 660-663.

Coatney, G. R., Collins, W. E., Warren, M., & Contacos, P. G. (1971). *The primate malarias.* Bethesda, MD: U.S. National Institute of Allergy and Infectious Diseases.

Coley, A. M., Campanale, N. V., Casey, J. L., Hodder, A. N., Crewther, P. E., Anders, R. F., Tilley, L. M., & Foley, M. (2001). Rapid and precise epitope mapping of monoclonal antibodies against *Plasmodium falciparum* AMA1 by combined phage display of fragments and random peptides. *Protein Engineering, Design and Selection, 14*(9), 691-698.

Conner, A. C., Barwell, J., Poyner, D. R., & Wheatley, M. (2011). The use of site-directed mutagenesis to study GPCRs. *Methods in Molecular Biology, 746*, 85-98.

Contacos, P. G., Coatney, G. R., Orihel, T. C., Collins, W. E., Chin, W., & Jeter, M. H. (1970). Transmission of *Plasmodium schwetzi* from the chimpanzee to man by mosquito bite. *The American Journal of Tropical Medicine and Hygiene, 19*(2), 190-195.

Corey, E., Wegner, S. K., Corey, M. J., & Vessella, R. L. (1997). Prostate-specific antigen: characterization of epitopes by synthetic peptide mapping and inhibition studies. *Clinical Chemistry, 43*(4), 575-584.

Cowan, G. J., Creasey, A. M., Dhanasarnsombut, K., Thomas, A. W., Remarque, E. J., & Cavanagh, D. R. (2011). A malaria vaccine based on the polymorphic block 2 region of MSP-1 that elicits a broad serotype-spanning immune response. *PloS One, 6*(10), e26616.

Cox-Singh, J. (2009). Knowlesi malaria in Vietnam. *Malaria Journal, 8*, 269.

Cox-Singh, J., Davis, T. M., Lee, K. S., Shamsul, S. S., Matusop, A., Ratnam, S., Rahman, H. A., Conway, D. J., & Singh, B. (2008). *Plasmodium knowlesi* malaria in humans is widely distributed and potentially life threatening. *Clinical Infectious Diseases, 46*(2), 165-171.

Cox-Singh, J., Hiu, J., Lucas, S. B., Divis, P. C., Zulkarnaen, M., Chandran, P., Wong, K. T., Adem, P., Zaki, S. R., Singh, B., & Krishna, S. (2010). Severe malaria - a case of fatal *Plasmodium knowlesi* infection with post-mortem findings: a case report. *Malaria Journal, 9*, 10.

Cox-Singh, J., & Singh, B. (2008). Knowlesi malaria: newly emergent and of public health importance? *Trends in Parasitology, 24*(9), 406-410.

Cox-Singh, J., Singh, B., Daneshvar, C., Planche, T., Parker-Williams, J., & Krishna, S. (2011). Anti-inflammatory cytokines predominate in acute human *Plasmodium knowlesi* infections. *PloS One, 6*(6), e20541.

Cragg, M. S. (2011). CD20 antibodies: doing the time warp. *Blood, 118*(2), 219-220.

Creative Diagnostics. (2014). In *Epitope Mapping*. Retrieved June 22, 2014, from http://www.creative-diagnostics.com/Epitope-Mapping.html

Cwirla, S. E., Peters, E. A., Barrett, R. W., & Dower, W. J. (1990). Peptides on phage: a vast library of peptides for identifying ligands. *Proceedings of the National Academy of Sciences of the United States of America, 87*(16), 6378-6382.

D'Andrea, A., Aste-Amezaga, M., Valiante, N. M., Ma, X., Kubin, M., & Trinchieri, G. (1993). Interleukin 10 (IL-10) inhibits human lymphocyte interferon gamma-production by suppressing natural killer cell stimulatory factor/IL-12 synthesis in accessory cells. *The Journal of Experimental Medicine, 178*(3), 1041-1048.

Daly, T. M., & Long, C. A. (1993). A recombinant 15-kilodalton carboxyl-terminal fragment of *Plasmodium yoelii yoelii* 17XL merozoite surface protein 1 induces a protective immune response in mice. *Infection and Immunity, 61*(6), 2462-2467.

Daneshvar, C., Davis, T. M., Cox-Singh, J., Rafa'ee, M. Z., Zakaria, S. K., Divis, P. C., & Singh, B. (2009). Clinical and laboratory features of human *Plasmodium knowlesi* infection. *Clinical Infectious Diseases, 49*(6), 852-860.

Daneshvar, C., Davis, T. M., Cox-Singh, J., Rafa'ee, M. Z., Zakaria, S. K., Divis, P. C., & Singh, B. (2010). Clinical and parasitological response to oral chloroquine and primaquine in uncomplicated human *Plasmodium knowlesi* infections. *Malaria Journal, 9*, 238.

Darko, C. A., Angov, E., Collins, W. E., Bergmann-Leitner, E. S., Girouard, A. S., Hitt, S. L., McBride, J. S., Diggs, C. L., Holder, A. A., Long, C. A., Barnwell, J. W.,

& Lyon, J. A. (2005). The clinical-grade 42-kilodalton fragment of merozoite surface protein 1 of *Plasmodium falciparum* strain FVO expressed in *Escherichia coli* protects *Aotus nancymai* against challenge with homologous erythrocytic-stage parasites. *Infection and Immunity, 73*(1), 287-297.

Devlin, J. J., Panganiban, L. C., & Devlin, P. E. (1990). Random peptide libraries: a source of specific protein binding molecules. *Science, 249*(4967), 404-406.

Diggs, C. L., & Sadun, E. H. (1965). Serological cross reactivity between *Plasmodium vivax* and *Plasmodium falciparum* as determined by a modified fluorescent antibody test. *Experimental Parasitology, 16*, 217-223.

Dondorp, A., Nosten, F., Stepniewska, K., Day, N., & White, N. (2005). Artesunate versus quinine for treatment of severe falciparum malaria: a randomised trial. *Lancet, 366*(9487), 717-725.

Dondorp, A. M., Fanello, C. I., Hendriksen, I. C., Gomes, E., Seni, A., Chhaganlal, K. D., Bojang, K., Olaosebikan, R., Anunobi, N., Maitland, K., Kivaya, E., Agbenyega, T., Nguah, S. B., Evans, J., Gesase, S., Kahabuka, C., Mtove, G., Nadjm, B., Deen, J., Mwanga-Amumpaire, J., Nansumba, M., Karema, C., Umulisa, N., Uwimana, A., Mokuolu, O. A., Adedoyin, O. T., Johnson, W. B., Tshefu, A. K., Onyamboko, M. A., Sakulthaew, T., Ngum, W. P., Silamut, K., Stepniewska, K., Woodrow, C. J., Bethell, D., Wills, B., Oneko, M., Peto, T. E., von Seidlein, L., Day, N. P., & White, N. J. (2010). Artesunate versus quinine in the treatment of severe falciparum malaria in African children (AQUAMAT): an open-label, randomised trial. *Lancet, 376*(9753), 1647-1657.

Draper, S. J., Goodman, A. L., Biswas, S., Forbes, E. K., Moore, A. C., Gilbert, S. C., & Hill, A. V. (2009). Recombinant viral vaccines expressing merozoite surface protein-1 induce antibody- and T cell-mediated multistage protection against malaria. *Cell Host & Microbe, 5*(1), 95-105.

Dutta, S., Kaushal, D. C., Ware, L. A., Puri, S. K., Kaushal, N. A., Narula, A., Upadhyaya, D. S., & Lanar, D. E. (2005). Merozoite surface protein 1 of *Plasmodium vivax* induces a protective response against *Plasmodium cynomolgi* challenge in rhesus monkeys. *Infection and Immunity, 73*(9), 5936-5944.

Dutta, S., Ware, L. A., Barbosa, A., Ockenhouse, C. F., & Lanar, D. E. (2001). Purification, characterization, and immunogenicity of a disulfide cross-linked *Plasmodium vivax* vaccine candidate antigen, merozoite surface protein 1, expressed in *Escherichia coli*. *Infection and Immunity, 69*(9), 5464-5470.

Dworschak, J., Recke, A., Freitag, M., Ludwig, R. J., Langenhan, J., Kreuzer, O. J., Zillikens, D., & Schmidt, E. (2012). Mapping of B cell epitopes on desmoglein 3 in pemphigus vulgaris patients by the use of overlapping peptides. *Journal of Dermatological Science, 65*(2), 102-109.

Eda, K., Eda, S., & Sherman, I. W. (2004). Identification of peptides targeting the surface of *Plasmodium falciparum*-infected erythrocytes using a phage display peptide library. *The American Journal of Tropical Medicine and Hygiene, 71*(2), 190-195.

Egan, A., Waterfall, M., Pinder, M., Holder, A., & Riley, E. (1997). Characterization of human T- and B-cell epitopes in the C terminus of *Plasmodium falciparum* merozoite surface protein 1: evidence for poor T-cell recognition of polypeptides with numerous disulfide bonds. *Infection and Immunity, 65*(8), 3024-3031.

Egan, A. F., Burghaus, P., Druilhe, P., Holder, A. A., & Riley, E. M. (1999). Human antibodies to the 19kDa C-terminal fragment of *Plasmodium falciparum* merozoite surface protein 1 inhibit parasite growth *in vitro*. *Parasite Immunology, 21*(3), 133-139.

Egan, A. F., Morris, J., Barnish, G., Allen, S., Greenwood, B. M., Kaslow, D. C., Holder, A. A., & Riley, E. M. (1996). Clinical immunity to *Plasmodium*

falciparum malaria is associated with serum antibodies to the 19-kDa C-terminal fragment of the merozoite surface antigen, PfMSP-1. *The Journal of Infectious Diseases, 173*(3), 765-769.

Epp, C., Kauth, C. W., Bujard, H., & Lutz, R. (2003). Expression and purification of *Plasmodium falciparum* MSP-1(42): A malaria vaccine candidate. *Journal of Chromatography B, 786*(1-2), 61-72.

Eyles, D. E., Coatney, G. R., & Getz, M. E. (1960). Vivax-type malaria parasite of macaques transmissible to man. *Science, 131*, 1812-1813.

Eyles, D. E., Warren, M., Guinn, E., Wharton, R. H., & Ramachandran, C. P. (1963). Identification of *Anopheles balabacensis introlatus* as a vector of monkey malaria in Malaya. *Bulletin of the World Health Organization, 28*(1), 134-135.

Fernando, S. D., Rodrigo, C., & Rajapakse, S. (2011). Chemoprophylaxis in malaria: drugs, evidence of efficacy and costs. *Asian Pacific Journal of Tropical Medicine, 4*(4), 330-336.

Figtree, M., Lee, R., Bain, L., Kennedy, T., Mackertich, S., Urban, M., Cheng, Q., & Hudson, B. J. (2010). *Plasmodium knowlesi* in human, Indonesian Borneo. *Emerging Infectious Diseases, 16*(4), 672-674.

Finkelman, F. D., Katona, I. M., Mosmann, T. R., & Coffman, R. L. (1988). IFN-gamma regulates the isotypes of Ig secreted during *in vivo* humoral immune responses. *The Journal of Immunology, 140*(4), 1022-1027.

Fong, Y. L., Cadigan, F. C., & Coatney, G. R. (1971). A presumptive case of naturally occurring *Plasmodium knowlesi* malaria in man in Malaysia. *Transactions of the Royal Society of Tropical Medicine and Hygiene, 65*(6), 839-840.

Garman, S. C., Simcoke, W. N., Stowers, A. W., & Garboczi, D. N. (2003). Structure of the C-terminal domains of merozoite surface protein-1 from *Plasmodium*

knowlesi reveals a novel histidine binding site. *The Journal of Biological Chemistry, 278*(9), 7264-7269.

Garnham, P. C., Lainson, R., & Cooper, W. (1957). The tissue stages and sporogony of *Plasmodium knowlesi*. *Transactions of the Royal Society of Tropical Medicine and Hygiene, 51*(5), 384-396.

Gaseitsiwe, S., Valentini, D., Mahdavifar, S., Reilly, M., Ehrnst, A., & Maeurer, M. (2010). Peptide microarray-based identification of *Mycobacterium tuberculosis* epitope binding to HLA-DRB1*0101, DRB1*1501, and DRB1*0401. *Clinical and Vaccine Immunology, 17*(1), 168-175.

Gershoni, J. M., Roitburd-Berman, A., Siman-Tov, D. D., Tarnovitski Freund, N., & Weiss, Y. (2007). Epitope mapping: the first step in developing epitope-based vaccines. *BioDrugs, 21*(3), 145-156.

Geysen, H. M., Meloen, R. H., & Barteling, S. J. (1984). Use of peptide synthesis to probe viral antigens for epitopes to a resolution of a single amino acid. *Proceedings of the National Academy of Sciences of the United States of America, 81*(13), 3998-4002.

Geysen, H. M., Rodda, S. J., & Mason, T. J. (1986). A priori delineation of a peptide which mimics a discontinuous antigenic determinant. *Molecular Immunology, 23*(7), 709-715.

Geysen, H. M., Rodda, S. J., Mason, T. J., Tribbick, G., & Schoofs, P. G. (1987). Strategies for epitope analysis using peptide synthesis. *Journal of Immunological Methods, 102*(2), 259-274.

Goel, V. K., Li, X., Chen, H., Liu, S. C., Chishti, A. H., & Oh, S. S. (2003). Band 3 is a host receptor binding merozoite surface protein 1 during the *Plasmodium falciparum* invasion of erythrocytes. *Proceedings of the National Academy of Sciences of the United States of America, 100*(9), 5164-5169.

Goldsby, R. A., Kindt, T. J., Kuby, J., & Osborne, B. A. (2002). *Immunology* (5th ed.). New York, NY: W. H. Freeman.

Good, M. F. (2001). Towards a blood-stage vaccine for malaria: are we following all the leads? *Nature Reviews Immunology, 1*(2), 117-125.

Guthridge, J. M., Young, K., Gipson, M. G., Sarrias, M. R., Szakonyi, G., Chen, X. S., Malaspina, A., Donoghue, E., James, J. A., Lambris, J. D., Moir, S. A., Perkins, S. J., & Holers, V. M. (2001). Epitope mapping using the X-ray crystallographic structure of complement receptor type 2 (CR2)/CD21: identification of a highly inhibitory monoclonal antibody that directly recognizes the CR2-C3d interface. *The Journal of Immunology, 167*(10), 5758-5766.

Haghi, A. M., Khoramizade, M. R., Nateghpour, M., Mohebali, M., Edrissian, G. H., Eshraghian, M. R., & Sepehrizadeh, Z. (2012). A recombinant *Plasmodium vivax* apical membrane antigen-1 to detect human infection in Iran. *The Korean Journal of Parasitology, 50*(1), 15-21.

Harris, K. S., Casey, J. L., Coley, A. M., Masciantonio, R., Sabo, J. K., Keizer, D. W., Lee, E. F., McMahon, A., Norton, R. S., Anders, R. F., & Foley, M. (2005). Binding hot spot for invasion inhibitory molecules on *Plasmodium falciparum* apical membrane antigen 1. *Infection and Immunity, 73*(10), 6981-6989.

Haste Andersen, P., Nielsen, M., & Lund, O. (2006). Prediction of residues in discontinuous B-cell epitopes using protein 3D structures. *Protein Science, 15*(11), 2558-2567.

Herrera, S., Rudin, W., Herrera, M., Clavijo, P., Mancilla, L., de Plata, C., Matile, H., & Certa, U. (1993). A conserved region of the MSP-1 surface protein of *Plasmodium falciparum* contains a recognition sequence for erythrocyte spectrin. *The EMBO Journal, 12*(4), 1607-1614.

Hertveldt, K., Belien, T., & Volckaert, G. (2009). General M13 phage display: M13 phage display in identification and characterization of protein-protein interactions. *Methods in Molecular Biology, 502*, 321-339.

Hightower, A., Kiptui, R., Manya, A., Wolkon, A., Vanden Eng, J. L., Hamel, M., Noor, A., Sharif, S. K., Buluma, R., Vulule, J., Laserson, K., Slutsker, L., & Akhwale, W. (2010). Bed net ownership in Kenya: the impact of 3.4 million free bed nets. *Malaria Journal, 9*, 183.

Hirunpetcharat, C., Tian, J. H., Kaslow, D. C., van Rooijen, N., Kumar, S., Berzofsky, J. A., Miller, L. H., & Good, M. F. (1997). Complete protective immunity induced in mice by immunization with the 19-kilodalton carboxyl-terminal fragment of the merozoite surface protein-1 (MSP1[19]) of *Plasmodium yoelii* expressed in *Saccharomyces cerevisiae*: correlation of protection with antigen-specific antibody titer, but not with effector CD4+ T cells. *The Journal of Immunology, 159*(7), 3400-3411.

Holder, A. A., & Freeman, R. R. (1982). Biosynthesis and processing of a *Plasmodium falciparum* schizont antigen recognized by immune serum and a monoclonal antibody. *The Journal of Experimental Medicine, 156*(5), 1528-1538.

Holder, A. A., Sandhu, J. S., Hillman, Y., Davey, L. S., Nicholls, S. C., Cooper, H., & Lockyer, M. J. (1987). Processing of the precursor to the major merozoite surface antigens of *Plasmodium falciparum*. *Parasitology, 94*, 199-208.

Hopp, T. (1985). Computer prediction of protein surface features and antigenic determinants. *Progress in Clinical and Biological Research, 172*, 367-377.

Hopp, T. P., & Woods, K. R. (1981). Prediction of protein antigenic determinants from amino acid sequences. *Proceedings of the National Academy of Sciences of the United States of America, 78*(6), 3824-3828.

Huang, J., & Honda, W. (2006). CED: a conformational epitope database. *BMC Immunology, 7*, 7.

Hui, G. S., Nikaido, C., Hashiro, C., Kaslow, D. C., & Collins, W. E. (1996). Dominance of conserved B-cell epitopes of the *Plasmodium falciparum* merozoite surface protein, MSP1, in blood-stage infections of naive *Aotus* monkeys. *Infection and Immunity, 64*(5), 1502-1509.

Hussain, R., Dawood, G., Abrar, N., Toossi, Z., Minai, A., Dojki, M., & Ellner, J. J. (1995). Selective increases in antibody isotypes and immunoglobulin G subclass responses to secreted antigens in tuberculosis patients and healthy household contacts of the patients. *Clinical and Diagnostic Laboratory Immunology, 2*(6), 726-732.

Ibiwoye, M. O., Howard, C. V., Sibbons, P., Hasan, M., & van Velzen, D. (1993). Cerebral malaria in the rhesus monkey (*Macaca mulatta*): observations on host pathology. *Journal of Comparative Pathology, 108*(3), 303-310.

Imwong, M., Tanomsing, N., Pukrittayakamee, S., Day, N. P., White, N. J., & Snounou, G. (2009). Spurious amplification of a *Plasmodium vivax* small-subunit RNA gene by use of primers currently used to detect *P. knowlesi*. *Journal of Clinical Microbiology, 47*(12), 4173-4175.

Jiang, N., Chang, Q., Sun, X., Lu, H., Yin, J., Zhang, Z., Wahlgren, M., & Chen, Q. (2010). Co-infections with *Plasmodium knowlesi* and other malaria parasites, Myanmar. *Emerging Infectious Diseases, 16*(9), 1476-1478.

Jongwutiwes, S., Putaporntip, C., Iwasaki, T., Sata, T., & Kanbara, H. (2004). Naturally acquired *Plasmodium knowlesi* malaria in human, Thailand. *Emerging Infectious Diseases, 10*(12), 2211-2213.

Kam-Morgan, L. N., Smith-Gill, S. J., Taylor, M. G., Zhang, L., Wilson, A. C., & Kirsch, J. F. (1993). High-resolution mapping of the HyHEL-10 epitope of

chicken lysozyme by site-directed mutagenesis. *Proceedings of the National Academy of Sciences of the United States of America*, *90*(9), 3958-3962.

Kamboj, K. K., Barnwell, J. W., Nussenzweig, R. S., & Cochrane, A. H. (1988). Characterization of cross-reactive blood-stage antigens of the *Plasmodium cynomolgi* complex using anti-*Plasmodium vivax* monoclonal antibodies. *The Journal of Parasitology, 74*(3), 403-408.

Kantele, A., & Jokiranta, T. S. (2011). Review of cases with the emerging fifth human malaria parasite, *Plasmodium knowlesi*. *Clinical Infectious Diseases, 52*(11), 1356-1362.

Kantele, A., Marti, H., Felger, I., Muller, D., & Jokiranta, T. S. (2008). Monkey malaria in a European traveler returning from Malaysia. *Emerging Infectious Diseases, 14*(9), 1434-1436.

Kaushal, D. C., Kaushal, N. A., Narula, A., Kumar, N., Puri, S. K., Dutta, S., & Lanar, D. E. (2007). Biochemical and immunological characterization of *E. coli* expressed 42 kDa fragment of *Plasmodium vivax* and *P. cynomolgi bastianelli* merozoite surface protein-1. *Indian Journal of Biochemistry & Biophysics, 44*(6), 429-436.

Kawai, S., Hirai, M., Haruki, K., Tanabe, K., & Chigusa, Y. (2009). Cross-reactivity in rapid diagnostic tests between human malaria and zoonotic simian malaria parasite *Plasmodium knowlesi* infections. *Parasitology International, 58*(3), 300-302.

Kidd, P. (2003). Th1/Th2 balance: the hypothesis, its limitations, and implications for health and disease. *Alternative Medicine Review, 8*(3), 223-246.

Kim, Y. M., Hwang, H. A., Yun, W. S., Kim, S. I., Lee, K. W., Park, S. K., Lee, Y. J., Kim, T. K., Wongsrichanalai, C., Sakanari, J. A., & Park, H. (2004). Efficacy of

the merozoite surface protein 1 of *Plasmodium vivax* as an antigen for ELISA to diagnose malaria. *Yonsei Medical Journal, 45*(1), 129-134.

King, R. A., Anders, D. L., & Christie, G. E. (1992). Site-directed mutagenesis of an amino acid residue in the bacteriophage P2 ogr protein implicated in interaction with *Escherichia coli* RNA polymerase. *Molecular Microbiology, 6*(22), 3313-3320.

Konthur, Z., & Crameri, R. (2003). High-throughput applications of phage display in proteomic analyses. *Targets, 2*(6), 261-270.

Krotoski, W. A., & Collins, W. E. (1982). Failure to detect hypnozoites in hepatic tissue containing exoerythrocytic schizonts of *Plasmodium knowlesi*. *The American Journal of Tropical Medicine and Hygiene, 31*(4), 854-856.

Lauterbach, S. B., Lanzillotti, R., & Coetzer, T. L. (2003). Construction and use of *Plasmodium falciparum* phage display libraries to identify host parasite interactions. *Malaria Journal, 2*(1), 47.

Laver, W. G., Air, G. M., Webster, R. G., & Smith-Gill, S. J. (1990). Epitopes on protein antigens: misconceptions and realities. *Cell, 61*(4), 553-556.

Lee, K. S., Cox-Singh, J., Brooke, G., Matusop, A., & Singh, B. (2009a). *Plasmodium knowlesi* from archival blood films: further evidence that human infections are widely distributed and not newly emergent in Malaysian Borneo. *International Journal for Parasitology, 39*(10), 1125-1128.

Lee, K. S., Cox-Singh, J., & Singh, B. (2009b). Morphological features and differential counts of *Plasmodium knowlesi* parasites in naturally acquired human infections. *Malaria Journal, 8*, 73.

Lee, W. C., Chin, P. W., Lau, Y. L., Chin, L. C., Fong, M. Y., Yap, C. J., Supramaniam, R. R., & Mahmud, R. (2013). Hyperparasitaemic human *Plasmodium knowlesi*

infection with atypical morphology in peninsular Malaysia. *Malaria Journal, 12*, 88.

Levine, N. D. (1988). Progress in taxonomy of the Apicomplexan protozoa. *Journal of Protozoology, 35*(4), 518-520.

Li, X., Chen, H., Oo, T. H., Daly, T. M., Bergman, L. W., Liu, S. C., Chishti, A. H., & Oh, S. S. (2004). A co-ligand complex anchors *Plasmodium falciparum* merozoites to the erythrocyte invasion receptor band 3. *The Journal of Biological Chemistry, 279*(7), 5765-5771.

Lima-Junior, J. C., Jiang, J., Rodrigues-da-Silva, R. N., Banic, D. M., Tran, T. M., Ribeiro, R. Y., Meyer, V. S., De-Simone, S. G., Santos, F., Moreno, A., Barnwell, J. W., Galinski, M. R., & Oliveira-Ferreira, J. (2011). B cell epitope mapping and characterization of naturally acquired antibodies to the *Plasmodium vivax* merozoite surface protein-3alpha (PvMSP-3alpha) in malaria exposed individuals from Brazilian Amazon. *Vaccine, 29*(9), 1801-1811.

Ling, I. T., Ogun, S. A., & Holder, A. A. (1994). Immunization against malaria with a recombinant protein. *Parasite Immunology, 16*(2), 63-67.

Linke, A., Kuhn, R., Muller, W., Honarvar, N., Li, C., & Langhorne, J. (1996). *Plasmodium chabaudi chabaudi*: differential susceptibility of gene-targeted mice deficient in IL-10 to an erythrocytic-stage infection. *Experimental Parasitology, 84*(2), 253-263.

Luchavez, J., Espino, F., Curameng, P., Espina, R., Bell, D., Chiodini, P., Nolder, D., Sutherland, C., Lee, K. S., & Singh, B. (2008). Human Infections with *Plasmodium knowlesi*, the Philippines. *Emeriging Infectious Diseases, 14*(5), 811-813.

Maksyutov, A. Z., & Zagrebelnaya, E. S. (1993). ADEPT: a computer program for prediction of protein antigenic determinants. *Computer Applications in the Biosciences, 9*(3), 291-297.

Malaria Site. (2009). In *Control of Malaria*. Retrieved June 5, 2014, from http://www.malariasite.com/malaria/ControlOfMalaria.htm

Malhotra, I., Wamachi, A. N., Mungai, P. L., Mzungu, E., Koech, D., Muchiri, E., Moormann, A. M., & King, C. L. (2008). Fine specificity of neonatal lymphocytes to an abundant malaria blood-stage antigen: epitope mapping of *Plasmodium falciparum* MSP1(33). *The Journal of Immunology, 180*(5), 3383-3390.

McBride, J. S., & Heidrich, H. G. (1987). Fragments of the polymorphic Mr 185,000 glycoprotein from the surface of isolated *Plasmodium falciparum* merozoites form an antigenic complex. *Molecular and Biochemical Parasitology, 23*(1), 71-84.

McCutchan, T. F., Piper, R. C., & Makler, M. T. (2008). Use of malaria rapid diagnostic test to identify *Plasmodium knowlesi* infection. *Emerging Infectious Diseases, 14*(11), 1750-1752.

McKean, P. G., O'Dea, K., & Brown, K. N. (1993). Nucleotide sequence analysis and epitope mapping of the merozoite surface protein 1 from *Plasmodium chabaudi chabaudi* AS. *Molecular and Biochemichal Parasitology, 62*(2), 199-209.

Medina, T. S., Costa, S. P., Oliveira, M. D., Ventura, A. M., Souza, J. M., Gomes, T. F., Vallinoto, A. C., Povoa, M. M., Silva, J. S., & Cunha, M. G. (2011). Increased interleukin-10 and interferon-gamma levels in *Plasmodium vivax* malaria suggest a reciprocal regulation which is not altered by IL-10 gene promoter polymorphism. *Malaria Journal, 10*, 264.

Miller, L. H., Johnson, J. G., Schmidt-Ullrich, R., Haynes, J. D., Wallach, D. F., & Carter, R. (1980). Determinants on surface proteins of *Plasmodium knowlesi* merozoites common to *Plasmodium falciparum* schizonts. *The Journal of Experimental Medicine*, *151*(4), 790-798.

Moss, D. K., Remarque, E. J., Faber, B. W., Cavanagh, D. R., Arnot, D. E., Thomas, A. W., & Holder, A. A. (2012). *Plasmodium falciparum* 19-kilodalton merozoite surface protein 1 (MSP1)-specific antibodies that interfere with parasite growth *in vitro* can inhibit MSP1 processing, merozoite invasion, and intracellular parasite development. *Infection and Immunity*, *80*(3), 1280-1287.

Mumey, B. M., Bailey, B. W., Kirkpatrick, B., Jesaitis, A. J., Angel, T., & Dratz, E. A. (2003). A new method for mapping discontinuous antibody epitopes to reveal structural features of proteins. *Journal of Computational Biology*, *10*(3-4), 555-567.

Mustafa, B., Jenneby, M., Esther, K. A., Hastings, O. S., & Michael, G. M. (2010). Immunity to *Plasmodium knowlesi* H strain malaria in olive baboons. *International Journal of Integrative Biology*, *10*(3), 147-152.

New England Biolabs. (2014). In *Ph.D.™-12 Phage Display Peptide Library Kit*. Retrieved May 28, 2014, from https://www.neb.com/products/e8110-phd-12-phage-display-peptide-library-kit

Ng, O. T., Ooi, E. E., Lee, C. C., Lee, P. J., Ng, L. C., Pei, S. W., Tu, T. M., Loh, J. P., & Leo, Y. S. (2008). Naturally acquired human *Plasmodium knowlesi* infection, Singapore. *Emerging Infectious Diseases*, *14*(5), 814-816.

O'Donnell, R. A., de Koning-Ward, T. F., Burt, R. A., Bockarie, M., Reeder, J. C., Cowman, A. F., & Crabb, B. S. (2001). Antibodies against merozoite surface protein (MSP)-1(19) are a major component of the invasion-inhibitory response

in individuals immune to malaria. *The Journal of Experimental Medicine, 193*(12), 1403-1412.

Odorico, M., & Pellequer, J. L. (2003). BEPITOPE: predicting the location of continuous epitopes and patterns in proteins. *Journal of Molecular Recognition, 16*(1), 20-22.

Ogunbanwo, J. A., Pendyala, P. R., Malhotra, P., & Chauhan, V. S. (2006). Expression, purification and characterization of a recombinant *Plasmodium vivax* thrombospondin related adhesive protein (PvTRAP). *International Journal of Biomedical Science, 2*(3), 251-259.

Orth, H., Jensen, B. O., Holtfreter, M. C., Kocheril, S. J., Mallach, S., MacKenzie, C., Muller-Stover, I., Henrich, B., Imwong, M., White, N. J., Haussinger, D., & Richter, J. (2013). *Plasmodium knowlesi* infection imported to Germany, January 2013. *Eurosurveillance, 18*(40), pii=20603.

Palaeya, V., Lau, Y. L., Mahmud, R., Chen, Y., & Fong, M. Y. (2013). Cloning, expression, and immunocharacterization of surface protein containing an altered thrombospondin repeat domain (SPATR) from *Plasmodium knowlesi*. *Malaria Journal, 12*, 182.

Pan, W., Ravot, E., Tolle, R., Frank, R., Mosbach, R., Turbachova, I., & Bujard, H. (1999). Vaccine candidate MSP-1 from *Plasmodium falciparum*: a redesigned 4917 bp polynucleotide enables synthesis and isolation of full-length protein from *Escherichia coli* and mammalian cells. *Nucleic Acids Research, 27*(4), 1094-1103.

Parham, P. (2009). *The immune system* (3rd ed.). New York, NY: Garland Science.

Parmley, S. F., & Smith, G. P. (1988). Antibody-selectable filamentous fd phage vectors: affinity purification of target genes. *Gene, 73*(2), 305-318.

Perlmann, P., & Troye-Blomberg, M. (2000). Malaria blood-stage infection and its control by the immune system. *Folia Biologica, 46*(6), 210-218.

Polley, S. D., Tetteh, K. K., Cavanagh, D. R., Pearce, R. J., Lloyd, J. M., Bojang, K. A., Okenu, D. M., Greenwood, B. M., McBride, J. S., & Conway, D. J. (2003). Repeat sequences in block 2 of *Plasmodium falciparum* merozoite surface protein 1 are targets of antibodies associated with protection from malaria. *Infection and Immunity, 71*(4), 1833-1842.

Praba-Egge, A. D., Montenegro, S., Cogswell, F. B., Hopper, T., & James, M. A. (2002). Cytokine responses during acute simian *Plasmodium cynomolgi* and *Plasmodium knowlesi* infections. *The American Journal of Tropical Medicine and Hygiene, 67*(6), 586-596.

Putaporntip, C., Jongwutiwes, S., Sakihama, N., Ferreira, M. U., Kho, W. G., Kaneko, A., Kanbara, H., Hattori, T., & Tanabe, K. (2002). Mosaic organization and heterogeneity in frequency of allelic recombination of the *Plasmodium vivax* merozoite surface protein-1 locus. *Proceedings of the National Academy of Sciences of the United States of America, 99*(25), 16348-16353.

Putaporntip, C., Thongaree, S., & Jongwutiwes, S. (2013). Differential sequence diversity at merozoite surface protein-1 locus of *Plasmodium knowlesi* from humans and macaques in Thailand. *Infection, Genetics and Evolution, 18*, 213-219.

Quin, S. J., & Langhorne, J. (2001). Different regions of the malaria merozoite surface protein 1 of *Plasmodium chabaudi* elicit distinct T-cell and antibody isotype responses. *Infection and Immunity, 69*(4), 2245-2251.

Rajahram, G. S., Barber, B. E., William, T., Menon, J., Anstey, N. M., & Yeo, T. W. (2012). Deaths due to *Plasmodium knowlesi* malaria in Sabah, Malaysia:

association with reporting as *Plasmodium malariae* and delayed parenteral artesunate. *Malaria Journal, 11*, 284.

Reid, J. A., & Weitz, B. (1961). Anopheline mosquitoes as vectors of animal malaria in Malaya. *Annals of Tropical Medicine and Parasitology, 55*, 180-186.

Renia, L., Ling, I. T., Marussig, M., Miltgen, F., Holder, A. A., & Mazier, D. (1997). Immunization with a recombinant C-terminal fragment of *Plasmodium yoelii* merozoite surface protein 1 protects mice against homologous but not heterologous *P. yoelii* sporozoite challenge. *Infection and Immunity, 65*(11), 4419-4423.

Ricchiuti, V., Briand, J. P., Meyer, O., Isenberg, D. A., Pruijn, G., & Muller, S. (1994). Epitope mapping with synthetic peptides of 52-kD SSA/Ro protein reveals heterogeneous antibody profiles in human autoimmune sera. *Clinical and Experimental Immunology, 95*(3), 397-407.

Richards, J. S., & Beeson, J. G. (2009). The future for blood-stage vaccines against malaria. *Immunology and Cell Biology, 87*(5), 377-390.

Riley, E. M., Allen, S. J., Wheeler, J. G., Blackman, M. J., Bennett, S., Takacs, B., Schonfeld, H. J., Holder, A. A., & Greenwood, B. M. (1992). Naturally acquired cellular and humoral immune responses to the major merozoite surface antigen (PfMSP1) of *Plasmodium falciparum* are associated with reduced malaria morbidity. *Parasite Immunology, 14*(3), 321-337.

Rowley, M. J., Scealy, M., Whisstock, J. C., Jois, J. A., Wijeyewickrema, L. C., & Mackay, I. R. (2000). Prediction of the immunodominant epitope of the pyruvate dehydrogenase complex E2 in primary biliary cirrhosis using phage display. *The Journal of Immunology, 164*(6), 3413-3419.

Russel, M., Linderoth, N. A., & Sali, A. (1997). Filamentous phage assembly: variation on a protein export theme. *Gene, 192*(1), 23-32.

Sachdeva, S., Ahmad, G., Malhotra, P., Mukherjee, P., & Chauhan, V. S. (2004). Comparison of immunogenicities of recombinant *Plasmodium vivax* merozoite surface protein 1 19- and 42-kiloDalton fragments expressed in *Escherichia coli*. *Infection and Immunity, 72*(10), 5775-5782.

Sachdeva, S., Mohmmed, A., Dasaradhi, P. V., Crabb, B. S., Katyal, A., Malhotra, P., & Chauhan, V. S. (2006). Immunogenicity and protective efficacy of *Escherichia coli* expressed *Plasmodium falciparum* merozoite surface protein-1(42) using human compatible adjuvants. *Vaccine, 24*(12), 2007-2016.

Schall, J. J. (2000). Transmission success of the malaria parasite *Plasmodium mexicanum* into its vector: role of gametocyte density and sex ratio. *Parasitology, 121(Pt 6)*, 575-580.

Scott, J. K., & Smith, G. P. (1990). Searching for peptide ligands with an epitope library. *Science, 249*(4967), 386-390.

Severinson, E., Naito, T., Tokumoto, H., Fukushima, D., Hirano, A., Hama, K., & Honjo, T. (1987). Interleukin 4 (IgG1 induction factor): a multifunctional lymphokine acting also on T cells. *European Journal of Immunology, 17*(1), 67-72.

Singh, A. P., Ozwara, H., Kocken, C. H., Puri, S. K., Thomas, A. W., & Chitnis, C. E. (2005). Targeted deletion of *Plasmodium knowlesi* Duffy binding protein confirms its role in junction formation during invasion. *Molecular Microbiology, 55*(6), 1925-1934.

Singh, B., Bobogare, A., Cox-Singh, J., Snounou, G., Abdullah, M. S., & Rahman, H. A. (1999). A genus- and species-specific nested polymerase chain reaction malaria detection assay for epidemiologic studies. *The American Journal of Tropical Medicine and Hygiene, 60*(4), 687-692.

Singh, B., Lee., K. S., Matusop, A., Radhakrishnan, A., Shamsul, S. S., Cox-Singh, J., Thomas, A., & Conway, D. J. (2004). A large focus of naturally acquired *Plasmodium knowlesi* infections in human beings. *Lancet, 363*(9414), 1017-1024.

Singh, S., Kennedy, M. C., Long, C. A., Saul, A. J., Miller, L. H., & Stowers, A. W. (2003). Biochemical and immunological characterization of bacterially expressed and refolded *Plasmodium falciparum* 42-kilodalton C-terminal merozoite surface protein 1. *Infection and Immunity, 71*(12), 6766-6774.

Singh, S., Miura, K., Zhou, H., Muratova, O., Keegan, B., Miles, A., Martin, L. B., Saul, A. J., Miller, L. H., & Long, C. A. (2006). Immunity to recombinant *Plasmodium falciparum* merozoite surface protein 1 (MSP1): protection in *Aotus nancymai* monkeys strongly correlates with anti-MSP1 antibody titer and *in vitro* parasite-inhibitory activity. *Infection and Immunity, 74*(8), 4573-4580.

Sinton, J. A., & Mulligan, H. W. (1933). A critical review of the literature relating to the identification of the malarial parasites recorded from monkeys of the families Cercopithecidae and Colobidae. *Records of the Malaria Survey of India, 3*, 381-443.

Smith-Gill, S. J. (1994). Protein epitopes: functional vs. structural definitions. *Research in Immunology, 145*(1), 67-70.

Smith, G. P. (1985). Filamentous fusion phage: novel expression vectors that display cloned antigens on the virion surface. *Science, 228*(4705), 1315-1317.

Spano, F., Matsuoka, H., Ozawa, R., Chinzei, Y., & Sinden, R. E. (1996). Epitope mapping on the ookinete surface antigen Pbs21 of *Plasmodium berghei*: identification of the site of binding of transmission-blocking monoclonal antibody 13.1. *Parassitologia, 38*(3), 559-563.

Spillner, E., Deckers, S., Grunwald, T., & Bredehorst, R. (2003). Paratope-based protein identification by antibody and peptide phage display. *Analytical Biochemistry, 321*(1), 96-104.

Stowers, A. W., Chen Lh, L. H., Zhang, Y., Kennedy, M. C., Zou, L., Lambert, L., Rice, T. J., Kaslow, D. C., Saul, A., Long, C. A., Meade, H., & Miller, L. H. (2002). A recombinant vaccine expressed in the milk of transgenic mice protects *Aotus* monkeys from a lethal challenge with *Plasmodium falciparum*. *Proceedings of the National Academy of Sciences of the United States of America, 99*(1), 339-344.

Stowers, A. W., Cioce, V., Shimp, R. L., Lawson, M., Hui, G., Muratova, O., Kaslow, D. C., Robinson, R., Long, C. A., & Miller, L. H. (2001). Efficacy of two alternate vaccines based on *Plasmodium falciparum* merozoite surface protein 1 in an *Aotus* challenge trial. *Infection and Immunity, 69*(3), 1536-1546.

Suchankova, A., Ritterova, L., Krcmar, M., Krchnak, V., Vagner, J., Jochmus, I., Gissmann, L., Kanka, J., & Vonka, V. (1991). Comparison of ELISA and western blotting for human papillomavirus type 16 E7 antibody determination. *The Journal of General Virology, 72(Pt 10)*, 2577-2581.

Sugimura, Y., Hosono, M., Wada, F., Yoshimura, T., Maki, M., & Hitomi, K. (2006). Screening for the preferred substrate sequence of transglutaminase using a phage-displayed peptide library: identification of peptide substrates for TGASE 2 and Factor XIIIA. The *Journal of Biological Chemistry, 281*(26), 17699-17706.

Sun, T., Holowka, T., Song, Y., Zierow, S., Leng, L., Chen, Y., Xiong, H., Griffith, J., Nouraie, M., Thuma, P. E., Lolis, E., Janse, C. J., Gordeuk, V. R., Augustijn, K., & Bucala, R. (2012). A *Plasmodium*-encoded cytokine suppresses T-cell immunity during malaria. *Proceedings of the National Academy of Sciences of the United States of America, 109*(31), E2117-2126.

Ta, T. T., Salas, A., Ali-Tammam, M., Martinez Mdel, C., Lanza, M., Arroyo, E., & Rubio, J. M. (2010). First case of detection of *Plasmodium knowlesi* in Spain by Real Time PCR in a traveller from Southeast Asia. *Malaria Journal, 9*, 219.

Tan, C. H., Vythilingam, I., Matusop, A., Chan, S. T., & Singh, B. (2008). Bionomics of *Anopheles latens* in Kapit, Sarawak, Malaysian Borneo in relation to the transmission of zoonotic simian malaria parasite *Plasmodium knowlesi*. *Malaria Journal, 7*, 52.

Tanabe, K., Mackay, M., Goman, M., & Scaife, J. G. (1987). Allelic dimorphism in a surface antigen gene of the malaria parasite *Plasmodium falciparum*. *Journal of Molecular Biology, 195*(2), 273-287.

Tanizaki, R., Ujiie, M., Kato, Y., Iwagami, M., Hashimoto, A., Kutsuna, S., Takeshita, N., Hayakawa, K., Kanagawa, S., Kano, S., & Ohmagari, N. (2013). First case of *Plasmodium knowlesi* infection in a Japanese traveller returning from Malaysia. *Malaria Journal, 12*, 128.

Terpe, K. (2006). Overview of bacterial expression systems for heterologous protein production: from molecular and biochemical fundamentals to commercial systems. *Applied Microbiology and Biotechnology, 72*(2), 211-222.

Thwing, J., Hochberg, N., Vanden Eng, J., Issifi, S., Eliades, M. J., Minkoulou, E., Wolkon, A., Gado, H., Ibrahim, O., Newman, R. D., & Lama, M. (2008). Insecticide-treated net ownership and usage in Niger after a nationwide integrated campaign. *Tropical Medicine & Intternational Health, 13*(6), 827-834.

Tian, J. H., Good, M. F., Hirunpetcharat, C., Kumar, S., Ling, I. T., Jackson, D., Cooper, J., Lukszo, J., Coligan, J., Ahlers, J., Saul, A., Berzofsky, J. A., Holder, A. A., Miller, L. H., & Kaslow, D. C. (1998). Definition of T cell epitopes within the 19 kDa carboxylterminal fragment of *Plasmodium yoelii* merozoite surface

protein 1 (MSP1(19)) and their role in immunity to malaria. *Parasite Immunology*, *20*(6), 263-278.

Tian, J. H., Kumar, S., Kaslow, D. C., & Miller, L. H. (1997). Comparison of protection induced by immunization with recombinant proteins from different regions of merozoite surface protein 1 of *Plasmodium yoelii*. *Infection and Immunity*, *65*(8), 3032-3036.

Udhayakumar, V., Anyona, D., Kariuki, S., Shi, Y. P., Bloland, P. B., Branch, O. H., Weiss, W., Nahlen, B. L., Kaslow, D. C., & Lal, A. A. (1995). Identification of T and B cell epitopes recognized by humans in the C-terminal 42-kDa domain of the *Plasmodium falciparum* merozoite surface protein (MSP)-1. *The Journal of Immunology*, *154*(11), 6022-6030.

Valderrama-Aguirre, A., Quintero, G., Gomez, A., Castellanos, A., Perez, Y., Mendez, F., Arevalo-Herrera, M., & Herrera, S. (2005). Antigenicity, immunogenicity, and protective efficacy of *Plasmodium vivax* MSP1 PV200l: a potential malaria vaccine subunit. *The American Journal of Tropical Medicine and Hygiene*, *73*(5 Suppl), 16-24.

Van den Eede, P., Van, H. N., Van Overmeir, C., Vythilingam, I., Duc, T. N., Hung le, X., Manh, H. N., Anne, J., D'Alessandro, U., & Erhart, A. (2009). Human *Plasmodium knowlesi* infections in young children in central Vietnam. *Malaria Journal*, *8*, 249.

van Hellemond, J. J., Rutten, M., Koelewijn, R., Zeeman, A. M., Verweij, J. J., Wismans, P. J., Kocken, C. H., & van Genderen, P. J. (2009). Human *Plasmodium knowlesi* infection detected by rapid diagnostic tests for malaria. *Emerging Infectious Diseases*, *15*(9), 1478-1480.

Van Nieuwenhove, L., Buscher, P., Balharbi, F., Humbert, M., Dieltjens, T., Guisez, Y., & Lejon, V. (2012). Identification of mimotopes with diagnostic potential for

Trypanosoma brucei gambiense variant surface glycoproteins using human antibody fractions. *PLoS Neglected Tropical Diseases, 6*(6), e1682.

van Rooyen, C. E., & Pile, G. R. (1935). Observations on infection by *Plasmodium knowlesi* (Ape malaria) in the treatment of general paralysis of the insane. *British Medical Journal, 2*(3901), 662-666.

Vanniasinkam, T., Barton, M. D., & Heuzenroeder, M. W. (2001). B-Cell epitope mapping of the VapA protein of *Rhodococcus equi*: implications for early detection of *R. equi* disease in foals. *Journal of Clinical Microbiology, 39*(4), 1633-1637.

Villard, V., Agak, G.W., Frank, G., Jafarshad, A., Servis, C., Nebie, I., Sirima, S.B., Felger, I., Arevalo-Herrera, M., Herrera, S., Heitz, F., Backer, V., Druilhe, P., Kajava, A.V., & Corradin, G. (2007). Rapid identification of malaria vaccine candidates based on alpha-helical coiled coil protein motif. *PloS One, 2*(7), e645.

Vythilingam, I., Foo, L. C., Chiang, G. L., Chan, S. T., Eng, K. L., Mahadevan, S., Mak, J. W., & Singh, K. I. (1995). The impact of permethrin impregnated bednets on the malaria vector *Anopheles maculatus* (Diptera: Culicidae) in aboriginal villages of Pos Betau Pahang, Malaysia. *The Southeast Asian Journal of Tropical Medicine and Public Health, 26*(2), 354-358.

Vythilingam, I., Noorazian, Y. M., Huat, T. C., Jiram, A. I., Yusri, Y. M., Azahari, A. H., Norparina, I., Noorrain, A., & Lokmanhakim, S. (2008). *Plasmodium knowlesi* in humans, macaques and mosquitoes in peninsular Malaysia. *Parasites & Vectors, 1*(1), 26.

Vythilingam, I., Tan, C. H., Asmad, M., Chan, S. T., Lee, K. S., & Singh, B. (2006). Natural transmission of *Plasmodium knowlesi* to humans by *Anopheles latens* in Sarawak, Malaysia. *Transactions of the Royal Society of Tropical Medicine and Hygiene, 100*(11), 1087-1088.

Wang, L. F., & Yu, M. (2009). Epitope mapping using phage-display random fragment libraries. *Methods in Molecular Biology, 524*, 315-332.

Wang, Z., Shao, D., Zhong, X., Han, C., Cai, P., & Wang, H. (2009). Epitope mapping of monoclonal antibody 1B9 against *Plasmodium falciparum*-derived macrophage migration inhibitory factor. *Immunological Investigations, 38*(5), 422-433.

Wharton, R. H., & Eyles, D. E. (1961). *Anopheles hackeri*, a vector of *Plasmodium knowlesi* in Malaya. *Science, 134*, 279-280.

Wharton, R. H., Eyles, D. E., Warren, M., & Moorhouse, D. E. (1962). *Anopheles leucosphyrus* identified as a vector of monkey malaria in Malaya. *Science, 137*, 758.

White, N. J. (2008). *Plasmodium knowlesi*: the fifth human malaria parasite. *Clinical Infectious Diseases, 46*(2), 172-173.

White, W. I., Evans, C. B., & Taylor, D. W. (1991). Antimalarial antibodies of the immunoglobulin G2a isotype modulate parasitemias in mice infected with *Plasmodium yoelii*. *Infection and Immunity, 59*(10), 3547-3554.

Wiersch, S. C., Maier, W. A., & Kampen, H. (2005). *Plasmodium* (*Haemamoeba*) *cathemerium* gene sequences for phylogenetic analysis of malaria parasites. *Parasitology Research, 96*(2), 90-94.

William, T., Menon, J., Rajahram, G., Chan, L., Ma, G., Donaldson, S., Khoo, S., Frederick, C., Jelip, J., Anstey, N. M., & Yeo, T. W. (2011). Severe *Plasmodium knowlesi* malaria in a tertiary care hospital, Sabah, Malaysia. *Emerging Infectious Diseases, 17*(7), 1248-1255.

Williams, S. C., Badley, R. A., Davis, P. J., Puijk, W. C., & Meloen, R. H. (1998). Identification of epitopes within beta lactoglobulin recognised by polyclonal

antibodies using phage display and PEPSCAN. *Journal of Immunological Methods, 213*(1), 1-17.

Winkler, S., Willheim, M., Baier, K., Schmid, D., Aichelburg, A., Graninger, W., & Kremsner, P. G. (1998). Reciprocal regulation of Th1- and Th2-cytokine-producing T cells during clearance of parasitemia in *Plasmodium falciparum* malaria. *Infection and Immunity, 66*(12), 6040-6044.

Wipasa, J., Hirunpetcharat, C., Mahakunkijcharoen, Y., Xu, H., Elliott, S., & Good, M. F. (2002). Identification of T cell epitopes on the 33-kDa fragment of *Plasmodium yoelii* merozoite surface protein 1 and their antibody-independent protective role in immunity to blood stage malaria. *The Journal of Immunology, 169*(2), 944-951.

Wipasa, J., Suphavilai, C., Okell, L. C., Cook, J., Corran, P. H., Thaikla, K., Liewsaree, W., Riley, E. M., & Hafalla, J. C. (2010). Long-lived antibody and B Cell memory responses to the human malaria parasites, *Plasmodium falciparum* and *Plasmodium vivax*. *PLoS Pathogens, 6*(2), e1000770.

World Health Organization. (2013). *World Malaria Report*. Geneva, Switzerland: World Health Organization.

Xainli, J., Cole-Tobian, J. L., Baisor, M., Kastens, W., Bockarie, M., Yazdani, S. S., Chitnis, C. E., Adams, J. H., & King, C. L. (2003). Epitope-specific humoral immunity to *Plasmodium vivax* Duffy binding protein. *Infection and Immunity, 71*(5), 2508-2515.

Yang, C., Collins, W. E., & Millet, P. (1994). Immunologic characterization of *Plasmodium vivax* antigens using *Plasmodium cynomolgi* liver stage-primed immune sera. *The American Journal of Tropical Medicine and Hygiene, 51*(3), 365-371.

Youn, J. H., Myung, H. J., Liav, A., Chatterjee, D., Brennan, P. J., Choi, I. H., Cho, S. N., & Shin, J. S. (2004). Production and characterization of peptide mimotopes of phenolic glycolipid-I of *Mycobacterium leprae*. *FEMS Immunology and Medical Microbiology*, *41*(1), 51-57.

Yusof, R., Lau, Y. L., Mahmud, R., Fong, M. Y., Jelip, J., Ngian, H. U., Mustakim, S., Hussin, H. M., Marzuki, N., & Ali, M. M. (2014). High proportion of knowlesi malaria in recent malaria cases in Malaysia. *Malaria Journal, 13*, 168.